KAROLINSKA INSTITUTET 200-YEAR ANNIVERSARY SYMPOSIUM ON INJURIES TO THE SPINAL CORD AND PERIPHERAL NERVOUS SYSTEM - AN UPDATE ON RECENT ADVANCES IN REGENERATIVE NEUROSCIENCE

EDITED BY: Mattias K. Sköld and Michael G. Fehlings
PUBLISHED IN: Frontiers in Neurology

frontiers Research Topics

frontiers

ISSN 1664-8714
ISBN 978-2-88945-324-5
DOI 10.3389/978-2-88945-324-5

About Frontiers

Frontiers is more than just an open-access publisher of scholarly articles: it is a pioneering approach to the world of academia, radically improving the way scholarly research is managed. The grand vision of Frontiers is a world where all people have an equal opportunity to seek, share and generate knowledge. Frontiers provides immediate and permanent online open access to all its publications, but this alone is not enough to realize our grand goals.

Frontiers Journal Series

The Frontiers Journal Series is a multi-tier and interdisciplinary set of open-access, online journals, promising a paradigm shift from the current review, selection and dissemination processes in academic publishing. All Frontiers journals are driven by researchers for researchers; therefore, they constitute a service to the scholarly community. At the same time, the Frontiers Journal Series operates on a revolutionary invention, the tiered publishing system, initially addressing specific communities of scholars, and gradually climbing up to broader public understanding, thus serving the interests of the lay society, too.

Dedication to quality

Each Frontiers article is a landmark of the highest quality, thanks to genuinely collaborative interactions between authors and review editors, who include some of the world's best academicians. Research must be certified by peers before entering a stream of knowledge that may eventually reach the public - and shape society; therefore, Frontiers only applies the most rigorous and unbiased reviews.
Frontiers revolutionizes research publishing by freely delivering the most outstanding research, evaluated with no bias from both the academic and social point of view.
By applying the most advanced information technologies, Frontiers is catapulting scholarly publishing into a new generation.

What are Frontiers Research Topics?

Frontiers Research Topics are very popular trademarks of the Frontiers Journals Series: they are collections of at least ten articles, all centered on a particular subject. With their unique mix of varied contributions from Original Research to Review Articles, Frontiers Research Topics unify the most influential researchers, the latest key findings and historical advances in a hot research area! Find out more on how to host your own Frontiers Research Topic or contribute to one as an author by contacting the Frontiers Editorial Office: **researchtopics@frontiersin.org**

KAROLINSKA INSTITUTET 200-YEAR ANNIVERSARY SYMPOSIUM ON INJURIES TO THE SPINAL CORD AND PERIPHERAL NERVOUS SYSTEM - AN UPDATE ON RECENT ADVANCES IN REGENERATIVE NEUROSCIENCE

Topic Editors:
Mattias K. Sköld, Uppsala University and Karolinska Institute, Sweden
Michael G. Fehlings, University of Toronto and Toronto Western Hospital, Canada

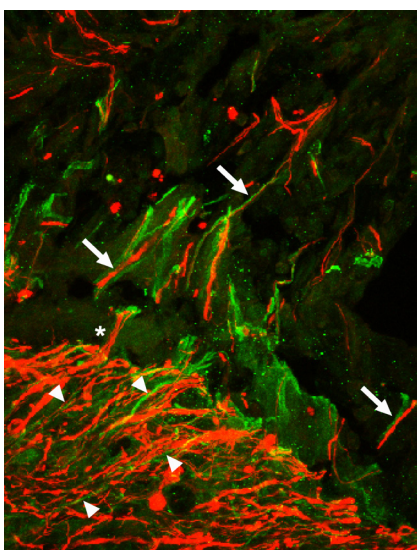

Detailed description of cover image: Axons (neurofilament, red) and astrocytes (GFAP, green) are seen at the border between the central and peripheral parts of the spinal cord at the site of replantation of the avulsed ventral root at 3 weeks after injury. In the more central parts astrocyte processes can be seen growing alongside axons (arrowheads) in a pattern that can also be found in the more peripheral parts where axons and astrocytic processess do align (arrows). Marked is also one single axon growing alongside an astrocytic processess over the border between the central parts and the peripheral nerve graft (asterisk*).

Image from *Front. Neur.* 2:29. doi: 10.3389/fneur.2011.00029.

The present E-book consists of original articles and reviews published in our Research Topic on injuries to the spinal cord and peripheral nerves and presents a wide array of novel findings and in depth discussions on topics within the field of nerve injury and repair.

Our aim with this Research Topic is to bring together knowledge spanning from basic laboratory studies to clinical findings and strategies within the field of spinal cord and nerve injury and repair. We hope this publication will provide a basis for accelerated knowlegde exchange within the field and hopefully a subsequent increase in research efforts and collaborations.

Citation: Sköld, M. K., Fehlings, M. G., eds. (2017). Karolinska Institutet 200-Year Anniversary Symposium on Injuries to the Spinal Cord and Peripheral Nervous System - An Update on Recent Advances in Regenerative Neuroscience. Lausanne: Frontiers Media. doi: 10.3389/978-2-88945-324-5

Table of Contents

frontiers in Neurology

EDITORIAL
published: 26 September 2017
doi: 10.3389/fneur.2017.00510

Editorial: Karolinska Institutet 200-Year Anniversary Symposium on Injuries to the Spinal Cord and Peripheral Nervous System—An Update on Recent Advances in Regenerative Neuroscience

Mattias K. Sköld[1,2] and Michael G. Fehlings[3,4]*

[1] Department of Neuroscience, Section of Neurosurgery, Uppsala University, Uppsala, Sweden, [2] Department of Neuroscience, Karolinska Institutet, Stockholm, Sweden, [3] Department of Neurosurgery, University of Toronto, Toronto, ON, Canada, [4] Spine Program, Toronto Western Hospital, Toronto, ON, Canada

Keywords: spinal cord injuries, brachial plexus injury, neuronal regeneration, nerve injury, neuronal plasticity and repair

Editorial on the Research Topic

Karolinska Institutet 200-Year Anniversary Symposium on Injuries to the Spinal Cord and Peripheral Nervous System—An Update on Recent Advances in Regenerative Neuroscience

OPEN ACCESS

Edited and Reviewed by:
Firas H. Kobeissy, University of Florida, United States

****Correspondence:***
Mattias K. Sköld
mattias.skold@akademiska.se

Specialty section:
This article was submitted to Neurotrauma, a section of the journal Frontiers in Neurology

Received: *21 August 2017*
Accepted: *12 September 2017*
Published: *26 September 2017*

Citation:
Sköld MK and Fehlings MG (2017) Editorial: Karolinska Institutet 200-Year Anniversary Symposium on Injuries to the Spinal Cord and Peripheral Nervous System—An Update on Recent Advances in Regenerative Neuroscience. Front. Neurol. 8:510. doi: 10.3389/fneur.2017.00510

The Karolinska Institutet 200-year anniversary symposium on injuries to the spinal cord and peripheral nerves in 2010 gathered expertise in the spinal cord, spinal nerve, and peripheral nerve injury fields, covering topics from molecular prerequisites for nerve regeneration to clinical methods in nerve repair and rehabilitation (Skold et al.). The present Research Topic recognizes the remarkable advances in regenerative neuroscience that have occurred over the past years.

In this Research Topic, we are pleased to present contributions from basic laboratory studies to new clinical strategies in the spirit of highlighting advancements in regenerative neuroscience and functional repair of traumatic injuries to the spinal cord and peripheral nerves.

As the main conduits of information from the periphery to the brain and vice versa, the spinal cord and the spinal nerves are of fundamental importance. The location of spinal motor and sensory neurons within both the central and peripheral nervous systems, with profoundly different responses to nerve injury, make these neurons especially interesting for understanding fundamental aspects of nerve injury and regeneration.

In injuries to the spinal cord, the primary injury results in damage of cells, extracellular matrix, and vasculature, that in turn give rise to a secondary injury cascade with consequent ischemia, inflammation, and death of glial cells and neurons. Formation of glial scars and cystic cavities are the result of posttraumatic changes in the structural architecture of the posttraumatic spinal cord which are of importance for the capacity of regrowth of axons, the poor recovery potential and resulting neurological capacity.

The glial scar is formed in a dynamic process after injury to the spinal cord and its potentially inhibitory as well as supportive effect on nerve regrowth has been studied widely (1–4).

In the zone around the lesion, activated astrocytes, microglia, invading macrophages, and fibroblast are arranged together with secreted extracellular matrix molecules to form the glial scar. Myelin forming oligodendrocytes are commonly lost after spinal cord injuries leaving axons demyelinated (5)

while surviving and new oligodendrocytes may not contribute to effective functional remyelination (6, 7). On the other hand, it is well known that oligodendrocyte progenitor cells, the so-called NG2 cells, do migrate to the spinal cord lesion and probably play a multifold function therein; secreting nerve growth inhibitory ECM molecules (chondroitin sulfate proteoglycans) and differentiating to myelin-producing oligodendrocytes and even astrocytes, although much of their function remains elusive. In the contribution to this Research Topic by Hackett and Lee, we do get a comprehensive review on NG2 cells and their role in health and disease. Hackett et al. point out that NG2 cells are, besides astrocytes, one major part of the glial scar. However, unlike astrocytes, they can differentiate into oligodendrocytes, astrocytes, and perhaps even Schwann cells and, thus, be a target in many aspects of spinal cord injury and repair.

Even though lack of nerve regeneration, or at least successful nerve regeneration, is the rule after injuries to the central nervous system (CNS), endogenous mechanisms and exceptions to this dogma of unsuccessful nerve regeneration do exist and hold promise of a wider understanding of how, when, and where nerve regeneration can occur and be supported. Anatomical and synaptic plasticity (8) as well as activation and development of neural precursor cells in to neurons and glia (9) after spinal cord injury are endogenous reparative attempts that need further exploration.

One interesting example of successful CNS nerve regeneration is the avulsion-replantation injury of spinal nerves (Carlstedt). When spinal roots, typically in high velocity traffic accidents, are torn from the spinal cord, this results in an interruption of the local transverse segmental spinal cord motor and sensory fibers. This will lead to dying back of the centrally located axon and, eventually, the motor neuron in the ventral horn of the spinal cord. However, if the avulsed spinal root is replanted to the spinal cord, survival of motor neurons and successful regeneration of axons from the motor neurons within the CNS will occur (10), which has resulted in a surgical method to restore function after this kind of longitudinal spinal cord injury (11).

In his perspectives article, Carlstedt elaborates on recent findings regarding the return of sensory function. Replantation of avulsed spinal roots leads to useful motor function if the procedure is performed before 1 month after injury (12), but sensory recovery cannot be achieved by replanting avulsed dorsal roots since the dorsal root ganglion neurons are unable to regenerate into the adult spinal cord (13).

Different strategies have been developed to overcome this problem and both use of implanted PNS conduits (14) and adjuvant therapy with a retinoic acid receptor agonist (15) has shown promising results in the restoration of sensory functions after spinal root avulsion.

In their original research paper, Bigbee et al. describe further progress in the field of sensory dysfunction after spinal root avulsion injuries in the lumbosacral plexus where replantation of ventral roots can ameliorate the otherwise resulting allodynia. In the dorsal horn after replantation of avulsed ventral roots on L6 + S1 level, they can demonstrate selective plasticity for vesicular glutamate transporter (VGLUT1) and isolectin B4 (IB4) in primary afferent projections. Given that VGLUT1 is a marker for cutaneous and muscle afferents and that IB4 is a marker for non-peptidergic primary afferents, these findings are suggestive of a restoration alternatively preservation of primary afferent phenotype expressions.

Neuronal guidance molecules are of fundamental importance in the establishment of the neuronal system during development, and a multifold of such factors and their receptors work in a complex and precisely orchestrated manner in CNS and PNS development. One such family of guidance molecules is the semaphorins (16). If and how such guidance molecules are of importance after injury and in the endogenous repair efforts in the injured CNS remains unclear and, therefore, under investigation. Previous findings in a model with regeneration of injured neurons in the spinal cord shows expression of semaphorins and their receptors in a specific pattern (17) as well as a possible interplay with growth factors related to angiogenesis (18), which is specifically interesting since vasculature and nerves share common growth factors and receptors during their establishment (19). In the contribution from Lindholm et al., the importance of the semaphorins is investigated further but now in primary sensory neurons after dorsal root injury. If such injuries are applied to the peripheral axon of the dorsal root ganglion it will be followed by vigorous regrowth, but if applied to the central part of the axon the regrowth will be much weaker. Interestingly, the expression pattern of both semaphorins and their receptors neuropilins differ distinctly between the different injuries and with specific temporal patterns, indicating an involvement in regenerative efforts of dorsal root ganglion neurites rather than inhibitory.

Anatomical variations are a common challenge, both in clinical practice and research. In their contribution to this Research Topic, Frostell et al. have made a welcomed contribution to spinal research by their effort to calculate the standard the size of the spinal cord based on 11 previous studies presenting measurements of spinal cord cross-sectional diameters. With this large and combined sample, they are able to compute population estimates of the transverse and anteroposterior diameter of the entire human spinal cord on a normalized craniocaudal axis. Information from this study will be useful in diagnosing and monitoring patients with neurodegenerative spinal disorders but also in different conditions, both in clinical and research settings, where neuronal segment relation to vertebral landmarks has to be achieved.

One important endogenous repair strategy is cerebral plasticity, i.e., the rearrangement of neuronal circuits as an answer to the new input injury (20). Thus, in surgical reconstruction of nerve injuries recovery, after such operations is a function of nerve regeneration and cerebral reorganization. In two interesting contributing original research papers and one case report, we get new insights into these mechanisms.

Dahlin et al. show in his case report an example of how the plastic capacity of the brain can be guided to improve function that has been lost in brachial plexus injuries where restoration with use of peripheral nerves, in this case phrenic nerve and intercostal nerves, have been used.

From the same group comes an original research paper (Bjorkman et al.) investigating the cerebral response to active movements in the shoulder and elbow in a group of patients with

residual shoulder problems after brachial plexus birth injuries. In this study, reorganization in both contralateral and, more surprisingly, ipsilateral sensorimotor cerebral areas were demonstrated, which shows how strong the endogenous compensatory plasticity mechanisms are. Hopefully a broader understanding of this dynamic capacity of the nervous system can be used to facilitate axon regeneration in CNS injuries (21).

An example of aberrant plasticity is phantom sensation/pain after limb amputation. When amputation occurs, nerves attempt to make new connections causing reorganization within both the residual limb and the brain (22).

In their study, Collins et al. investigate if face-representing somatosensory cortical regions are able to take over the arm area in upper extremity amputees and can show that in 42% of upper extremity amputees stimulation of the face evokes phantom limb arm and hand sensations. These results demonstrate that upper limb amputation causes changes within somatosensory cortical areas, knowledge that will help understand the phantom limb pain better and holds promises for future therapeutic strategies to this debilitating condition.

We are thankful to all authors who have contributed to this Research Topic and believe that the articles offer the reader an overview of the diverse scientific approaches and latest advancements in the field of spinal cord and peripheral nerve injury and repair. It is clear from the collection of findings presented in the published papers that the progress in this field, both methodological and conceptual, will help push forward our understanding of nerve injury and repair to the benefit of our patients.

We trust that the contributions will be of interest to both basic scientists and clinical researchers and hope they will inspire further research in the fields of neurotrauma and regenerative neuroscience.

AUTHOR CONTRIBUTIONS

MS and MGF wrote the editorial. MS is the corresponding author.

ACKNOWLEDGMENTS

We do thank Prof. Mårten Risling for organizing the original Karolinska Institutet 200-year anniversary Symposium on Traumatic Injuries in the Nervous System and for his kind support on this follow up Research Topic.

REFERENCES

1. Chen MS, Huber AB, van der Haar ME, Frank M, Schnell L, Spillmann AA, et al. Nogo-A is a myelin-associated neurite outgrowth inhibitor and an antigen for monoclonal antibody IN-1. *Nature* (2000) 403(6768):434–9. doi:10.1038/35000219
2. Silver J, Miller JH. Regeneration beyond the glial scar. *Nat Rev Neurosci* (2004) 5(2):146–56. doi:10.1038/nrn1326
3. Anderson MA, Burda JE, Ren Y, Ao Y, O'Shea TM, Kawaguchi R, et al. Astrocyte scar formation aids central nervous system axon regeneration. *Nature* (2016) 532(7598):195–200. doi:10.1038/nature17623
4. Ahuja CS, Martin AR, Fehlings M. Recent advances in managing a spinal cord injury secondary to trauma. *F1000Res* (2016) 5. doi:10.12688/f1000research.7586.1
5. Crowe MJ, Bresnahan JC, Shuman SL, Masters JN, Beattie MS. Apoptosis and delayed degeneration after spinal cord injury in rats and monkeys. *Nat Med* (1997) 3(1):73–6. doi:10.1038/nm0197-73
6. Crawford AH, Tripathi RB, Foerster S, McKenzie I, Kougioumtzidou E, Grist M, et al. Pre-existing mature oligodendrocytes do not contribute to remyelination following toxin-induced spinal cord demyelination. *Am J Pathol* (2016) 186(3):511–6. doi:10.1016/j.ajpath.2015.11.005
7. Nashmi R, Fehlings MG. Changes in axonal physiology and morphology after chronic compressive injury of the rat thoracic spinal cord. *Neuroscience* (2001) 104(1):235–51. doi:10.1016/S0306-4522(01)00009-4
8. Raineteau O, Schwab ME. Plasticity of motor systems after incomplete spinal cord injury. *Nat Rev Neurosci* (2001) 2(4):263–73. doi:10.1038/35067570
9. Meletis K, Barnabe-Heider F, Carlen M, Evergren E, Tomilin N, Shupliakov O, et al. Spinal cord injury reveals multilineage differentiation of ependymal cells. *PLoS Biol* (2008) 6(7):e182. doi:10.1371/journal.pbio.0060182
10. Cullheim S, Carlstedt T, Linda H, Risling M, Ulfhake B. Motoneurons reinnervate skeletal muscle after ventral root implantation into the spinal cord of the cat. *Neuroscience* (1989) 29(3):725–33. doi:10.1016/0306-4522(89)90144-9
11. Carlstedt T, Grane P, Hallin RG, Noren G. Return of function after spinal cord implantation of avulsed spinal nerve roots. *Lancet* (1995) 346(8986):1323–5. doi:10.1016/S0140-6736(95)92342-X
12. Htut M, Misra VP, Anand P, Birch R, Carlstedt T. Motor recovery and the breathing arm after brachial plexus surgical repairs, including re-implantation of avulsed spinal roots into the spinal cord. *J Hand Surg Eur Vol* (2007) 32(2):170–8. doi:10.1016/J.JHSB.2006.11.011
13. Carlstedt T. Regenerating axons form nerve terminals at astrocytes. *Brain Res* (1985) 347(1):188–91. doi:10.1016/0006-8993(85)90911-4
14. Carlstedt T, Misra VP, Papadaki A, McRobbie D, Anand P. Return of spinal reflex after spinal cord surgery for brachial plexus avulsion injury. *J Neurosurg* (2012) 116(2):414–7. doi:10.3171/2011.7.JNS111106
15. Goncalves MB, Malmqvist T, Clarke E, Hubens CJ, Grist J, Hobbs C, et al. Neuronal RARbeta signaling modulates PTEN activity directly in neurons and via exosome transfer in astrocytes to prevent glial scar formation and induce spinal cord regeneration. *J Neurosci* (2015) 35(47):15731–45. doi:10.1523/JNEUROSCI.1339-15.2015
16. O'Malley AM, Shanley DK, Kelly AT, Barry DS. Towards an understanding of semaphorin signalling in the spinal cord. *Gene* (2014) 553(2):69–74. doi:10.1016/j.gene.2014.10.005
17. Lindholm T, Skold MK, Suneson A, Carlstedt T, Cullheim S, Risling M. Semaphorin and neuropilin expression in motoneurons after intraspinal motoneuron axotomy. *Neuroreport* (2004) 15(4):649–54. doi:10.1097/00001756-200403220-00015
18. Skold M, Cullheim S, Hammarberg H, Piehl F, Suneson A, Lake S, et al. Induction of VEGF and VEGF receptors in the spinal cord after mechanical spinal injury and prostaglandin administration. *Eur J Neurosci* (2000) 12(10):3675–86. doi:10.1046/j.1460-9568.2000.00263.x
19. Carmeliet P, Tessier-Lavigne M. Common mechanisms of nerve and blood vessel wiring. *Nature* (2005) 436(7048):193–200. doi:10.1038/nature03875
20. Duffau H. Brain plasticity: from pathophysiological mechanisms to therapeutic applications. *J Clin Neurosci* (2006) 13(9):885–97. doi:10.1016/j.jocn.2005.11.045
21. Rosenkranz K, Rothwell JC. Differences between the effects of three plasticity inducing protocols on the organization of the human motor cortex. *Eur J Neurosci* (2006) 23(3):822–9. doi:10.1111/j.1460-9568.2006.04605.x
22. Flor H. Phantom-limb pain: characteristics, causes, and treatment. *Lancet Neurol* (2002) 1(3):182–9. doi:10.1016/S1474-4422(02)00074-1

Conflict of Interest Statement: The authors declare that the research was conducted in the absence of any commercial or financial relationships that could be construed as a potential conflict of interest.

frontiers in Neurology

REVIEW
published: 15 November 2016
doi: 10.3389/fneur.2016.00199

Understanding the NG2 Glial Scar after Spinal Cord Injury

*Amber R. Hackett and Jae K. Lee**

Miami Project to Cure Paralysis, The Neuroscience Graduate Program, Department of Neurological Surgery, University of Miami Miller School of Medicine, Miami, FL, USA

NG2 cells, also known as oligodendrocyte progenitor cells, are located throughout the central nervous system and serve as a pool of progenitors to differentiate into oligodendrocytes. In response to spinal cord injury (SCI), NG2 cells increase their proliferation and differentiation into remyelinating oligodendrocytes. While astrocytes are typically associated with being the major cell type in the glial scar, many NG2 cells also accumulate within the glial scar but their function remains poorly understood. Similar to astrocytes, these cells hypertrophy, upregulate expression of chondroitin sulfate proteoglycans, inhibit axon regeneration, contribute to the glial-fibrotic scar border, and some even differentiate into astrocytes. Whether NG2 cells also have a role in other astrocyte functions, such as preventing the spread of infiltrating leukocytes and expression of inflammatory cytokines, is not yet known. Thus, NG2 cells are not only important for remyelination after SCI but are also a major component of the glial scar with functions that overlap with astrocytes in this region. In this review, we describe the signaling pathways important for the proliferation and differentiation of NG2 cells, as well as the role of NG2 cells in scar formation and tissue repair.

Keywords: OPCs, oligodendrocytes, scar formation, astroglial scar, oligodendrocyte progenitor cells, axon regeneration

OPEN ACCESS

Edited by:
Mattias K. Sköld,
Uppsala University, Sweden

Reviewed by:
Linda Noble,
University of California San Francisco, USA
Bridgette D. Semple,
University of Melbourne, Australia

***Correspondence:**
Jae K. Lee
jlee22@med.miami.edu

Specialty section:
This article was submitted to Neurotrauma, a section of the journal Frontiers in Neurology

Received: *12 September 2016*
Accepted: *31 October 2016*
Published: *15 November 2016*

Citation:
Hackett AR and Lee JK (2016) Understanding the NG2 Glial Scar after Spinal Cord Injury. Front. Neurol. 7:199. doi: 10.3389/fneur.2016.00199

INTRODUCTION

Many oligodendrocytes are lost after contusive spinal cord injury (SCI) (1, 2), leaving axons demyelinated and impairing proper conduction of action potentials (3–6). Although new remyelinating oligodendrocytes are formed after SCI (7–11), normal levels of myelination are not achieved (6). Pre-existing oligodendrocytes do not contribute to remyelination (12); however, NG2 cells, also known as oligodendrocyte progenitor cells (OPCs), are ubiquitously distributed throughout the central nervous system (CNS) and are capable of differentiating into oligodendrocytes in the adult CNS (13). Thus, targeting their proliferation and differentiation is an appealing target to promote remyelination after CNS injury. NG2 cells are present in increased numbers surrounding the lesion site (2, 7, 8, 14), and many studies have investigated the mechanisms underlying their differentiation into oligodendrocytes and their contribution to remyelination (15–17).

However, a large number of NG2 cells that do not differentiate into oligodendrocytes are present within the glial scar, which has been traditionally synonymous with reactive astrocytes. Interestingly, similar to astrocytes, these NG2 cells hypertrophy and upregulate expression of chondroitin sulfate proteoglycans (CSPGs) after CNS injury (18). In fact, NG2 is itself a CSPG (gene name is *cspg4*) and can inhibit axon growth *in vitro* (19). Interestingly, NG2 cells have the capacity to differentiate into astrocytes at the CNS injury site, as discussed in more detail below. Thus, NG2 cells are potentially

a major contributor to the axon regeneration inhibition by the glial scar.

In addition to their role in axon growth inhibition, NG2 cells may share other properties with astrocytes. For example, astrocytes play an important role in preventing the spread of infiltrating leukocytes, and their ablation leads to increased neuron and oligodendrocyte loss (20, 21). Astrocytes also play a major role in the immune response after contusive SCI through secretion of pro-inflammatory cytokines and chemokines (22, 23). In this review article, we will discuss methods of investigating NG2 cells in the context of SCI, the mechanisms underlying the proliferation of NG2 cells after SCI, as well as their contribution to the glial scar including axon regeneration, wound healing and inflammation.

SCAR FORMATION AFTER CONTUSIVE SCI

Figure 1 depicts a diagram of the cellular reactions after contusive SCI in mice. Differences between mice, rat, and human SCI will be addressed where appropriate. In the uninjured spinal cord, astrocytes, oligodendrocytes, and NG2 cells are located throughout the parenchyma (**Figure 1A**). Contusive SCI leads to large scale death of neurons and glia at the site of injury, shearing of ascending and descending axons, and damage to the vasculature. This damage leads to large-scale hemorrhage at the site of the lesion, which leads to the release of factors that contribute to the immune response, and responses from resident glia (24, 25). Microglia reacts within hours after injury by accumulating around the lesion site and secreting pro-inflammatory cytokines and chemokines that which contribute to the immune response (26). While NG2 cells have been shown to proliferate and migrate short distances toward the lesion site after laser induced injury (27), their migration capacity has not been investigated in more clinically relevant traumatic injuries. Astrocytes also proliferate, hypertrophy, and upregulate expression of glial fibrillary acidic protein (GFAP), and secrete cytokines, chemokines, growth factors, and CSPGs (28). Increased inflammation leads to secondary damage to neurons and oligodendrocytes, as well as axonal dieback characterized by dystrophic endings (1, 29) (**Figures 1B–D**). Myelin debris and CSPGs, both inhibitory to axon regeneration, accumulate in the lesion core and the glial scar. Hematogenous macrophages start to infiltrate the lesion (30, 31) and attract perivascular fibroblasts that separate from

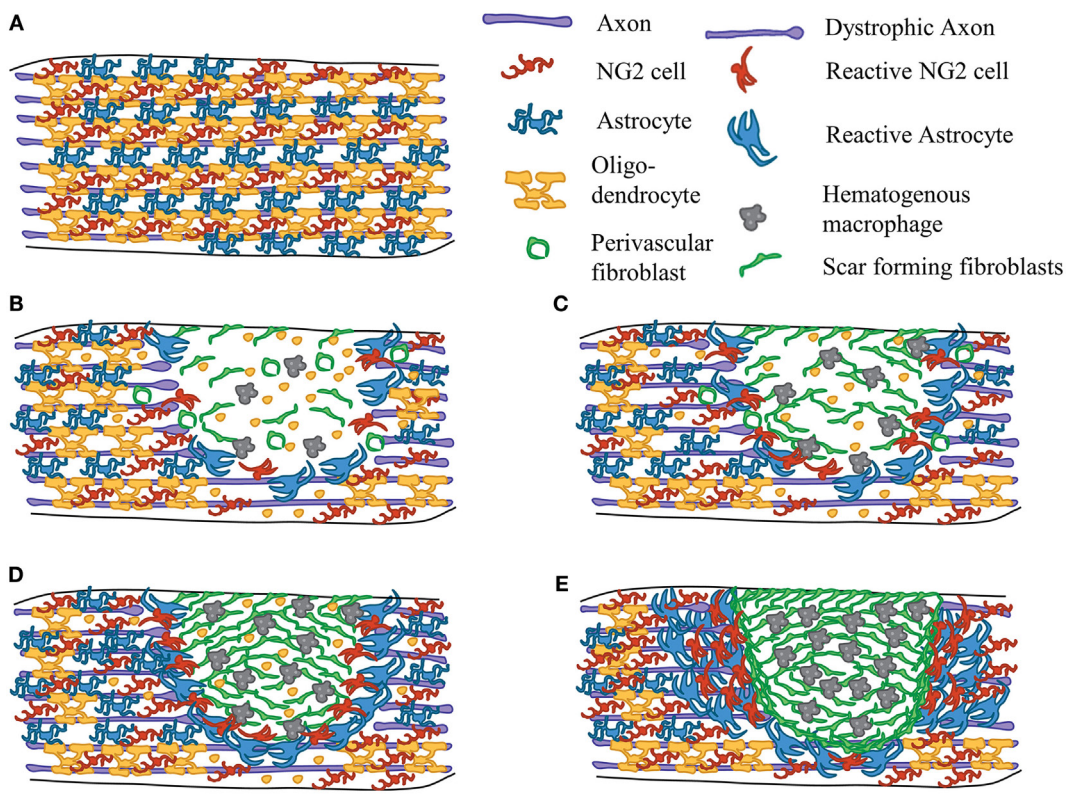

FIGURE 1 | Scar formation after SCI. Diagram depicting the events of scar formation after contusive SCI in mice. Astrocytes (blue), NG2 cells (red), and myelinating oligodendrocytes (yellow) in the uninjured spinal cord white matter **(A)**. Early after SCI, cell death occurs within the lesion site and axons are damaged. Microglia (not shown) and astrocytes respond by secreting cytokines and chemokines. NG2 cells react and proliferate around the lesion site. Macrophages (gray) begin to infiltrate the lesion core and perivascular fibroblasts (green) begin to delaminate from blood vessels **(B)**. Inflammation causes secondary death of oligodendrocytes and neurons leading to accumulation of myelin debris in the injury site **(C)**. Macrophage and fibroblast density peaks at 7 days after SCI **(D)**. By 2 weeks after SCI, the scar has matured. There are tight borders between the fibrotic scar (consisting of fibroblasts and macrophages) and the glial scar (consisting of astrocytes, NG2 cells, and microglia) **(E)**. The relative number of cells may not accurately reflect actual *in vivo* pathology.

blood vessels and form the fibrotic scar (32, 33) peaking in density by 7 days after SCI. By 14 days after SCI, the scar has started to mature and form tight borders between the glial and fibrotic components of the scar (20, 21, 33) (**Figure 1E**). (At around this time in rats and humans, a fluid-filled cavity starts to form in parts of the fibrotic scar, whereas in mice, the fibrotic scar contracts slightly over time.) The formation of this scar is dependent on the interactions between CNS cells, namely microglia, NG2 cells, and astrocytes, with non-CNS cells, namely hematogenous macrophages and fibroblasts. In human SCI, astrocytes and NG2 cells were readily detected in the glial scar, and macrophages in the lesion core, within days after SCI (34). Understanding their individual contributions to scar formation is essential for designing both regenerative and neuroprotective therapies for SCI. In this review, we will focus primarily on the role of NG2 cells in the context of the glial scar formation after SCI.

NG2 CELL FATE MAPPING STRATEGIES AFTER CNS INJURY

Proper understanding of NG2 cells after SCI requires proper understanding of the tools that have been used to study them, namely antibodies and transgenic mouse lines. In the uninjured brain and spinal cord, antibodies against NG2 and PDGFRα (platelet-derived growth factor receptor alpha) label NG2$^+$ glia, but NG2 antibodies also label pericytes that express this CSPG (35–37) (**Table 1**). After CNS injury, NG2 expression is upregulated at the injury site (18), but many cells including pericytes, non-myelinating Schwann cells, and macrophages also express NG2 (38, 39) (**Table 1**), making the use of the NG2 antibody alone insufficient to definitively identify NG2$^+$ glial cells. Similarly, PDGFRα antibodies can label fibroblasts, rather than NG2 glia, at the injury site (39) (**Table 1**). Since cells that are NG2$^+$ macrophages, NG2$^+$ pericytes, or PDGFRα$^+$ fibroblasts are often counted as NG2 glia, the use of these antibodies as sole markers for NG2 glia has led to the misconception that NG2 glia are located within the injury core (GFAP-negative region) and has mostly likely contributed to the highly variable reports of NG2 cell density across different studies (40). For the remainder of this review, our use of NG2 cells refers to NG2$^+$ glia (and not pericytes), and we use these two terms along with OPC interchangeably. Antibodies against Olig2 has also been used to identify NG2 cells, but they also label mature oligodendrocytes, and several reports have shown that a small population of protoplasmic astrocytes (10, 41) and reactive astrocytes can also express the transcription factor Olig2 after CNS injury (42, 43) (**Table 1**). Thus, co-labeling with NG2 and Olig2 antibodies may be the best method of histologically detecting NG2 cells after SCI.

Prior to the advent of genetic fate mapping using transgenic mice expressing cell type-specific Cre recombinase, several attempts to understand the fate of NG2 cells after SCI were made. One of the first attempts to study the fate of NG2 cells after SCI utilized a Mahoney retrovirus with reporter expression driven by the NG2 promoter (9). Injection of this virus into the injury site-labeled dividing NG2 cells, however, due to the fact that it was administered after SCI, it also labeled a large number of macrophages (since some of them upregulate NG2 as discussed above) (39, 44). This study also reported that a high percentage of NG2 cells differentiate into GFAP$^+$ astrocytes (35–50%); however, this could have included astrocytes that upregulated NG2 after SCI. Shortly after, Lytle et al. (43) used the CNP-EGFP mice (which labels 2′,3′-cyclic-nucleotide 3′-phosphodiesterase$^+$ NG2 cells and oligodendrocytes) to determine the response of NG2 cells after contusive SCI and reported that a large population of NG2$^+$ cells were EGFP$^-$. This could have been due to CNPase only being expressed in NG2 cells that have already committed to the oligodendrocyte lineage since CNPase is expressed later than PDGFRα and NG2 during development (45, 46). However, it is also possible that scar forming NG2 cells downregulate CNPase expression after injury. Together, these results suggest that NG2 glia comprise both myelinating cells as well as non-myelinating, scar forming cells after contusive SCI.

Transgenic mice expressing tamoxifen-inducible Cre under cell-specific promoters (Cre-ER mice) have been particularly useful for studying fate of NG2 cells after SCI. Although PDGFRα-CreER (13, 47), NG2-CreER (48), and Olig2-CreER (41) mice have been used extensively to either fate map and/or conditionally delete genes in NG2 cells, each mouse line has its advantages and disadvantages. The NG2-CreER mouse line has a recombination efficiency of about 30–40% of NG2 cells (48, 49), while the PDGFRα-CreER has a recombination efficiency of over 90% (47). Low recombination efficiency is often desirable for lineage tracing studies, while high recombination efficiency is often desirable for functional studies. Similar to the limitations of antibodies as discussed above, these transgenic lines label cells other than NG2 glia. The NG2-CreER mice label pericytes (49, 50) whereas the PDGFRα-CreER mice label fibroblasts at the injury site (unpublished observations), and the Olig2-CreER mice label oligodendrocytes as well as a small population of

TABLE 1 | Antibodies used to label NG2 cells after SCI.

Antibody	NG2 glia	Pericytes	Astrocytes	OLs	Macrophages	Schwann cells
Uninjured						
NG2 (39)	+	+				
PDGFRα (39)	+	+				
Olig2 (42, 43)	+			+		
Injured						
NG2 (39)	+	+			+	+
PDGFRα (39)	+	+				
Olig2 (42, 43)	+		+	+		

astrocytes (10, 51). Although we did not observe contributions of $NG2^+$ pericytes to scar formation after SCI in mice, it is possible that experimental manipulations (drugs, viruses, or genes deletions) could induce them to contribute to scar formation (49). Thus, these off-target labeling must be carefully considered when interpreting any NG2 cell genetic fate mapping studies involving these mouse lines.

One possible solution to circumvent these technical hurdles is to combine genetic labeling of NG2 cells with antibody co-labeling. Genetically labeled cells in NG2-CreER mice can be co-labeled with Olig2 or PDGFRβ antibody to distinguish NG2 cells from pericytes/fibroblasts respectively. Alternatively, instead of using Rosa26 reporter mice, Olig2 promoter-driven reporter mice can be used in combination with NG2-CreER or PDGFRα-CreER mice, which would label NG2 glia without labeling pericytes. This Olig2 strategy can be used to express not only fluorescent reporters but also proteins such as diphtheria toxin receptor (52) that can be used to probe the function of NG2 cells more specifically. However, such Olig2 reporter mice have not yet been reported in the literature.

PROLIFERATION AND OLIGODENDROGENESIS

NG2 cells have been shown to react to CNS injuries such as traumatic brain injury (18), demyelination (53), and contusive SCI (2). This response is reminiscent of astrocyte reactivity as they surround the lesion site and hypertrophy (18). Whereas NG2 cells are normally evenly dispersed throughout the spinal cord (13) and maintain territories due to the dynamic filopodia being repulsed by neighboring NG2 cells (27), their processes become intertwined as they form the glial scar. Two-photon live imaging has revealed NG2 cells react to laser injury by migrating only short distances toward the lesion (27), suggesting that the large number of NG2 cells at the injury site is most likely due to local proliferation rather than migration. In fact, the percentage of proliferating NG2 cells is increased sixfold (2) and NG2 cells comprise nearly one half of bromodeoxyuridine (BrdU)-labeled cells, 3 days after SCI (7). This is most likely an underestimate since it does not account for NG2 cells that differentiated into oligodendrocytes and/or astrocytes after injury. Overall, these data suggest that NG2 cells have a significant capacity to proliferate after SCI.

As NG2 cells differentiate into oligodendrocytes, they lose expression of the NG2 antigen. NG2 cells are capable of differentiating directly into oligodendrocytes without cell division (27), but they often differentiate after division, where one or both differentiate into oligodendrocytes within 6–8 days. This represents a critical window where their fate after proliferation can be determined by the microenvironment of the injury site (48, 54). For example, myelin damage can accelerate and promote NG2 cell differentiation into oligodendrocytes (54). Sensory deprivation induced by whisker clipping can reduce oligodendrogenesis after NG2 cell division, suggesting that neuronal activity promotes differentiation of NG2 cells into oligodendrocytes (54). Conversely, optogenetic stimulation of neurons can increase the proliferation of NG2 cells and their subsequent differentiation into oligodendrocytes (55). This raises the possibility that the myelin and neuronal damage after SCI may create an environment that significantly influences NG2 cell differentiation.

Several factors important for proliferation and differentiation of NG2 cells are upregulated after SCI. These include fibroblast growth factor 2 (FGF2) (56, 57), glial growth factor 2 (GGF2) (58, 59), and Wnts (60). FGF2 is a potent mitogen for NG2 cells *in vitro* (56). Deletion of FGFR1 and FGFR2 in NG2 cells reduces oligodendrogenesis and remyelination chronically after cuprizone-induced demyelination (61). FGF2 is increased for at least a month after SCI (57) and intraspinal injection of FGF2 (62) was shown to improve functional recovery after SCI. GGF has been shown to increase the proliferation of NG2 cells while inhibiting their differentiation *in vitro* (63). Subcutaneous injection of GGF2 increases NG2 cell proliferation, oligodendrogenesis, and functional recovery after SCI (59) as well as increased functional recovery and myelination after experimental autoimmune encephalomyelitis (EAE) (64). Wnts have been shown to play a major role in proliferation of NG2 cells during development (65) and are upregulated after SCI (60). Overexpression of activated β-catenin, a downstream mediator of Wnt signaling, results in developmental hypomyelination and delayed remyelination after demyelination (65). Wnt3A-conditioned media increases proliferation of NG2 cells *in vitro* and deletion of β-catenin in NG2 cells leads to reduced proliferation of NG2 in the glial scar after contusive SCI (66).

Cytokines such as ciliary neurotrophic factor (CNTF), leukemia inhibitory factor (LIF), and tumor necrosis factor (TNF) are also important in the proliferation and differentiation of NG2 cells (67). CNTF and LIF promote oligodendrocyte differentiation *in vitro* (67), however, CNTF knockout (68) and LIF knockout mice (69) only have a developmental delay in oligodendrogenesis, indicating that these factors may be a mediator of oligodendrogenesis early in development. Daily intraperitoneal administration of CNTF increases numbers of NG2 cells, oligodendrocytes, and neurons and improves outcome after EAE (70). Deletion of the transcription factor signal transducer and activator of transcription 3 (STAT3), which is downstream of CNTF, LIF, and several other cytokines, delays oligodendrogenesis without affecting proliferation after SCI (49). Accordingly, overexpression of a constitutively active STAT3 using an adenovirus leads to increased oligodendrocyte differentiation *in vitro* (71). Deletion of suppressor of cytokine signaling 3 (SOCS3), a negative regulator of STAT3, leads to enhanced proliferation of NG2 cells in the glial scar but does not affect their differentiation after SCI, suggesting a non-canonical STAT3/SOCS3 signaling mechanism in NG2 cells after SCI (49). Although the proinflammatory cytokine TNFα is typically associated with oligodendrocyte death, it may have important roles in NG2 cell response to injury and subsequent remyelination. TNFα signaling through TNFR2 is important for NG2 cell proliferation and differentiation after cuprizone-induced demyelination (72). Similarly, genetic deletion of TNFR2 using the CNPase-Cre mouse resulted in impaired functional recovery, reduced number of NG2 cells, and impaired oligodendrocyte differentiation and remyelination after EAE (73). While similar genetic studies have not been performed

after SCI, pharmacological blockade of TNFR1, but not TNFR2, promotes functional recovery SCI (74).

NG2 CELL LINEAGE PLASTICITY AFTER INJURY

Astrogliogenesis

Both NG2 cells and astrocytes are derived from radial glia during development (75, 76). In addition, NG2 cells isolated *in vitro* differentiate into astrocytes as well as oligodendrocytes (77). Thus, while NG2 cells differentiate only into oligodendrocytes in the normal CNS, these observations provide a mechanistic basis for the potential of NG2 cells to differentiate into astrocytes in the injured CNS. The advent of Cre-loxP technology has allowed rigorous testing of NG2 cell lineage plasticity *in vivo*. The NG2-Cre mouse line revealed that, indeed, a population of NG2 cells could differentiate into protoplasmic astrocytes in the ventrolateral forebrain gray matter (78) and spinal cord (79) during development. As mentioned above, Sellers et al. injected Mahoney retrovirus with a reporter driven by the NG2 promoter into the injured spinal cord, and found that 35–54% of reporter-labeled cells were GFAP$^+$ astrocytes (limitations of this technique is discussed above).

Using CreER mice to permanently label a population of NG2 cells prior to injury has led to similar results. The NG2-CreER and PDGFRα-CreER mouse lines both revealed that NG2 cells can only differentiate into oligodendrocytes in the uninjured adult CNS (13, 47, 48). To determine if NG2 cells had lineage plasticity after injury, the Olig2-CreER mice were used in cortical stab injury (41) and dorsal hemisection SCI (10). However, due to the fact that 5% of labeled cells were GFAP$^+$ in the uninjured condition, it was difficult to determine if NG2 cells had astroglial fate. Using the NG2-CreER mice in which astrocytes are not labeled in the uninjured spinal cord, 8% of NG2 cells expressed GFAP at 10 days post cortical stab injury (80). Since the percentage of reporter-labeled cells that co-localized with GFAP decreased to 2% by 30 days after injury and many cells retained NG2 expression, it has been suggested that these NG2 cells transiently express GFAP after injury and that NG2 cell-derived astrocytes are not major contributors to the astroglial scar (80). However, after contusive SCI where inflammation, secondary damage, and astrogliosis is much greater than stab wounds, 25% of reporter-labeled cells in the NG2-CreER mice expressed GFAP at 1 week after SCI and 8% by 4 weeks after injury (49).

Possible mechanisms by which NG2 cells differentiate into astrocytes after SCI could be similar to the mechanisms underlying astrogliogenesis during development. These include the Janus kinase (JAK)/STAT3 (81), bone morphogenetic protein (BMP) (82), and/or Olig2 signaling pathways (83, 84). BMP2 and BMP4 are known to promote astrogliogenesis from NG2 cells *in vitro* (85). Both BMP2 and BMP4 are upregulated after SCI (86), and intraspinal injection of BMP4 leads to increased differentiation of transplanted NG2 progenitors into GFAP$^+$ astrocytes (9). When NG2 cells are treated with conditioned media from reactive astrocytes isolated from injured spinal cords, it reduces their differentiation into O1$^+$ oligodendrocytes and increases their expression of GFAP (87), suggesting that the injured spinal cord could provide a niche for NG2 cell differentiation into astrocytes. Astrocytes isolated from the injured spinal cord have increased expression of BMP2/BMP4 compared to uninjured spinal cord astrocytes and BMP2 is increased in reactive astrocyte conditioned media, suggesting that astrocytes are a major source of BMPs after SCI (87). NG2 cells increase expression of the BMP downstream effector Smad after exposure to reactive astrocyte-conditioned media with an associated decrease in MBP and increase in GFAP expression, which is reversed upon treatment with the BMP inhibitor noggin (87). Together, these data suggest that BMPs may be derived from reactive astrocytes and promote NG2 cell differentiation into astrocytes after contusive SCI.

In addition to BMPs, the JAK-STAT3 signaling pathway could also be important in astrogliogenesis from NG2 cells after CNS injury. The JAK-STAT3 signaling pathway is important for astrocyte differentiation from nestin$^+$ cortical precursor cells and STAT3 binds to the GFAP promoter (81, 88). In addition, developmental astrogliogenesis is impaired in LIF knockout mice and gp130 knockout mice (89, 90). However, neither deletion of STAT3 nor its negative regulator SOCS3 significantly affects NG2 cell differentiation into astrocytes after SCI (49). Overexpression of the oligodendrocyte transcription factor Olig2 reduced astrocyte differentiation from neural stem cells *in vitro* (83) while deletion of Olig2 in developing NG2 cells leads to increased astrocyte production at the expense of oligodendrogenesis and myelination (91). However, genetic deletion of Olig2 does not affect astrogliogenesis from NG2 cells after cortical stab injury (80). Together, these data suggest that NG2 cells might differentiate into astrocytes by a mechanism different from developmental processes.

Differentiation into Schwann Cells

After contusive SCI, there are many Schwann cells at the injury site (92, 93). Since there are no Schwann cells in the normal spinal cord and since the majority of the myelin protein 0 (P0$^+$) myelinating Schwann cells are located in the dorsal column after SCI, it was thought that these Schwann cells had migrated from the dorsal roots. However, genetic lineage tracing revealed that, after focal demyelination in the dorsal column white matter, the majority of Schwann cells were derived from NG2 cells (94). This is also supported by a recent study in which a dorsal rhizotomy did not lead to a significant decrease in Schwann cells at the SCI site, indicating that the peripheral nervous system (PNS) is not a major source of Schwann cells present at the injury site (95). While there is accumulating evidence that NG2 cells can differentiate into Schwann cells after SCI, there are several issues that need to be carefully considered. First, in addition to dorsal roots, the ventral roots as well as nerve fibers on blood vessels may also serve as sources of Schwann cells (96). Second, unlike the ability of NG2 cells to differentiate into astrocytes *in vitro*, there have been no reports of NG2 cells differentiating into Schwann cells *in vitro*. Last, whereas NG2 cells and astrocytes are derived from the neural tube, Schwann cells are derived from the neural crest, thereby making the mechanism by which NG2 cells differentiate into Schwann cells ontogenetically more complex than the mechanism of their differentiation into astrocytes.

CONTRIBUTIONS TO AXON REGENERATION

Increased CSPG expression is widely considered to be a major inhibitory barrier to axon regeneration after CNS injury. Phosphocan, neurocan, versican, and brevican are all upregulated after SCI (97). While reactive astrocytes are considered a major source of CSPGs (98), NG2 cells have also been shown to secrete versican and neurocan *in vitro* (99–101). Unlike other CSPGs, NG2 is typically expressed on the cell membrane rather than as a secreted factor. However, its extracellular domain can be shed from the cell surface *via* cleavage by metalloproteinases (MMPs) (102). Increased expression of NG2 in the glial scar and its ability to inhibit neurite outgrowth *in vitro* indicate that NG2 cells may be major inhibitors of axon regeneration (19). The NG2 proteoglycan leads to inhibition of cerebellar granule neuron neurite outgrowth even after digestion with chrondroitinase ABC (ChABC), indicating that it is not just the glycosaminoglycan (GAG) side chains but also the core proteoglycan that is inhibitory to axon growth (19). Treatment with intraspinal injection of NG2 neutralizing antibody leads to enhanced regeneration of ascending sensory axons after SCI (103), and long-term delivery of NG2 neutralizing antibody through an osmotic pump improves conduction and functional recovery after SCI (104). Together, these studies suggest that NG2 proteoglycan is inhibitory to axon regeneration.

However, the inhibitory properties of NG2 proteoglycan does not necessarily mean that NG2 cells themselves are inhibitory. Despite the increased levels of NG2, several studies have noted that NG2 cells are often associated with regenerating axons, and similar findings have been reported for astrocytes (105–107). Neonatal hippocampal neurites grow better on NG2 cells than on poly-L-lysine and laminin (PLL), even after overexpressing NG2 using an adenovirus (108). In addition, regenerating axons are observed more frequently in areas of the spinal cord that are $NG2^+$ after SCI (39, 109) and may facilitate axon entry into Schwann cell grafts after SCI (110). Also, *cspg4* knockout mice display less serotonergic axons that are able to cross into the lesion (111), as well as increased dieback of sensory axons after SCI (112). In addition, regenerating dorsal root ganglion (DRG) axons associate with NG2-expressing cells after dorsal column crush (112). These data suggest that while NG2 proteoglycan may inhibit axon regeneration, NG2 cells themselves may be permissive to axon growth (108, 112). This is similar to the role of reactive astrocytes where even though their expression of CSPG is inhibitory to axon regeneration, reactive astrocytes themselves may be permissive to, and even necessary for, axon regeneration (105–107). Thus, we must be cautious in classifying

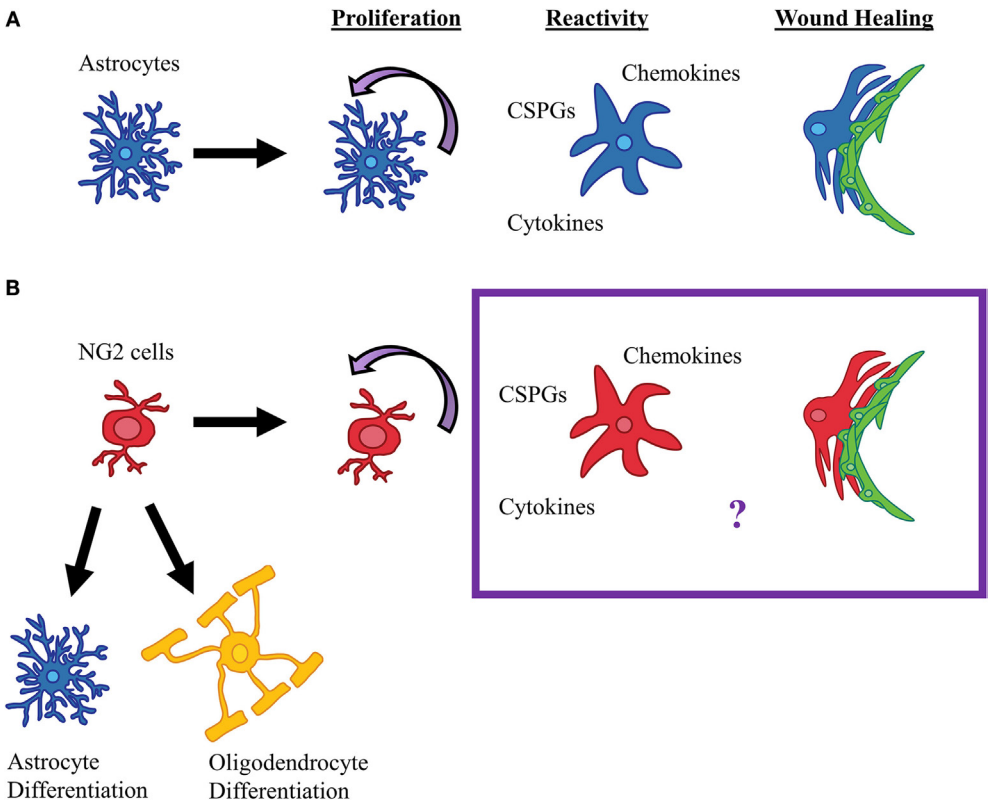

FIGURE 2 | Reactive gliosis after SCI. (A) After SCI in mice and rats, astrocytes proliferate; secrete cytokines, chemokines, and CSPGs; and form glial-fibrotic borders. **(B)** It is known that NG2 cells proliferate, differentiate into oligodendrocytes and astrocytes, and contribute to scar formation after SCI, however, whether NG2 cells contribute to the glial scar by secreting cytokines or contribute to the wound healing process is currently unknown.

cells as inhibitory to axon regeneration based solely on their expression of CSPGs.

While axons may be able to use NG2 cells as a growth-permissive substrate, the fact that regenerating axons can form terminal synaptic contacts with NG2 cells implies that the net effect prevents axonal growth (112–114). The ability of NG2 cells to form synapse with axons has been known for quite some time (115), but its significance in the context of axon regeneration is just beginning to be appreciated. NG2 cells form "synaptic-like" structures with DRG axons *in vitro* (112), and NG2 cells are associated with dystrophic sensory axons (116). Furthermore, there is presynaptic differentiation of injured sensory axons along the CNS/PNS border after dorsal root crush injury (117). Together, these data indicate that NG2 cells may inhibit axon regeneration by both expression of the inhibitory NG2 proteoglycan as well as formation of synaptic contacts.

CONTRIBUTIONS TO INFLAMMATION

Astrocytes contribute to the inflammatory response after CNS injury and attenuating their expression of proinflammatory cytokines and chemokines leads to improved functional outcome (118–123). While astrocytes and microglia have been the focus of neuroinflammatory studies, there is accumulating evidence that NG2 cells may also contribute to the inflammatory response. Genetic deletion of Act1, an activator of NFκB (nuclear factor kappa-light-chain-enhancer of activated B cells) *via* interleukin-17 (IL-17) signaling, in NG2 cells, leads to reduced expression of proinflammatory chemokines, reduced leukocyte infiltration, and improved functional outcome after EAE (124). Upon stimulation *in vitro*, NG2 cells increase expression of multiple proinflammatory chemokines and cytokines as well as MMPs (124, 125). In addition, NG2 cells upregulate IL1β and C-C motif chemokine ligand 2 (CCL2) after cuprizone demyelination (126). Interestingly, deletion of β-catenin in NG2 cells leads to reduced Iba1$^+$ macrophage/microglia density around the lesion after SCI and also reduced astrogliosis, suggesting that NG2 cells may play a role in attracting macrophages after CNS injury (66). Therefore, these studies raise the possibility that NG2 cells may be a major contributor to inflammation after CNS injury, and future studies need to directly address this possibility, especially in the context of SCI.

SUMMARY

The glial scar has been synonymous with reactive astrocytes, but there is substantial evidence indicating that NG2 cells are also a major part of the glial scar, both physically and functionally. Similar to astrocytes, NG2 cells react to SCI by proliferating, becoming hypertrophic, and upregulating CSPG expression (**Figure 2**). However, unlike astrocytes, NG2 cells can differentiate into other cell types, namely oligodendrocytes, astrocytes, and perhaps even Schwann cells. This lineage plasticity of NG2 cells raise the possibility that they can be targeted to promote endogenous repair of the injured spinal cord. Most NG2 cells remain undifferentiated in the glial scar region, and these NG2 cells contribute to axon regeneration failure by expressing CSPGs and forming synaptic structures that prevent further axonal growth. Similar to astrocytes, NG2 cells may also contribute to neuroinflammation, which remains an area that has been underappreciated in the field (**Figure 2**). Therefore, NG2 cells share similarities and differences with astrocytes as a part of the glial scar, which present novel mechanisms that may be targeted to promote repair after SCI.

AUTHOR CONTRIBUTIONS

AH and JL selected the content and wrote the manuscript.

ACKNOWLEDGMENTS

We thank Wolfgang Pita-Thomas for helpful comments.

FUNDING

This study was funded by NINDS R01NS081040, R21NS082835, U.S. Army W81XWH131007715, The Miami Project to Cure Paralysis, and the Buoniconti Fund. AH was funded by the Lois Pope LIFE Fellows Program.

REFERENCES

1. Crowe MJ, Bresnahan JC, Shuman SL, Masters JN, Beattie MS. Apoptosis and delayed degeneration after spinal cord injury in rats and monkeys. *Nat Med* (1997) 3:73–6. doi:10.1038/nm0197-73
2. McTigue DM, Wei P, Stokes BT. Proliferation of NG2-positive cells and altered oligodendrocyte numbers in the contused rat spinal cord. *J Neurosci* (2001) 21:3392–400.
3. Bunge RP, Puckett WR, Becerra JL, Marcillo A, Quencer RM. Observations on the pathology of human spinal cord injury. A review and classification of 22 new cases with details from a case of chronic cord compression with extensive focal demyelination. *Adv Neurol* (1993) 59:75–89.
4. Cao Q, Zhang YP, Iannotti C, Devries WH, Xu XM, Shields CB, et al. Functional and electrophysiological changes after graded traumatic spinal cord injury in adult rat. *Exp Neurol* (2005) 191(Suppl 1):S3–16. doi:10.1016/j.expneurol.2004.08.026
5. Guest JD, Hiester ED, Bunge RP. Demyelination and Schwann cell responses adjacent to injury epicenter cavities following chronic human spinal cord injury. *Exp Neurol* (2005) 192:384–93. doi:10.1016/j.expneurol.2004.11.033
6. Totoiu MO, Keirstead HS. Spinal cord injury is accompanied by chronic progressive demyelination. *J Comp Neurol* (2005) 486:373–83. doi:10.1002/cne.20517
7. Zai LJ, Wrathall JR. Cell proliferation and replacement following contusive spinal cord injury. *Glia* (2005) 50:247–57. doi:10.1002/glia.20176
8. Tripathi R, McTigue DM. Prominent oligodendrocyte genesis along the border of spinal contusion lesions. *Glia* (2007) 55:698–711. doi:10.1002/glia.20491
9. Sellers DL, Maris DO, Horner PJ. Postinjury niches induce temporal shifts in progenitor fates to direct lesion repair after spinal cord injury. *J Neurosci* (2009) 29:6722–33. doi:10.1523/JNEUROSCI.4538-08.2009
10. Barnabe-Heider F, Goritz C, Sabelstrom H, Takebayashi H, Pfrieger FW, Meletis K, et al. Origin of new glial cells in intact and injured adult spinal cord. *Cell Stem Cell* (2010) 7:470–82. doi:10.1016/j.stem.2010.07.014
11. Powers BE, Sellers DL, Lovelett EA, Cheung W, Aalami SP, Zapertov N, et al. Remyelination reporter reveals prolonged refinement of spontaneously

regenerated myelin. *Proc Natl Acad Sci U S A* (2013) 110:4075–80. doi:10.1073/pnas.1210293110
12. Crawford AH, Tripathi RB, Foerster S, Mckenzie I, Kougioumtzidou E, Grist M, et al. Pre-existing mature oligodendrocytes do not contribute to remyelination following toxin-induced spinal cord demyelination. *Am J Pathol* (2016) 186(3):511–6. doi:10.1016/j.ajpath.2015.11.005
13. Rivers LE, Young KM, Rizzi M, Jamen F, Psachoulia K, Wade A, et al. PDGFRA/NG2 glia generate myelinating oligodendrocytes and piriform projection neurons in adult mice. *Nat Neurosci* (2008) 11:1392–401. doi:10.1038/nn.2220
14. Lytle JM, Wrathall JR. Glial cell loss, proliferation and replacement in the contused murine spinal cord. *Eur J Neurosci* (2007) 25:1711–24. doi:10.1111/j.1460-9568.2007.05390.x
15. Almad A, Sahinkaya FR, Mctigue DM. Oligodendrocyte fate after spinal cord injury. *Neurotherapeutics* (2011) 8:262–73. doi:10.1007/s13311-011-0033-5
16. Miron VE, Kuhlmann T, Antel JP. Cells of the oligodendroglial lineage, myelination, and remyelination. *Biochim Biophys Acta* (2011) 1812:184–93. doi:10.1016/j.bbadis.2010.09.010
17. Franklin RJ, Goldman SA. Glia disease and repair-remyelination. *Cold Spring Harb Perspect Biol* (2015) 7:a020594. doi:10.1101/cshperspect.a020594
18. Levine JM. Increased expression of the NG2 chondroitin-sulfate proteoglycan after brain injury. *J Neurosci* (1994) 14:4716–30.
19. Dou CL, Levine JM. Inhibition of neurite growth by the NG2 chondroitin sulfate proteoglycan. *J Neurosci* (1994) 14:7616–28.
20. Faulkner JR, Herrmann JE, Woo MJ, Tansey KE, Doan NB, Sofroniew MV. Reactive astrocytes protect tissue and preserve function after spinal cord injury. *J Neurosci* (2004) 24:2143–55. doi:10.1523/JNEUROSCI.3547-03.2004
21. Wanner IB, Anderson MA, Song B, Levine J, Fernandez A, Gray-Thompson Z, et al. Glial scar borders are formed by newly proliferated, elongated astrocytes that interact to corral inflammatory and fibrotic cells via STAT3-dependent mechanisms after spinal cord injury. *J Neurosci* (2013) 33:12870–86. doi:10.1523/JNEUROSCI.2121-13.2013
22. Brambilla R, Bracchi-Ricard V, Hu WH, Frydel B, Bramwell A, Karmally S, et al. Inhibition of astroglial nuclear factor kappaB reduces inflammation and improves functional recovery after spinal cord injury. *J Exp Med* (2005) 202:145–56. doi:10.1084/jem.20041918
23. Pineau I, Sun L, Bastien D, Lacroix S. Astrocytes initiate inflammation in the injured mouse spinal cord by promoting the entry of neutrophils and inflammatory monocytes in an IL-1 receptor/MyD88-dependent fashion. *Brain Behav Immun* (2010) 24:540–53. doi:10.1016/j.bbi.2009.11.007
24. Rhodes KE, Raivich G, Fawcett JW. The injury response of oligodendrocyte precursor cells is induced by platelets, macrophages and inflammation-associated cytokines. *Neuroscience* (2006) 140:87–100. doi:10.1016/j.neuroscience.2006.01.055
25. Sahinkaya FR, Milich LM, Mctigue DM. Changes in NG2 cells and oligodendrocytes in a new model of intraspinal hemorrhage. *Exp Neurol* (2014) 255:113–26. doi:10.1016/j.expneurol.2014.02.025
26. Silver J, Schwab ME, Popovich PG. Central nervous system regenerative failure: role of oligodendrocytes, astrocytes, and microglia. *Cold Spring Harb Perspect Biol* (2014) 7:a020602. doi:10.1101/cshperspect.a020602
27. Hughes EG, Kang SH, Fukaya M, Bergles DE. Oligodendrocyte progenitors balance growth with self-repulsion to achieve homeostasis in the adult brain. *Nat Neurosci* (2013) 16:668–76. doi:10.1038/nn.3390
28. Silver J, Miller JH. Regeneration beyond the glial scar. *Nat Rev Neurosci* (2004) 5:146–56. doi:10.1038/nrn1326
29. Cregg JM, Depaul MA, Filous AR, Lang BT, Tran A, Silver J. Functional regeneration beyond the glial scar. *Exp Neurol* (2014) 253:197–207. doi:10.1016/j.expneurol.2013.12.024
30. Evans TA, Barkauskas DS, Myers JT, Hare EG, You JQ, Ransohoff RM, et al. High-resolution intravital imaging reveals that blood-derived macrophages but not resident microglia facilitate secondary axonal dieback in traumatic spinal cord injury. *Exp Neurol* (2014) 254:109–20. doi:10.1016/j.expneurol.2014.01.013
31. Zhu Y, Soderblom C, Krishnan V, Ashbaugh J, Bethea JR, Lee JK. Hematogenous macrophage depletion reduces the fibrotic scar and increases axonal growth after spinal cord injury. *Neurobiol Dis* (2015) 74:114–25. doi:10.1016/j.nbd.2014.10.024
32. Goritz C, Dias DO, Tomilin N, Barbacid M, Shupliakov O, Frisen J. A pericyte origin of spinal cord scar tissue. *Science* (2011) 333:238–42. doi:10.1126/science.1203165
33. Soderblom C, Luo X, Blumenthal E, Bray E, Lyapichev K, Ramos J, et al. Perivascular fibroblasts form the fibrotic scar after contusive spinal cord injury. *J Neurosci* (2013) 33:13882–7. doi:10.1523/JNEUROSCI.2524-13.2013
34. Buss A, Pech K, Kakulas BA, Martin D, Schoenen J, Noth J, et al. NG2 and phosphacan are present in the astroglial scar after human traumatic spinal cord injury. *BMC Neurol* (2009) 9:32. doi:10.1186/1471-2377-9-32
35. Levine JM, Stallcup WB. Plasticity of developing cerebellar cells in vitro studied with antibodies against the NG2 antigen. *J Neurosci* (1987) 7:2721–31.
36. Stallcup WB, Beasley L. Bipotential glial precursor cells of the optic nerve express the NG2 proteoglycan. *J Neurosci* (1987) 7:2737–44.
37. Nishiyama A, Lin XH, Giese N, Heldin CH, Stallcup WB. Co-localization of NG2 proteoglycan and PDGF alpha-receptor on O2A progenitor cells in the developing rat brain. *J Neurosci Res* (1996) 43:299–314. doi:10.1002/(SICI)1097-4547(19960201)43:3<299::AID-JNR5>3.0.CO;2-E
38. Jones LL, Yamaguchi Y, Stallcup WB, Tuszynski MH. NG2 is a major chondroitin sulfate proteoglycan produced after spinal cord injury and is expressed by macrophages and oligodendrocyte progenitors. *J Neurosci* (2002) 22:2792–803.
39. McTigue DM, Tripathi R, Wei P. NG2 colocalizes with axons and is expressed by a mixed cell population in spinal cord lesions. *J Neuropathol Exp Neurol* (2006) 65:406–20. doi:10.1097/01.jnen.0000218447.32320.52
40. Levine J. The reactions and role of NG2 glia in spinal cord injury. *Brain Res* (2015) 1638(Pt B):199–208. doi:10.1016/j.brainres.2015.07.026
41. Dimou L, Simon C, Kirchhoff F, Takebayashi H, Gotz M. Progeny of Olig2-expressing progenitors in the gray and white matter of the adult mouse cerebral cortex. *J Neurosci* (2008) 28:10434–42. doi:10.1523/JNEUROSCI.2831-08.2008
42. Buffo A, Vosko MR, Erturk D, Hamann GF, Jucker M, Rowitch D, et al. Expression pattern of the transcription factor Olig2 in response to brain injuries: implications for neuronal repair. *Proc Natl Acad Sci U S A* (2005) 102:18183–8. doi:10.1073/pnas.0506535102
43. Lytle JM, Chittajallu R, Wrathall JR, Gallo V. NG2 cell response in the CNP-EGFP mouse after contusive spinal cord injury. *Glia* (2009) 57:270–85. doi:10.1002/glia.20755
44. Bu J, Akhtar N, Nishiyama A. Transient expression of the NG2 proteoglycan by a subpopulation of activated macrophages in an excitotoxic hippocampal lesion. *Glia* (2001) 34:296–310. doi:10.1002/glia.1063
45. Zhang SC. Defining glial cells during CNS development. *Nat Rev Neurosci* (2001) 2:840–3. doi:10.1038/35097593
46. Pozniak CD, Langseth AJ, Dijkgraaf GJ, Choe Y, Werb Z, Pleasure SJ. Sox10 directs neural stem cells toward the oligodendrocyte lineage by decreasing suppressor of fused expression. *Proc Natl Acad Sci U S A* (2010) 107:21795–800. doi:10.1073/pnas.1016485107
47. Kang SH, Fukaya M, Yang JK, Rothstein JD, Bergles DE. NG2+ CNS glial progenitors remain committed to the oligodendrocyte lineage in postnatal life and following neurodegeneration. *Neuron* (2010) 68:668–81. doi:10.1016/j.neuron.2010.09.009
48. Zhu X, Hill RA, Dietrich D, Komitova M, Suzuki R, Nishiyama A. Age-dependent fate and lineage restriction of single NG2 cells. *Development* (2011) 138:745–53. doi:10.1242/dev.047951
49. Hackett AR, Lee DH, Dawood A, Rodriguez M, Funk L, Tsoulfas P, et al. STAT3 and SOCS3 regulate NG2 cell proliferation and differentiation after contusive spinal cord injury. *Neurobiol Dis* (2016) 89:10–22. doi:10.1016/j.nbd.2016.01.017
50. Honsa P, Pivonkova H, Dzamba D, Filipova M, Anderova M. Polydendrocytes display large lineage plasticity following focal cerebral ischemia. *PLoS One* (2012) 7:e36816. doi:10.1371/journal.pone.0036816
51. Tatsumi K, Takebayashi H, Manabe T, Tanaka KF, Makinodan M, Yamauchi T, et al. Genetic fate mapping of Olig2 progenitors in the injured adult cerebral cortex reveals preferential differentiation into astrocytes. *J Neurosci Res* (2008) 86:3494–502. doi:10.1002/jnr.21862
52. Birey F, Aguirre A. Age-dependent netrin-1 signaling regulates NG2+ glial cell spatial homeostasis in normal adult gray matter. *J Neurosci* (2015) 35:6946–51. doi:10.1523/JNEUROSCI.0356-15.2015

53. Keirstead HS, Levine JM, Blakemore WF. Response of the oligodendrocyte progenitor cell population (defined by NG2 labelling) to demyelination of the adult spinal cord. *Glia* (1998) 22:161–70. doi:10.1002/(SICI)1098-1136(199802)22:2<161::AID-GLIA7>3.0.CO;2-A
54. Hill RA, Patel KD, Goncalves CM, Grutzendler J, Nishiyama A. Modulation of oligodendrocyte generation during a critical temporal window after NG2 cell division. *Nat Neurosci* (2014) 17:1518–27. doi:10.1038/nn.3815
55. Gibson EM, Purger D, Mount CW, Goldstein AK, Lin GL, Wood LS, et al. Neuronal activity promotes oligodendrogenesis and adaptive myelination in the mammalian brain. *Science* (2014) 344:1252304. doi:10.1126/science.1252304
56. Wolswijk G, Noble M. Cooperation between PDGF and FGF converts slowly dividing O-2Aadult progenitor cells to rapidly dividing cells with characteristics of O-2Aperinatal progenitor cells. *J Cell Biol* (1992) 118:889–900. doi:10.1083/jcb.118.4.889
57. Tripathi RB, McTigue DM. Chronically increased ciliary neurotrophic factor and fibroblast growth factor-2 expression after spinal contusion in rats. *J Comp Neurol* (2008) 510:129–44. doi:10.1002/cne.21787
58. Zai LJ, Yoo S, Wrathall JR. Increased growth factor expression and cell proliferation after contusive spinal cord injury. *Brain Res* (2005) 1052:147–55. doi:10.1016/j.brainres.2005.05.071
59. Whittaker MT, Zai LJ, Lee HJ, Pajoohesh-Ganji A, Wu J, Sharp A, et al. GGF2 (Nrg1-beta3) treatment enhances NG2+ cell response and improves functional recovery after spinal cord injury. *Glia* (2012) 60:281–94. doi:10.1002/glia.21262
60. Fernandez-Martos CM, Gonzalez-Fernandez C, Gonzalez P, Maqueda A, Arenas E, Rodriguez FJ. Differential expression of Wnts after spinal cord contusion injury in adult rats. *PLoS One* (2011) 6:e27000. doi:10.1371/journal.pone.0027000
61. Furusho M, Roulois AJ, Franklin RJ, Bansal R. Fibroblast growth factor signaling in oligodendrocyte-lineage cells facilitates recovery of chronically demyelinated lesions but is redundant in acute lesions. *Glia* (2015) 63:1714–28. doi:10.1002/glia.22838
62. Kasai M, Jikoh T, Fukumitsu H, Furukawa S. FGF-2-responsive and spinal cord-resident cells improve locomotor function after spinal cord injury. *J Neurotrauma* (2014) 31:1584–98. doi:10.1089/neu.2009.1108
63. Canoll PD, Musacchio JM, Hardy R, Reynolds R, Marchionni MA, Salzer JL. GGF/neuregulin is a neuronal signal that promotes the proliferation and survival and inhibits the differentiation of oligodendrocyte progenitors. *Neuron* (1996) 17:229–43. doi:10.1016/S0896-6273(00)80155-5
64. Cannella B, Hoban CJ, Gao YL, Garcia-Arenas R, Lawson D, Marchionni M, et al. The neuregulin, glial growth factor 2, diminishes autoimmune demyelination and enhances remyelination in a chronic relapsing model for multiple sclerosis. *Proc Natl Acad Sci U S A* (1998) 95:10100–5. doi:10.1073/pnas.95.17.10100
65. Fancy SP, Baranzini SE, Zhao C, Yuk DI, Irvine KA, Kaing S, et al. Dysregulation of the Wnt pathway inhibits timely myelination and remyelination in the mammalian CNS. *Genes Dev* (2009) 23:1571–85. doi:10.1101/gad.1806309
66. Rodriguez JP, Coulter M, Miotke J, Meyer RL, Takemaru K, Levine JM. Abrogation of beta-catenin signaling in oligodendrocyte precursor cells reduces glial scarring and promotes axon regeneration after CNS injury. *J Neurosci* (2014) 34:10285–97. doi:10.1523/JNEUROSCI.4915-13.2014
67. Mayer M, Bhakoo K, Noble M. Ciliary neurotrophic factor and leukemia inhibitory factor promote the generation, maturation and survival of oligodendrocytes in vitro. *Development* (1994) 120:143–53.
68. Barres BA, Burne JF, Holtmann B, Thoenen H, Sendtner M, Raff MC. Ciliary neurotrophic factor enhances the rate of oligodendrocyte generation. *Mol Cell Neurosci* (1996) 8:146–56. doi:10.1006/mcne.1996.0053
69. Ishibashi T, Lee PR, Baba H, Fields RD. Leukemia inhibitory factor regulates the timing of oligodendrocyte development and myelination in the postnatal optic nerve. *J Neurosci Res* (2009) 87:3343–55. doi:10.1002/jnr.22173
70. Kuhlmann T, Remington L, Cognet I, Bourbonniere L, Zehntner S, Guilhot F, et al. Continued administration of ciliary neurotrophic factor protects mice from inflammatory pathology in experimental autoimmune encephalomyelitis. *Am J Pathol* (2006) 169:584–98. doi:10.2353/ajpath.2006.051086
71. Steelman AJ, Zhou Y, Koito H, Kim S, Payne HR, Lu QR, et al. Activation of oligodendroglial Stat3 is required for efficient remyelination. *Neurobiol Dis* (2016) 91:336–46. doi:10.1016/j.nbd.2016.03.023
72. Arnett HA, Mason J, Marino M, Suzuki K, Matsushima GK, Ting JP. TNF alpha promotes proliferation of oligodendrocyte progenitors and remyelination. *Nat Neurosci* (2001) 4:1116–22. doi:10.1038/nn738
73. Madsen PM, Motti D, Karmally S, Szymkowski DE, Lambertsen KL, Bethea JR, et al. Oligodendroglial TNFR2 mediates membrane TNF-dependent repair in experimental autoimmune encephalomyelitis by promoting oligodendrocyte differentiation and remyelination. *J Neurosci* (2016) 36:5128–43. doi:10.1523/JNEUROSCI.0211-16.2016
74. Novrup HG, Bracchi-Ricard V, Ellman DG, Ricard J, Jain A, Runko E, et al. Central but not systemic administration of XPro1595 is therapeutic following moderate spinal cord injury in mice. *J Neuroinflammation* (2014) 11:159. doi:10.1186/s12974-014-0159-6
75. Molofsky AV, Deneen B. Astrocyte development: a guide for the perplexed. *Glia* (2015) 63:1320–9. doi:10.1002/glia.22836
76. Bergles DE, Richardson WD. Oligodendrocyte development and plasticity. *Cold Spring Harb Perspect Biol* (2016) 8:a020453. doi:10.1101/cshperspect.a020453
77. Raff MC, Miller RH, Noble M. A glial progenitor cell that develops in vitro into an astrocyte or an oligodendrocyte depending on culture medium. *Nature* (1983) 303:390–6. doi:10.1038/303390a0
78. Zhu X, Bergles DE, Nishiyama A. NG2 cells generate both oligodendrocytes and gray matter astrocytes. *Development* (2008) 135:145–57. doi:10.1242/dev.004895
79. Zhu X, Hill RA, Nishiyama A. NG2 cells generate oligodendrocytes and gray matter astrocytes in the spinal cord. *Neuron Glia Biol* (2008) 4:19–26. doi:10.1017/S1740925X09000015
80. Komitova M, Serwanski DR, Lu QR, Nishiyama A. NG2 cells are not a major source of reactive astrocytes after neocortical stab wound injury. *Glia* (2011) 59:800–9. doi:10.1002/glia.21152
81. Bonni A, Sun Y, Nadal-Vicens M, Bhatt A, Frank DA, Rozovsky I, et al. Regulation of gliogenesis in the central nervous system by the JAK-STAT signaling pathway. *Science* (1997) 278:477–83. doi:10.1126/science.278.5337.477
82. Rajan P, McKay RD. Multiple routes to astrocytic differentiation in the CNS. *J Neurosci* (1998) 18:3620–9.
83. Fukuda S, Kondo T, Takebayashi H, Taga T. Negative regulatory effect of an oligodendrocytic bHLH factor OLIG2 on the astrocytic differentiation pathway. *Cell Death Differ* (2004) 11:196–202. doi:10.1038/sj.cdd.4401332
84. Setoguchi T, Kondo T. Nuclear export of OLIG2 in neural stem cells is essential for ciliary neurotrophic factor-induced astrocyte differentiation. *J Cell Biol* (2004) 166:963–8. doi:10.1083/jcb.200404104
85. Mabie PC, Mehler MF, Marmur R, Papavasiliou A, Song Q, Kessler JA. Bone morphogenetic proteins induce astroglial differentiation of oligodendroglial-astroglial progenitor cells. *J Neurosci* (1997) 17:4112–20.
86. Hampton DW, Asher RA, Kondo T, Steeves JD, Ramer MS, Fawcett JW. A potential role for bone morphogenetic protein signalling in glial cell fate determination following adult central nervous system injury in vivo. *Eur J Neurosci* (2007) 26:3024–35. doi:10.1111/j.1460-9568.2007.05940.x
87. Wang Y, Cheng X, He Q, Zheng Y, Kim DH, Whittemore SR, et al. Astrocytes from the contused spinal cord inhibit oligodendrocyte differentiation of adult oligodendrocyte precursor cells by increasing the expression of bone morphogenetic proteins. *J Neurosci* (2011) 31:6053–8. doi:10.1523/JNEUROSCI.5524-09.2011
88. Nakashima K, Yanagisawa M, Arakawa H, Kimura N, Hisatsune T, Kawabata M, et al. Synergistic signaling in fetal brain by STAT3-Smad1 complex bridged by p300. *Science* (1999) 284:479–82.
89. Bugga L, Gadient RA, Kwan K, Stewart CL, Patterson PH. Analysis of neuronal and glial phenotypes in brains of mice deficient in leukemia inhibitory factor. *J Neurobiol* (1998) 36:509–24.
90. Nakashima K, Wiese S, Yanagisawa M, Arakawa H, Kimura N, Hisatsune T, et al. Developmental requirement of gp130 signaling in neuronal survival and astrocyte differentiation. *J Neurosci* (1999) 19:5429–34.
91. Zhu X, Zuo H, Maher BJ, Serwanski DR, Loturco JJ, Lu QR, et al. Olig2-dependent developmental fate switch of NG2 cells. *Development* (2012) 139:2299–307. doi:10.1242/dev.078873

92. Bresnahan JC. An electron-microscopic analysis of axonal alterations following blunt contusion of the spinal cord of the rhesus monkey (*Macaca mulatta*). *J Neurol Sci* (1978) 37:59–82. doi:10.1016/0022-510X(78)90228-9
93. Bunge MB, Holets VR, Bates ML, Clarke TS, Watson BD. Characterization of photochemically induced spinal cord injury in the rat by light and electron microscopy. *Exp Neurol* (1994) 127:76–93. doi:10.1006/exnr.1994.1082
94. Zawadzka M, Rivers LE, Fancy SP, Zhao C, Tripathi R, Jamen F, et al. CNS-resident glial progenitor/stem cells produce Schwann cells as well as oligodendrocytes during repair of CNS demyelination. *Cell Stem Cell* (2010) 6:578–90. doi:10.1016/j.stem.2010.04.002
95. Bartus K, Galino J, James ND, Hernandez-Miranda LR, Dawes JM, Fricker FR, et al. Neuregulin-1 controls an endogenous repair mechanism after spinal cord injury. *Brain* (2016) 139(Pt 5):1394–416. doi:10.1093/brain/aww039
96. Doucette R. PNS-CNS transitional zone of the first cranial nerve. *J Comp Neurol* (1991) 312:451–66. doi:10.1002/cne.903120311
97. Jones LL, Margolis RU, Tuszynski MH. The chondroitin sulfate proteoglycans neurocan, brevican, phosphacan, and versican are differentially regulated following spinal cord injury. *Exp Neurol* (2003) 182:399–411. doi:10.1016/S0014-4886(03)00087-6
98. McKeon RJ, Jurynec MJ, Buck CR. The chondroitin sulfate proteoglycans neurocan and phosphacan are expressed by reactive astrocytes in the chronic CNS glial scar. *J Neurosci* (1999) 19:10778–88.
99. Asher RA, Morgenstern DA, Fidler PS, Adcock KH, Oohira A, Braistead JE, et al. Neurocan is upregulated in injured brain and in cytokine-treated astrocytes. *J Neurosci* (2000) 20:2427–38.
100. Asher RA, Morgenstern DA, Shearer MC, Adcock KH, Pesheva P, Fawcett JW. Versican is upregulated in CNS injury and is a product of oligodendrocyte lineage cells. *J Neurosci* (2002) 22:2225–36.
101. Crespo D, Asher RA, Lin R, Rhodes KE, Fawcett JW. How does chondroitinase promote functional recovery in the damaged CNS? *Exp Neurol* (2007) 206:159–71. doi:10.1016/j.expneurol.2007.05.001
102. Asher RA, Morgenstern DA, Properzi F, Nishiyama A, Levine JM, Fawcett JW. Two separate metalloproteinase activities are responsible for the shedding and processing of the NG2 proteoglycan in vitro. *Mol Cell Neurosci* (2005) 29:82–96. doi:10.1016/j.mcn.2005.02.001
103. Tan AM, Colletti M, Rorai AT, Skene JH, Levine JM. Antibodies against the NG2 proteoglycan promote the regeneration of sensory axons within the dorsal columns of the spinal cord. *J Neurosci* (2006) 26:4729–39. doi:10.1523/JNEUROSCI.3900-05.2006
104. Petrosyan HA, Hunanyan AS, Alessi V, Schnell L, Levine J, Arvanian VL. Neutralization of inhibitory molecule NG2 improves synaptic transmission, retrograde transport, and locomotor function after spinal cord injury in adult rats. *J Neurosci* (2013) 33:4032–43. doi:10.1523/JNEUROSCI.4702-12.2013
105. Lee JK, Chow R, Xie F, Chow SY, Tolentino KE, Zheng B. Combined genetic attenuation of myelin and semaphorin-mediated growth inhibition is insufficient to promote serotonergic axon regeneration. *J Neurosci* (2010) 30:10899–904. doi:10.1523/JNEUROSCI.2269-10.2010
106. Zukor K, Belin S, Wang C, Keelan N, Wang X, He Z. Short hairpin RNA against PTEN enhances regenerative growth of corticospinal tract axons after spinal cord injury. *J Neurosci* (2013) 33:15350–61. doi:10.1523/JNEUROSCI.2510-13.2013
107. Anderson MA, Burda JE, Ren Y, Ao Y, O'shea TM, Kawaguchi R, et al. Astrocyte scar formation aids central nervous system axon regeneration. *Nature* (2016) 532:195–200. doi:10.1038/nature17623
108. Yang Z, Suzuki R, Daniels SB, Brunquell CB, Sala CJ, Nishiyama A. NG2 glial cells provide a favorable substrate for growing axons. *J Neurosci* (2006) 26:3829–39. doi:10.1523/JNEUROSCI.4247-05.2006
109. Jones LL, Sajed D, Tuszynski MH. Axonal regeneration through regions of chondroitin sulfate proteoglycan deposition after spinal cord injury: a balance of permissiveness and inhibition. *J Neurosci* (2003) 23:9276–88.
110. Williams RR, Henao M, Pearse DD, Bunge MB. Permissive Schwann cell graft/spinal cord interfaces for axon regeneration. *Cell Transplant* (2015) 24:115–31. doi:10.3727/096368913X674657
111. de Castro R Jr, Tajrishi R, Claros J, Stallcup WB. Differential responses of spinal axons to transection: influence of the NG2 proteoglycan. *Exp Neurol* (2005) 192:299–309. doi:10.1016/j.expneurol.2004.11.027
112. Filous AR, Tran A, Howell CJ, Busch SA, Evans TA, Stallcup WB, et al. Entrapment via synaptic-like connections between NG2 proteoglycan+ cells and dystrophic axons in the lesion plays a role in regeneration failure after spinal cord injury. *J Neurosci* (2014) 34:16369–84. doi:10.1523/JNEUROSCI.1309-14.2014
113. Han SB, Kim H, Skuba A, Tessler A, Ferguson T, Son YJ. Sensory axon regeneration: a review from an in vivo imaging perspective. *Exp Neurobiol* (2012) 21:83–93. doi:10.5607/en.2012.21.3.83
114. Son YJ. Synapsing with NG2 cells (polydendrocytes), unappreciated barrier to axon regeneration? *Neural Regen Res* (2015) 10:346–8. doi:10.4103/1673-5374.153672
115. Bergles DE, Roberts JD, Somogyi P, Jahr CE. Glutamatergic synapses on oligodendrocyte precursor cells in the hippocampus. *Nature* (2000) 405:187–91. doi:10.1038/35012083
116. Busch SA, Horn KP, Cuascut FX, Hawthorne AL, Bai L, Miller RH, et al. Adult NG2+ cells are permissive to neurite outgrowth and stabilize sensory axons during macrophage-induced axonal dieback after spinal cord injury. *J Neurosci* (2010) 30:255–65. doi:10.1523/JNEUROSCI.3705-09.2010
117. Di Maio A, Skuba A, Himes BT, Bhagat SL, Hyun JK, Tessler A, et al. In vivo imaging of dorsal root regeneration: rapid immobilization and presynaptic differentiation at the CNS/PNS border. *J Neurosci* (2011) 31:4569–82. doi:10.1523/JNEUROSCI.4638-10.2011
118. Lau LT, Yu AC. Astrocytes produce and release interleukin-1, interleukin-6, tumor necrosis factor alpha and interferon-gamma following traumatic and metabolic injury. *J Neurotrauma* (2001) 18:351–9. doi:10.1089/08977150151071035
119. Brambilla R, Persaud T, Hu X, Karmally S, Shestopalov VI, Dvoriantchikova G, et al. Transgenic inhibition of astroglial NF-kappa B improves functional outcome in experimental autoimmune encephalomyelitis by suppressing chronic central nervous system inflammation. *J Immunol* (2009) 182:2628–40. doi:10.4049/jimmunol.0802954
120. Brambilla R, Morton PD, Ashbaugh JJ, Karmally S, Lambertsen KL, Bethea JR. Astrocytes play a key role in EAE pathophysiology by orchestrating in the CNS the inflammatory response of resident and peripheral immune cells and by suppressing remyelination. *Glia* (2014) 62:452–67. doi:10.1002/glia.22616
121. Choi SS, Lee HJ, Lim I, Satoh J, Kim SU. Human astrocytes: secretome profiles of cytokines and chemokines. *PLoS One* (2014) 9:e92325. doi:10.1371/journal.pone.0092325
122. Kim RY, Hoffman AS, Itoh N, Ao Y, Spence R, Sofroniew MV, et al. Astrocyte CCL2 sustains immune cell infiltration in chronic experimental autoimmune encephalomyelitis. *J Neuroimmunol* (2014) 274:53–61. doi:10.1016/j.jneuroim.2014.06.009
123. Mills Ko E, Ma JH, Guo F, Miers L, Lee E, Bannerman P, et al. Deletion of astroglial CXCL10 delays clinical onset but does not affect progressive axon loss in a murine autoimmune multiple sclerosis model. *J Neuroinflammation* (2014) 11:105. doi:10.1186/1742-2094-11-105
124. Kang Z, Wang C, Zepp J, Wu L, Sun K, Zhao J, et al. Act1 mediates IL-17-induced EAE pathogenesis selectively in NG2+ glial cells. *Nat Neurosci* (2013) 16:1401–8. doi:10.1038/nn.3505
125. Tirotta E, Ransohoff RM, Lane TE. CXCR2 signaling protects oligodendrocyte progenitor cells from IFN-gamma/CXCL10-mediated apoptosis. *Glia* (2011) 59:1518–28. doi:10.1002/glia.21195
126. Moyon S, Dubessy AL, Aigrot MS, Trotter M, Huang JK, Dauphinot L, et al. Demyelination causes adult CNS progenitors to revert to an immature state and express immune cues that support their migration. *J Neurosci* (2015) 35:4–20. doi:10.1523/JNEUROSCI.0849-14.2015

Conflict of Interest Statement: The authors declare that the research was conducted in the absence of any commercial or financial relationships that could be construed as a potential conflict of interest.

frontiers in Neurology

PERSPECTIVE
published: 23 August 2016
doi: 10.3389/fneur.2016.00135

New Treatments for Spinal Nerve Root Avulsion Injury

*Thomas Carlstedt**

Wolfson CARD, Kings College London, London, UK

Further progress in the treatment of the longitudinal spinal cord injury has been made. In an inverted translational study, it has been demonstrated that return of sensory function can be achieved by bypassing the avulsed dorsal root ganglion neurons. Dendritic growth from spinal cord sensory neurons could replace dorsal root ganglion axons and re-establish a reflex arch. Another research avenue has led to the development of adjuvant therapy for regeneration following dorsal root to spinal cord implantation in root avulsion injury. A small, lipophilic molecule that can be given orally acts on the retinoic acid receptor system as an agonist. Upregulation of dorsal root ganglion regenerative ability and organization of glia reaction to injury were demonstrated in treated animals. The dual effect of this substance may open new avenues for the treatment of root avulsion and spinal cord injuries.

Keywords: nerve plexus, root avulsion, neurotization, adjuvant therapy, sensory recovery, spinal cord regeneration

OPEN ACCESS

Edited by:
Michael G. Fehlings,
University of Toronto, Canada

Reviewed by:
Åsa Fex-Svenningsen,
University of Southern Denmark, Denmark
Peter John Shortland,
Western Sydney University, Australia

***Correspondence:**
Thomas Carlstedt
carlstedt.thomas@googlemail.com

Specialty section:
This article was submitted to Neurotrauma, a section of the journal Frontiers in Neurology

Received: *25 May 2016*
Accepted: *05 August 2016*
Published: *23 August 2016*

Citation:
Carlstedt T (2016) New Treatments for Spinal Nerve Root Avulsion Injury. Front. Neurol. 7:135. doi: 10.3389/fneur.2016.00135

INTRODUCTION

In a previous communication, the basic science background and its clinical translation to the first surgical method that results in functional return after a spinal cord injury was given (1). The traumatic tear of nerve roots from the spinal cord interrupts the segmental transverse sensory and motor nerve fibers causing a longitudinal spinal cord injury. If left untreated, the affected spinal cord segments can deteriorate over about 1 month, with disintegration of neuronal networks and death of motor (2), sensory (3), and autonomic (4) nerve cells. The clinical effect of such lesion is loss of motor and sensory and autonomic function. Such injury in the human occurs most frequently in road traffic accidents affecting mainly the nerve plexus formations for limb function mostly for the arm, i.e., the origin of the brachial plexus. The cure of this condition depends on regeneration in the central nervous system (CNS).

By reimplanting avulsed nerve roots into the spinal cord functional useful motor but not sensory function is restored if the procedure is performed before 1 month after injury. This unique surgical strategy has since 25 years been a routine procedure in centers for brachial plexus injury in Stockholm and London (5). Close to 100 patients with at least subtotal brachial plexus root avulsions have been treated. In most patients, there is motor recovery which is functional in about 70% of the cases (6). Like in other types of brachial plexus or proximal nerve injuries mainly the proximally situated muscles recover good function. Distal muscles such as in the hand rarely regain any useful activity, although this has been described in some patients (7, 8). Remaining problems with this technique are injury-induced neuronal death, direction and specificity of reinnervation, and muscle and sensory receptor disintegration from long time of denervation.

Sensory recovery is not possible to restore only by reimplanting avulsed dorsal roots. The dorsal root ganglion neurons are unable to regenerate into the adult spinal cord (9). The molecular and cellular events that repel or arrest axons in the PNS–CNS transitional region remain elusive, but the

idea that axons may terminate regeneration by synapsing with non-neuronal cells was originally proposed (9). This provocative idea has recently been supported (10). Proteoglycan producing NG2 cells have been indicated to participate in such process (11), and it is therefore pertinent to further study these cells in conjunction with dorsal root de- and regeneration across the PNS–CNS transitional region (see below). Since the previous communication (1), experimental and clinical studies have been performed in order to overcome the problem of sensory recovery after dorsal root avulsion injury.

INTRAMEDULLARY NEURON TRANSFER TO RE-ESTABLISH SENSORY FUNCTION

A type of palliative "neurotization" procedure to replace the avulsed dorsal root and its ganglion containing the primary sensory neurons was developed. The concept of ventral root or nerve graft implantation to promote growth from spinal cord motoneurons to the periphery was the basis for a procedure to reconnect the periphery with spinal cord sensory systems. Sensory nerve cells in the spinal cord could hypothetically in accordance with CNS motoneurons potentially elongate new processes into a PNS graft implanted into the dorsal spinal cord to reconnect with the periphery. When asking spinal cord neurons to extend new processes into the PNS, it is likely that not axons but dendrites would be recruited by the PNS conduit implanted into the dorsal horn. It is well established that dendrites can produce aberrant or supernumerary axons after injury. Such processes have been shown to extend from dendrites into the PNS and are called dendraxons (12) or unusual distal processes (UDP) (13). Extension of supernumerary axons or dendraxons into a PNS conduit has previously been demonstrated for motoneurons (12, 14). It has also been shown that such processes can transmit impulses and contain transmitter substances for synaptic communication (14).

Experimentally, it was shown that intrinsic sensory spinal cord neurons can extend new (non-regenerative) processes into an implanted PNS conduit. Immunohistochemical technique (MAP2 staining) showed that these neurites were dendrites that had extended into the implanted PNS conduit and have functional properties (9). Electrophysiology verified that the new growth from sensory spinal cord neurons can transmit impulses. There was also a demonstration of transsynaptically provoked muscle contraction when stimulating these neurites which demonstrates that an integration of this new growth of spinal cord neurons with segmental spinal cord circuits in particularly ventral horn motoneurons occurred.

The implantation of a PNS conduit into both the ventral for motor recovery and dorsal part of the spinal cord for sensory recovery was performed in clinical cases of brachial plexus avulsion injury. Following such procedures, proprioception together with muscle function could be demonstrated (8). The biceps tendon reflex was confirmed clinically and H-reflex by means of electrophysiology (8). This is intriguing as proprioceptive function has been demonstrated to disappear and not to recover after a nerve injury with regeneration (15). With this extended spinal cord surgery including also sensory neurons, it was obvious that movements had become more controlled without the usual synkinesis seen in cases were motor conduits only had been reconstructed. In contrast to recovery of proprioception, there were no clinical, electrophysiological, or structural signs of exteroception (8).

ADJUVANT THERAPY FOR SPINAL CORD SENSORY REGENERATION

The dorsal root injury is considered as a type of spinal cord injury and as such the most common spinal cord injury (16). The palliative neurotization procedure described earlier has not resulted in a full sensory recovery. It is obvious that adjuvant therapy is necessary to complement surgery in order to recover better sensation after dorsal root injury or avulsion from the spinal cord. There are at least two major reasons for the failure of injured dorsal root axons to regrow back into the spinal cord. There is a lack of intrinsic neuronal growth, based largely on inactivity in the phosphoinositide3-kinase (PI3K)/Akt/mammalian target of rapamycin (mTOR) pathway, which is negatively regulated by phosphatase and tensin homolog (PTEN) (17). Another major impediment to regeneration into the spinal cord is the formation of an inhibitory environment by a glia scar.

The retinoic acid signaling system is very powerful in neuron growth and regeneration. Previous work has shown that retinoic acid receptor (RAR) beta 2 signaling stimulates axonal outgrowth in human, mouse, and rat (18, 19). In the adult, retinoic acid-responsive elements are locally activated in the regenerating rat nerve after a peripheral nerve injury (20). In adult spinal cord explants and dorsal root ganglion neurons where RARbeta 2 is absent, overexpression of RARbeta stimulates neurite outgrowth (21). Furthermore, delivery of RARbeta 2 to adult neurons induces axonal regeneration programs within injured neurons and encourages axonal growth also in the inhibitory CNS (22).

A small lipophilic molecule which is an agonist to the nuclear receptor RAR beta has been developed to be used in conjunction with dorsal root to spinal cord reimplantation surgery. In a rat model of cervical dorsal root avulsion (C5–T1), the newly developed RARbeta agonist was given (23). After 4 weeks of treatment, behavioral tests showed recovery of sensory (the sticky tape test; sensing and removal) and locomotor function (the horizontal ladder test). Dorsal root fiber regeneration across the dorsal root peripheral–central transitional region (PNS–CNS TR) was shown by biotinylated dextran amine (BDA) labeling and by means of tractography which showed a robust ingrowth of neurites. Synaptic recovery was demonstrated by analysis of noxious heat stimuli response, synaptic density, and mechano- and proprioceptive synapses in the dorsal horn showing that new connections had been established in the spinal cord (23).

Of paramount importance is how the regenerated dorsal root axons re-entered the spinal cord. In the naive adult situation, there is a specialized transitional region between a stereotype peripheral nerve compartment of the dorsal root and the central nervous fiber tracts of the spinal cord, which involves a number of unique structural entities (24). Among these are the occurrences of fibrous astrocytic processes surrounding and separating the

most proximal peripheral paranodes and a compound PNS–CNS type of node of Ranvier at the crossing of nerve fibers from the PNS to the CNS of organization (25). In the treated animals, a glia construct of a similar organization had been re-established at the passing of regenerated dorsal root axons into the spinal cord. This is of conceptual importance as it seems as a naive structural glia organization has to be repeated to allow a successful regeneration. This is presently the subject of further studies in particular what the role of the NG2 cells are in this context.

Studies of the mechanisms of the switch from a non-permissive environment in the CNS and an increased regenerative activity in the dorsal root neurons to allow for regeneration demonstrated that the RARbeta agonist modulates the PTEN signaling pathway in both neurons and astrocytes. In neurons RARbeta, *via* a cytoplasmic effect, induces PTEN to move from the membrane where it blocks axonal growth *via* the PI3K inhibition (17), into the cytoplasm, where it becomes phosphorylated and hence inactive (26). In addition, stimulation of RARbeta results in an increased secretion of PTEN in exosomes. These are taken up by astrocytes, resulting in hampered proliferation and glia scar formation as well as causing them to arrange in a normal-appearing scaffold around the regenerating axons allowing them to grow back into the spinal cord (23). The dual effect of RARbeta signaling, both neuronal and neuronal–glial, results in axonal regeneration in the spinal cord after dorsal root injury.

In summary, there is the potential of new growth and plasticity rather than regeneration of spinal cord sensory neurons that can replace the injured primary sensory dorsal root neurons and reconnect to the periphery for reestablishment of some but not all sensory qualities. In order for a more complete return of sensory function after dorsal root avulsion from the spinal cord, a unique adjuvant therapy has been developed.

AUTHOR CONTRIBUTIONS

The author confirms being the sole contributor of this work and approved it for publication.

ACKNOWLEDGMENT

The generous support by Dr M. Risling is highly appreciated.

FUNDING

Wellcome Trust, Karolinska Institutet, Swedish Defence FOT-AF.9221006, and Darwin Trust of Edinburgh.

REFERENCES

1. Carlstedt T. Perspective on the treatment of the longitudinal spinal cord injury. *Front Neurol* (2011) 2:11. doi:10.3389/fneur.2010.00011
2. Bergerot A, Shortland PJ, Annand P, Hunt SP, Carlstedt T. Co-treatment with riluzole and GDNF is necessary for functional recovery after ventral root avulsion injury. *Exp Neurol* (2004) 187:359–66. doi:10.1016/j.expneurol.2004.02.003
3. Chew DJ, Linster VHL, Sakthithasan M, Robson ML, Carlstedt T, Shortland PJ. Cell death after dorsal root injury. *Neurosci Lett* (2008) 433:231–4. doi:10.1016/j.neulet.2008.01.012
4. Hoang TX, Akhavan M, Wu J, Havton LA. Minocyline protects motor but not autonomic neurons after cauda equina injury. *Exp Brain Res* (2008) 187:71–7. doi:10.1007/s00221-008-1398-5
5. Carlstedt T. *Central Nerve Plexus Injury*. London: Imperial College Press (2007).
6. Htut M, Misra P, Anand P, Birch R, Carlstedt T. Motor recovery and the breathing arm after brachial plexus surgical repairs, including re-implantation of avulsed spinal roots into the spinal cord. *J Hand Surg Eur* (2007) 31:596–605. doi:10.1016/j.jhsb.2006.04.027
7. Carlstedt T, Hultgren T, Nyman T, Hansson T. Cortical activity and hand function restoration in a patient after spinal cord surgery. *Nat Rev Neurol* (2009) 5:571–4. doi:10.1038/nrneurol.2009.137
8. Carlstedt T, Misra PV, Papadaki A, MacRobbie D, Anand P. Return of spinal reflex after spinal cord surgery for brachial plexus avulsion injury. *J Neurosurg* (2012) 116(Spine 2):414–7. doi:10.3171/2011.7.JNS111106
9. Carlstedt T. Regenerating axons form nerve terminals at astrocytes. *Brain Res* (1985) 347:188–91. doi:10.1016/0006-8993(85)90911-4
10. Han SB, Kim H, Skuba A, Tessler A, Fergusson T, Son Y-J. Sensory axon regeneration: a review from an in vivo imaging perspective. *Exp Neurol* (2012) 3:83–93. doi:10.5607/en.2012.21.3.83
11. Son Y-J. Synapsing with NG2 cells (polydendrocytes), unappreciated barrier to axon regeneration. *Neural Regen Res* (2015) 10:346–8. doi:10.4103/1673-5374.153672
12. Lindå H, Risling M, Cullheim S. "Dendraxons" in regenerating motoneurons in the cat: do dendrites generate new axons after central axotomy? *Brain Res* (1985) 385:329–33. doi:10.1016/0006-8993(85)90978-3
13. Rose PK, Odlozinski M. Extension of the dendritic tree of motoneurons innervating neck muscles of the adult cat after permanent axotomy. *J Comp Neurol* (1998) 390:392–411. doi:10.1002/(SICI)1096-9861(19980119)390:3<392::AID-CNE7>3.0.CO;2-X
14. Hoang TX, Nieto JH, Havton LA. Regenerating supernumerary axons are cholinergic and emerge from both autonomic and motor neurons in the rat spinal cord. *Neuroscience* (2005) 136:417–23. doi:10.1016/j.neuroscience.2005.08.022
15. Alvarez FJ, Titus-Mitchell HE, Bullinger KL, Kraszpulski M, Nardelli P, Cope TC. Permanent central synaptic disconnection of proprioceptors after nerve injury and regeneration. 1. Los of VGLUT/1A synapses on motoneuron. *J Neurophysiol* (2011) 106:2450–70. doi:10.1152/jn.01095.2010
16. Ramer MS, McMahon SB, Priestly JV. Axon regeneration across the dorsal root entry zone. *Prog Brain Res* (2001) 136:621–39. doi:10.1016/S0079-6123(01)32107-6
17. Park KK, Liu K, Hu Y, Kanter JL, He Z. PTEN/mTOR and axon regeneration. *Exp Neurol* (2010) 223:45–50. doi:10.1016/j.expneurol.2009.12.032
18. Agudo M, Yin P, Davies M, Bradbury E, Doherty P, McMahon S, et al. A retinoic acid receptor beta agonist (CD2019) overcomes inhibition of axonal outgrowth via phosphoinositide 3-kinase signalling in the injured adult spinal cord. *Neurobiol Dis* (2010) 37:147–55. doi:10.1016/j.nbd.2009.09.018
19. Wong L-F, Yip PK, Battaglia A, Grist J, Corcoran J, Maden M, et al. Retinoic acid receptor beta2 promotes functional regeneration of sensory axons in the spinal cord. *Nature* (2006) 9:243–50. doi:10.1038/nn1622
20. Zhelvaznik N, Schrage K, McKaffery P, Mev J. Activation of retinoic acid signalling after sciatic nerve injury: upregulation of cellular retinoic binding proteins. *Eur J Neurosci* (2003) 18:1033–40. doi:10.1046/j.1460-9568.2003.02834.x
21. Corcoran J, So PL, Barber RD, Vincent KL, Mazarakis ND, Mitrophanous KA, et al. Retinoic acid receptor beta 2 and neurite outgrowth in the adult mouse spinal cord in vitro. *J Cell Sci* (2002) 115:3779–86. doi:10.1242/jcs.00046
22. Yip PK, Wong LP, Pattison D, Battaglia A, Grist J, Bradbury EJ, et al. Lentiviral vector expressing retinoic acid receptor beta 2 promotes recovery of function after corticospinal tract injury in the adult rat spinal cord. *Hum Mol Genet* (2006) 15:3107–18. doi:10.1093/hmg/ddl251

23. Goncalves MB, Malmquist T, Clarke E, Hubens CJ, Grist J, Hobbs C, et al. Neuronal RARbeta signalling modulates PTEN activity directly in neurons and via exosome transfer in astrocytes to prevent glia scar formation and induce spinal cord regeneration. *J Neurosci* (2015) 35(47):15731–45. doi:10.1523/JNEUROSCI.1339-15.2015
24. Berthold C-H, Carlstedt T. Observations on the morphology at the transition between the peripheral and central nervous system in the cat. II. General organization of the transitional region in S1 dorsal rootlets. *Acta Physiol Scand Suppl* (1977) 446:23–42.
25. Berthold C-H, Carlstedt T. Observations on the morphology at the transition between the peripheral and central nervous system in the cat. III. Myelinated fibres in S1 dorsal rootlets. *Acta Physiol Scand Suppl* (1977) 446:43–60.
26. Ross AH, Gericke A. Phosphorylation keeps PTEN phosphatase closed for business. *Proc Natl Acad Sci U S A* (2009) 106:1297–8. doi:10.1073/pnas.0812473106

Conflict of Interest Statement: The author declares that the research was conducted in the absence of any commercial or financial relationships that could be construed as a potential conflict of interest.

frontiers in Neurology

CORRECTION
published: 05 July 2017
doi: 10.3389/fneur.2017.00326

Corrigendum: New Treatments for Spinal Nerve Root Avulsion Injury

*Thomas Carlstedt**

Wolfson CARD, Kings College London, London, United Kingdom

Keywords: nerve plexus, root avulsion, neurotization, adjuvant therapy, sensory recovery, spinal cord regeneration

A corrigendum on

New Treatments for Spinal Nerve Root Avulsion Injury
by Carlstedt T. Front Neurol (2016) 7:135. doi:10.3389/fneur.2016.00135

Missing Funding:
In the original article, I neglected to include the funders: Wellcome Trust, Karolinska Institutet, Swedish Defence FOT-AF.9221006, and Darwin Trust of Edinburgh. The author apologizes for this error and state that this does not change the scientific conclusions of the article in any way.

Text Correction:
In the original article, there were two errors with the inclusion of the texts:

"Pharmacokinetic and pharmacodynamics studies have demonstrated dose dependent efficacy in oral administration of the RARbeta agonist. Toxicological tests have shown little adverse effects. Clinical trials are now imminent in the most experienced centers for plexus injuries (London and Stockholm) using this first drug that can be given orally for direct treatment of a spinal cord injury."

and

"A new drug that can be given orally restores sensory functions and muscle coordination after such injury by means of regeneration within the spinal cord. If successful in clinical trials this drug can be considered for many other CNS injuries."

Corrections by deleting those texts have been done to section "Adjuvant therapy for spinal cord sensory regeneration" paragraph six and seven.

The author apologizes for this error and state that this does not change the scientific conclusions of the article in any way.

The original article has been updated.

OPEN ACCESS

Edited and Reviewed by:
Michael G. Fehlings, University Health Network, Canada

***Correspondence:**
Thomas Carlstedt
carlstedt.thomas@googlemail.com

Specialty section:
This article was submitted to Neurotrauma, a section of the journal Frontiers in Neurology

Received: *06 June 2017*
Accepted: *22 June 2017*
Published: *05 July 2017*

Citation:
Carlstedt T (2017) Corrigendum: New Treatments for Spinal Nerve Root Avulsion Injury. Front. Neurol. 8:326. doi: 10.3389/fneur.2017.00326

Conflict of Interest Statement: The author declares that the research was conducted in the absence of any commercial or financial relationships that could be construed as a potential conflict of interest.

frontiers in Neurology

ORIGINAL RESEARCH
published: 31 July 2017
doi: 10.3389/fneur.2017.00291

Plasticity of Select Primary Afferent Projections to the Dorsal Horn after a Lumbosacral Ventral Root Avulsion Injury and Root Replantation in Rats

Allison J. Bigbee[1†], *Mahnaz Akhavan*[2†] *and Leif A. Havton*[1,3*]

[1] *Department of Neurology, David Geffen School of Medicine at UCLA, Los Angeles, CA, United States,* [2] *Department of Molecular, Cell, and Developmental Biology, UCLA, Los Angeles, CA, United States,* [3] *Department of Neurobiology, David Geffen School of Medicine at UCLA, Los Angeles, CA, United States*

Injuries to the conus medullaris and cauda equina portions of the spinal cord result in neurological impairments, including paralysis, autonomic dysfunction, and pain. In experimental studies, earlier investigations have shown that a lumbosacral ventral root avulsion (VRA) injury results in allodynia, which may be ameliorated by surgical replantation of the avulsed ventral roots. Here, we investigated the long-term effects of an L6 + S1 VRA injury on the plasticity of three populations of afferent projections to the dorsal horn in rats. At 8 weeks after a unilateral L6 + S1 VRA injury, quantitative morphological studies of the adjacent L5 dorsal horn showed reduced immunoreactivity (IR) for the vesicular glutamate transporter, VGLUT1 and isolectin B4 (IB4) binding, whereas IR for calcitonin gene-related peptide (CGRP) was unchanged. The IR for VGLUT1 and CGRP as well as IB4 binding was at control levels in the L5 dorsal horn at 8 weeks following an acute surgical replantation of the avulsed L6 + S1 ventral roots. Quantitative morphological studies of the L5 dorsal root ganglia (DRGs) showed unchanged neuronal numbers for both the VRA and replanted series compared to shams. The portions of L5 DRG neurons expressing IR for VGLUT1 and CGRP, and IB4 binding were also the same between the VRA, replanted, and sham-operated groups. We conclude that the L5 dorsal horn shows selective plasticity for VGLUT1 and IB4 primary afferent projections after an L6 + S1 VRA injury and surgical repair.

Keywords: cauda equine, VGLUT1, isolectin B4, calcitonin gene-related peptide, dorsal root ganglion

OPEN ACCESS

Edited by:
Mattias K. Sköld,
Uppsala University, Sweden

Reviewed by:
Lev N. Novikov,
Umeå University, Sweden
Alexandre Leite Rodrigues Oliveira,
Universidade Estadual de Campinas, Brazil

***Correspondence:**
Leif A. Havton
lhavton@mednet.ucla.edu

†These authors have contributed equally to this work.

Specialty section:
This article was submitted to Neurotrauma, a section of the journal Frontiers in Neurology

Received: *18 November 2016*
Accepted: *06 June 2017*
Published: *31 July 2017*

Citation:
Bigbee AJ, Akhavan M and Havton LA (2017) Plasticity of Select Primary Afferent Projections to the Dorsal Horn after a Lumbosacral Ventral Root Avulsion Injury and Root Replantation in Rats. Front. Neurol. 8:291. doi: 10.3389/fneur.2017.00291

INTRODUCTION

Brachial plexus and lumbosacral nerve root injuries may result in a combination of paralysis of peripheral organs and sensory impairments, including the development of neuropathic pain (1, 2). Although injuries to peripheral nerves and dorsal roots, which carry sensory fibers, represent established causes of neuropathic pain, isolated ventral root transection injuries with degeneration of efferent motor fibers may represent another cause of hyperalgesia and allodynia in experimental models (3–5). An at-level neuropathic pain presentation with allodynia, but in the absence of hyperalgesia, may develop in response to a lumbosacral ventral root avulsion (VRA) injury in rats (6). Interestingly, acute surgical repair in the form of direct implantation of the avulsed lumbosacral

ventral roots into the lateral funiculus of the spinal cord promotes regenerative growth by spinal cord neurons with extension of axons into the replanted roots, functional reinnervation of the lower urinary tract, and amelioration of neuropathic pain (6–8). However, information on the effects of the VRA injury and repair on afferent projections into the dorsal horn as a potential contributor to sensory plasticity has remained sparse.

The main objective of this investigation was to study the effects of a unilateral L6 and S1 VRA injury, with and without surgical replantation of the avulsed ventral roots into the spinal cord, on the expression of select markers for subsets of primary afferents in the L5 dorsal horn. This experimental model interrupts the ventral horn exit zone at the junction between the central and peripheral nervous systems, but the dorsal horn entry zone remains anatomically intact and allows primary afferents to enter the spinal cord. We investigated the immunohistochemical expression patterns for the vesicular glutamate transporter (VGLUT1) and calcitonin gene-related peptide (CGRP), as well as the histochemical binding patterns for the isolectin B4 (IB4). VGLUT1 immunoreactivity (IR) is detected primarily within Rexed's laminae III and IV, and the medial portion of lamina V of the dorsal horn, and serves as a marker for cutaneous and muscle afferents (9, 10). CGRP IR is normally present in Rexed's laminae I and II and indicates small and thinly myelinated or non-myelinated peptidergic primary afferents (11). Staining for IB4 is also detected primarily in Rexed's laminae I and II and used to identify the presence of non-peptidergic primary afferents (12, 13). We first identified the labeling and staining patterns for VGLUT1, CGRP, and IB4 in the L5 dorsal horn, then examined the corresponding L5 dorsal root ganglion (DRG) using the same morphological markers to examine signs for intramedullary plasticity of afferent projections and neuronal counts. This morphological investigation represents a direct extension of prior studies on VRA-induced at-level neuropathic pain and its amelioration by a surgical root reimplantation procedure, and the spinal cord and DRG tissues used for the present study were obtained from the same animals as those providing behavioral and morphological data for our prior report (6).

MATERIALS AND METHODS

All animal procedures were approved by the Chancellor's Animal Research Committee at UCLA and performed according to the standards established by the National Institutes of Health (NIH) Guide for Care and Use of Laboratory Animals. All efforts were made to minimize the numbers of animals needed for the study and any suffering associated with the procedures. Adult female Sprague-Dawley rats (Charles River Laboratories, Wilmington, MA, USA) were included in the studies ($n = 25$; 200–220 g body weight). The rats were divided into three groups: (1) rats undergoing a sham operation procedure of a lumbar laminectomy and opening of the dura mater (LAM, $n = 13$); (2) rats undergoing an L6 and S1 VRA injury (VRA, $n = 7$); and (3) rats undergoing an L6 and S1 VRA injury followed by an acute implantation of lesioned ventral roots into the lateral funiculus of the corresponding segments (VRI, $n = 5$).

Surgical Procedures

Spine surgeries with ventral root procedures were performed according to established protocols (6, 7). In short, all subjects were maintained under a surgical plane of inhalational anesthesia (2% isoflurane). A midline incision was made over the lumbar spinous processes, and an L1–L3 hemi-laminectomy was performed with spinous processes left intact. The dura was opened, and the L6 and S1 ventral roots were identified and avulsed from the spinal cord surface using a fine jeweler's forceps to apply traction along the normal course of the ventral roots. In animals of the VRI series, the tip of a scalpel blade was used to make two small longitudinal incisions along the lateral funiculus of the L6 and S1 spinal cord segments, and the avulsed ventral roots were gently implanted into the spinal cord white matter. The reimplanted roots were held in place within the longitudinal spinal cord incision, aided by the application of adjacent coagulating blood, but without the use of any sutures or tissue glue. In the LAM series, the dura was opened, the L6 and S1 ventral roots identified, gently manipulated, but not injured. A layer of Gelfoam® was positioned over the exposed spinal cord, and a titanium mesh was attached over the laminectomy site, secured to the ligaments between the T11–T12 and L5–L6 spinous processes using a 6-0 silk suture, to provide added stabilization of the vertebral column and protect the exposed spinal cord segments against any direct pressure from the surrounding tissue (14). The paraspinous muscle and skin layers were closed separately, and all rats were allowed to recover from the procedure. Buprenex® (0.2–0.5 mg/kg s.c.) was given every 12 h for 2 days to provide postoperative pain control. All animals were checked daily for overall health, and bladders were manually expressed as needed during the recovery phase until independent voiding function was present.

Morphological Studies

At 8 weeks postoperatively, all animals received an overdose of sodium pentobarbital and were perfused intracardially with 0.1 M phosphate buffer followed by a 4% paraformaldehyde solution. The vertebral column was removed and the spinal cord dissected free to visualize individual lumbosacral DRGs and nerve roots. Only animals with an anatomically verified L6 + S1 ventral root lesion with or without root repair were included in the studies. For the repair series of animals, only rats with replanted ventral roots still attached at the surgical repair site were included in the study. The spinal cord and lumbosacral DRGs from each subject were post-fixed in the fixative solution overnight and rinsed in 0.1 M phosphate-buffered saline (PBS). The spinal cord and DRG tissues were cryoprotected in a 30% sucrose solution for 24 h, preserved in OCT compound (Sakura Finetek, Torrance, CA, USA), and stored in −80°C. Spinal cord tissues were cut at 30-μm thickness, and DRG tissues were cut at 10-μm thickness using a cryostat.

Established criteria for the rat lumbosacral cytoarchitecture were used to identify the location of the L5 spinal cord (15). Every fifth section of the L5 spinal cord segment or DRG was selected for morphological analysis, and a total of 4–8 sections were analyzed for each morphological marker. Adjacent sections were processed for the detection of CGRP, VGLUT1, and IB4.

Although the L6 + S1 ventral roots were avulsed, the morphological studies were performed using the adjacent L5 segment in order to minimize involvement of injured ventral root afferents of the L6 + S1 segments and to allow direct comparisons with prior pain behavioral and morphological studies in the same animals (6).

Sections of the L5 spinal cord segment and the L5 DRGs were initially rinsed in PBS. Next, the sections were blocked in 5% normal donkey serum for 1 h (Jackson Immuno Research Labs, Inc., West Grove, PA, USA) and processed for VGLUT1 (anti-rabbit, 1:1,000; Synaptic Systems, Göttingen, Germany), CGRP (anti-rabbit, 1:4,000, Millipore, Billerica, MA, USA), or IB4 FITC-conjugated lectin (1:100, Sigma, St. Louis, MO, USA). The primary antibodies were incubated overnight in 0.3% Triton X-100 in PBS at room temperature. Secondary antibodies (Alexa Fluor® 594 or Alexa Fluor® 488, 1:500, Invitrogen, Carlsbad, CA, USA) were incubated for 1 h at room temperature. The sections underwent a final rinse and were mounted on glass slides with Vectashield mounting medium (Vector Laboratories, Burlingame, CA, USA). The region of interest (ROI) for the analysis of VGLUT1 IR consisted of an outline of the dorsal horn gray matter with its ventral border at the same level as the ventral tip of the dorsal columns (**Figures 1A–C**). The ROI for the analysis of CGRP IR and IB4 labeling consisted of a total of 10 square boxes with an area of 1,225 μm^2 each across the inner portion of Rexed's lamina II (**Figures 2A** and **3A**). Fluorescent images were captured using a Spot camera (Diagnostic Instruments, Sterling Heights, MI, USA), which was attached to a Nikon E600 microscope. Magnification, light intensity, and exposure times were held constant during the image capturing. Densitometric analysis and quantitative studies were performed using C-Imaging software (Compix, Inc., Brandywine, PA, USA) and determined an area of immunopositive labeling above a constant threshold. ROIs included the dorsal horn gray matter for VGLUT1 IR studies and the superficial gray matter (laminae I–II) for CGRP IR and IB4 labeling. For quantitative studies of neuronal counts of the L5 DRGs, DAPI staining allowed for nuclear identification and for neuronal profile counts. Neuronal and non-neuronal nuclei showed distinct morphological differences with the neuronal nuclei being larger, round to oval in shape and showing less intense fluorescent labeling with uneven chromatin patterns, whereas glial nuclei showed small and round nuclei with bright fluorescent labeling. Each L5 DRG was cut serially at 10-μm thickness, and every fifth section was stained for DAPI and used to determine the total number of sensory neuron. Abercrombie's method was applied to correct for the presence of split nuclei in sections using the formula, $N = A \times (T/(D + T))$, wherein N is the corrected number of nuclei in a section, A is the crude count of nuclear profiles, T is the section thickness, and D is the average diameter of the nuclei (16). For each DRG, a total of 100 nuclei were measured to determine the average nuclear diameter. A total of 6–14 sections were used to determine the corrected neuronal count for each DRG. To calculate the proportion of sensory neurons labeled for VGLUT1, CGRP, IB4, and CGRP/IB4, profile counts for each of these subtypes of sensory neurons were determined and related to the corrected number of DAPI-stained DRG neurons in four sections from the mid portion of each DRG.

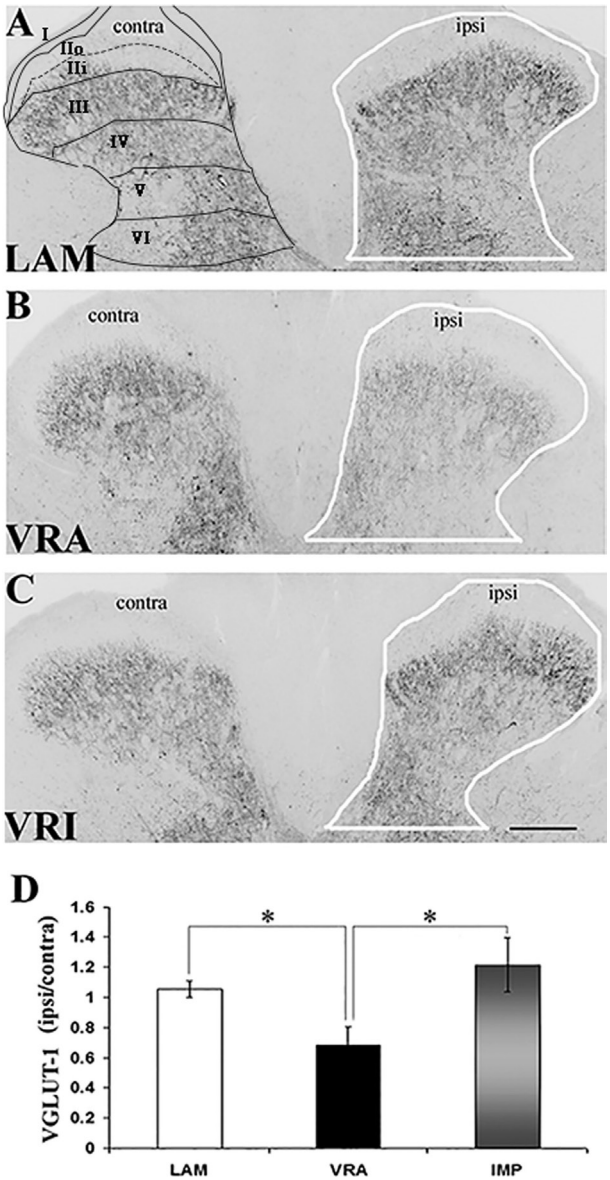

FIGURE 1 | Effects of a unilateral L6 + S1 ventral root avulsion (VRA) injury and VRA injury followed by acute root replantation (VRI) on VGLUT1 immunoreactivity (IR) in the L5 dorsal horn at 8 weeks postoperatively. **(A–C)** The results were compared with sham-operated animals (LAM) and expressed as a ratio for the labeling detected on the sides ipsilateral (ipsi) and contralateral (contra) to the surgical procedures. The region of interest is indicated by the outline of the dorsal horn on the ipsi side for the LAM, VRA, and VRI groups. Rexed's laminae of the dorsal horn are also indicated for LAM. **(D)** Note that VGLUT1 IR was decreased on the ipsi side after the VRA injury, whereas the corresponding VGLUT1 IR for the VRI group was symmetric and similar to the control group (LAM). Scale bar = 250 μm and * indicates a significant difference of $p < 0.05$ between groups.

Statistical Analyses

Data were expressed as mean ± SE. Analyses between experimental groups were performed using the non-parametric Kruskal–Wallis ANOVA with Dunn's *post hoc* test. We considered $p < 0.05$ as statistically significant.

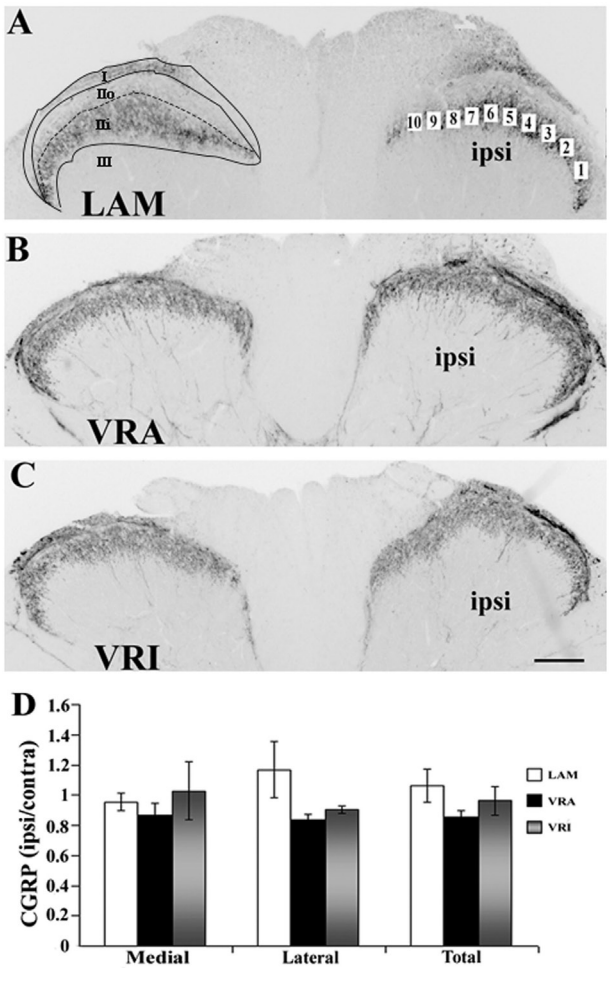

FIGURE 2 | Effects of a unilateral L6 + S1 ventral root avulsion (VRA) injury and VRA injury followed by acute root replantation (VRI) on CGRP immunoreactivity (IR) in the L5 dorsal horn at 8 weeks postoperatively. **(A–C)** The results were compared with sham-operated animals (LAM) and expressed as a ratio for the labeling detected on the sides ipsilateral (ipsi) and contralateral (contra) to the surgical procedures. The region of interest was indicated by the placement of 10 boxes of 1,225 μm^2 each across the superficial laminae of the dorsal horn for the LAM, VRA, and VRI groups. For comparisons between the lateral and medial portions of the dorsal horn, boxes 1–5 represented the lateral portion and boxes 6–10 represented the medial portion of the superficial laminae. Rexed's laminae for the superficial dorsal horn are indicated for LAM. **(D)** Note that there was no difference between the LAM, VRA, and VRI groups with regards to CGRP IR in the superficial laminae of the dorsal horn. Scale bar = 250 μm.

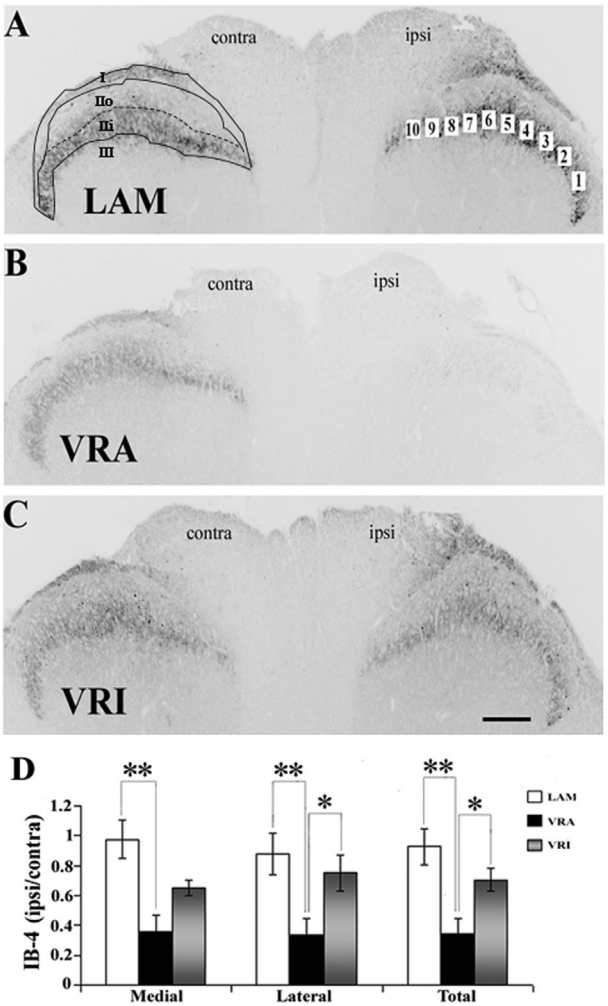

FIGURE 3 | Effects of a unilateral L6 + S1 ventral root avulsion (VRA) injury and VRA injury followed by acute root replantation (VRI) on isolectin B4 (IB4) binding in the L5 dorsal horn at 8 weeks postoperatively. **(A–C)** The results were compared with sham-operated animals (LAM) and expressed as a ratio for the labeling detected on the sides ipsilateral (ipsi) and contralateral (contra) to the surgical procedures. The region of interest was indicated by the placement of 10 boxes of 1,225 μm^2 each across the superficial laminae of the dorsal horn for the LAM, VRA, and VRI groups. For comparisons between the lateral and medial portions of the dorsal horn, boxes 1–5 represented the lateral portion and boxes 6–10 represented the medial portion of the superficial laminae. Rexed's laminae for the superficial dorsal horn are indicated for LAM. **(D)** Note that there was a reduced IB4 binding on the ipsi side after the VRA injury, whereas the corresponding IB4 binding was symmetric and similar between the LAM and VRI groups. Scale bar = 250 μm and * indicates a significant difference of $p < 0.05$ and ** indicates a significant difference of $p < 0.01$ between groups.

RESULTS

We investigated the effects of an L6 and S1 VRA injury and repair on the plasticity of primary sensory afferent projections to the dorsal horn of the L5 segment in rats. For this purpose, we examined the IR for the vesicular glutamate transporter, VGLUT1, and CGRP, as markers for the spinal cord projections of mechanoreceptive primary afferents and peptidergic nociceptive primary afferents, respectively. We also studied the binding of the Griffonia simplicifolia IB4, as a marker for non-peptidergic primary afferent projections to the dorsal horn.

VGLUT1 IR in the Dorsal Horn

VGLUT1 IR was detected in the dorsal horn of the L5 segment in all groups, especially within laminae IV–VI. Using densitometry,

IR for VGLUT1 was quantified in the dorsal horn (laminae I–VI) of both the ipsilateral (ipsi) and contralateral (contra) sides in rats of the LAM, VRA, and VRI groups (**Figure 1**). The VGLUT1 IR was markedly reduced in the dorsal horn after the VRA injury, as demonstrated by a decreased ratio of the ipsi to contra VGLUT1 IR in this ROI in rats of the VRA series (0.68 ± 0.13, $n = 6$) compared to the corresponding ratio in rats of the LAM series (1.05 ± 0.05, $n = 8$, $p < 0.05$). However, the ipsi to contra ratio of VGLUT1 IR was maintained in the VRI series (1.21 ± 0.18, $n = 5$) and not different from the corresponding ratio in rats of the LAM series but higher than the VGLUT1 IR in the VRA group ($p < 0.05$).

CGRP IR and Isolectin IB4 Binding in the Dorsal Horn

Both CGRP IR and isolectin IB4 were primarily detected within lamina I and II of the superficial dorsal horn in rats of all series. Double labeling for CGRP IR and IB4 binding combined with confocal light microscopy demonstrated that their territories largely overlapped in the superficial dorsal horn. Specifically, CGRP IR was primarily detected in lamina I and lamina IIo, whereas isolectin IB4 binding was mostly detected in lamina IIo and lamina IIi. There was no or minimal co-localization of CGRP IR and isolectin IB4 binding in the dorsal horn. Densitometry showed that the ratio of ipsi to contra values for CGRP in the superficial dorsal horn was not different between the LAM, VRA, and VRI groups (**Figure 2**).

The binding of IB4 was in the same ROI markedly reduced after the VRA injury, as demonstrated by a decreased ratio of ipsi to contra binding of IB4 in the superficial dorsal horn (0.35 ± 0.10, $n = 7$) compared to the corresponding ratio in rats of the LAM series (0.93 ± 0.12, $n = 8$, $p < 0.05$) (**Figure 3**). Interestingly, the ratio of ipsi to contra binding for binding for IB4 in the superficial dorsal horn was maintained in the VRI series (0.71 ± 0.08, $n = 5$) and not different from corresponding binding in the LAM series but significantly higher than IB4 binding ratio in the rats of the VRA series ($p < 0.05$) (**Figure 3**). When the medial and lateral portions of the superficial dorsal horn were analyzed separately, similar statistically significant differences between the experimental groups were identified.

Neuronal Numbers Functional Phenotypes in the L5 DRG

The effects of an L6 + S1 VRA or VRI on the L5 DRG were determined by quantitative light microscopy. The ratio of DAPI-stained DRG neurons of the ipsi and contra L5 DRG was determined for subjects of the LAM, VRA, and VRI series (**Figure 4**). The ipsi/contra ratio for the L5 DRG was 1.00 ± 0.07 ($n = 5$), 1.00 ± 0.04 ($n = 5$), and 1.09 ± 0.06 ($n = 5$), respectively. There were no differences between the groups.

The relative frequency for the expression of VGLUT1 IR, CGRP IR, and binding for IB4 was determined for the ipsi L5 DRG neurons of the LAM, VRA, and VRI series (**Figure 5**). No statistical differences were detected for the relative frequencies for VGLUT1 IR, CGRP IR, or IB4 binding between the groups. In addition, there was no difference between the experimental groups with regards to the frequency of co-labeling of CGRP IR and IB4 binding.

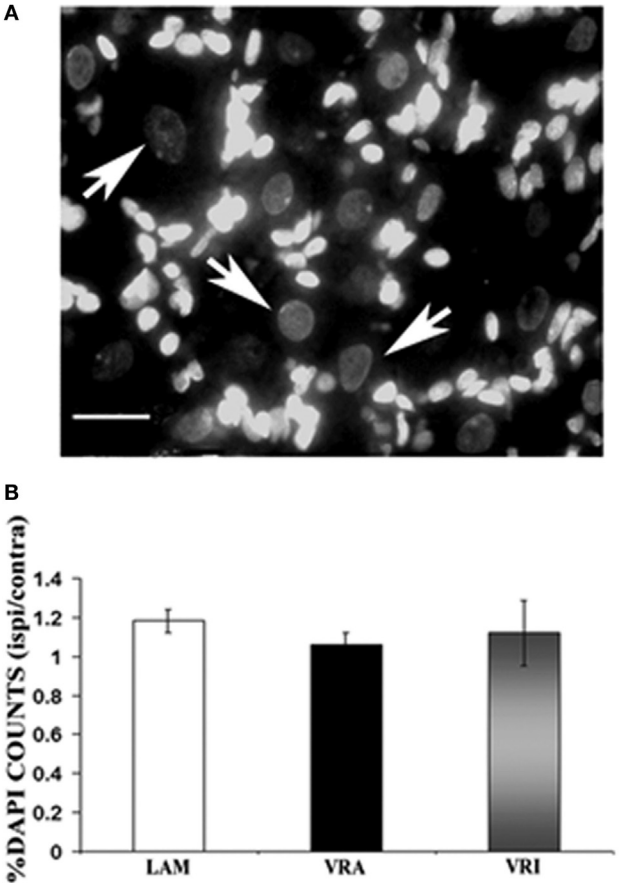

FIGURE 4 | Effects of a unilateral L6 + S1 ventral root avulsion (VRA) injury and VRA injury followed by acute root replantation (VRI) on neuronal counts in the L5 dorsal root ganglion (DRG) at 8 weeks postoperatively. The results were compared with sham-operated animals (LAM) and expressed as a ratio for the labeling detected on the sides ipsilateral (ipsi) and contralateral (contra) to the surgical procedures. **(A)** DAPI staining allowed for the identification and counting of neuronal nuclei in the L5 DRG (arrows). **(B)** Note that there was no difference with regards to neuronal counts of the L5 DRG between the LAM, VRA, and VRI groups. Scale bar = 20 μm.

DISCUSSION

The present study demonstrated differential plasticity for the expression of VGLUT1, IB4, and CGRP in the dorsal horn of the L5 spinal cord segment at 8 weeks after a combined L6 + S1 VRA injury as well as after a combined L6 + S1 VRA injury followed by acute replantation of the avulsed ventral roots. Specifically, the expression of VGLUT1 was reduced in the deep dorsal horn at 8 weeks after the VRA. In the superficial dorsal horn, the expression of IB4 was also reduced, whereas CGRP IR remained unchanged after the VRA injury. When the lumbosacral VRA injury was followed by an acute implantation of the lesioned roots into the lateral funiculus of the affected spinal cord segments, the

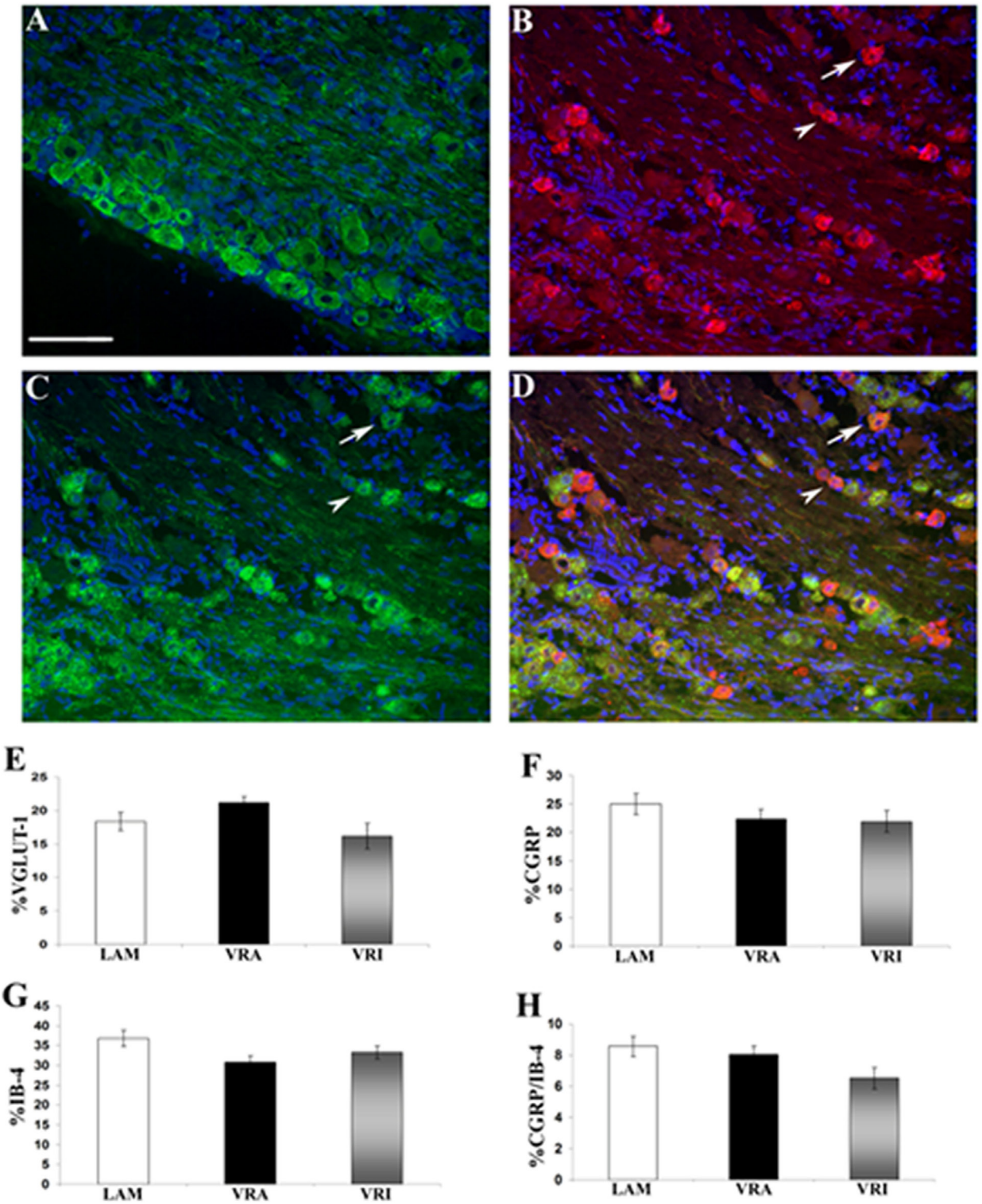

FIGURE 5 | Effects of a unilateral L6 + S1 ventral root avulsion (VRA) injury and VRA injury followed by acute root replantation (VRI) on the relative proportions of neurons showing immunoreactivity (IR) for **(A)** VGLUT1 or **(B)** calcitonin gene-related peptide (CGRP) or **(C)** binding for isolectin B4 (IB4) in the L5 dorsal horn at 8 weeks postoperatively. The results were compared with sham-operated animals (LAM) and expressed as a ratio for the labeling detected on the sides ipsilateral (ipsi) and contralateral (contra) to the surgical procedures. Note that there was no difference with regards to the percent dorsal root ganglion (DRG) neurons expressing IR for **(E)** VGLUT1 or **(F)** GCRP or **(G)** binding for IB4 between the LAM, VRA, and VRI groups. **(H)** In addition, there was no difference for the number of DRG neurons showing double labeling for CGRP and IB4 between the groups. Scale bar = 100 μm.

L5 dorsal exhibited baseline expression levels for VGLUT1, IB4, and CGRP, suggestive of a restoration or preservation of primary afferent phenotype expressions.

Plasticity of Primary Sensory Afferents after Peripheral Injury

It is well established that injuries to the peripheral nervous system, including a spinal nerve or sciatic nerve ligation, may result in neuropathic pain and plasticity of the intramedullary primary afferent projections (17–20). Prior studies have demonstrated a reduction of both VGLUT1 and isolectin IB4 in the lumbar dorsal horn after a sciatic nerve lesion (21, 22) and decreased CGRP and isolectin IB4 binding in the L4 and L5 dorsal horns after an L5 spinal nerve ligation (23). Such injuries to the peripheral nervous system may also result in the degeneration and death of axotomized DRG neurons (13, 24, 25). It is therefore possible that a loss of axotomized DRG neurons may have contributed to the reduced intramedullary labeling of markers for primary afferents after a mixed nerve or spinal nerve root lesion. In contrast, a VRA injury is sensory-sparing, and no DRG loss or change in the relative numbers of VGLUT1, CGRP, or IB4 positive neurons was detected in the L5 DRG after an L6 + S1 VRA injury. Our observed downregulation of VGLUT1 IR and isolectin IB4 staining in the L5 dorsal horn in the VRA series is therefore likely a representation of plasticity within select primary afferent projections.

In addition to the at-level injury and effects seen in the present study at the L5 segment after an L6 + S1 VRA injury and repair, plasticity may also take place at more remote spinal segments, which are involved with autonomic functions. The lower urinary tract is under parasympathetic control by autonomic innervation that originates primarily from the L6 and S1 segments, and it receives sympathetic innervation with origin at the lower thoracic and upper lumbar segments (26, 27). Both CGRP and VGLUT1 are present in distinct autonomic fibers that innervate the dorsal horn and autonomic nuclei at the thoracolumbar and lumbosacral segments (28–31). Following an L6 + S1 VRA injury, there was a selective decrease of CGRP in the dorsal horn of the L1 + L2 dorsal horn and no detectable effect on the VGLUT1 innervation of the same segments at 8 weeks postoperatively, whereas an acute reimplantation of the avulsed ventral root resulted in a partial restoration of the CGRP levels in the L1 + L2 dorsal horn (32). We conclude that the L6 + S1 VRA injury and repair may have parallel but different effects on spinal cord innervation by both somatosensory and visceral afferents.

Neuroprotective Effects of Avulsed Ventral Root Reimplantation

A neuroprotective effect provided by acute reimplantation of avulsed lumbosacral ventral roots is well established. Surgical reimplantation of avulsed L6 and S1 ventral roots into the lateral funiculus of the rat spinal cord augments motoneuron survival and regeneration of axons into the grafted roots (7), promotes reinnervation of peripheral targets (8), ameliorates neuropathic pain and intramedullary inflammatory and glial reactions in the dorsal horn (6), and reduces intramedullary degeneration of primary afferent axon collaterals in the spinal dorsal columns (33). In the present study, surgical reimplantation of avulsed L6 + S1 ventral roots resulted in the preservation of the intramedullary phenotype of VGLUT1 and CGRP IR and IB4 staining in the L5 dorsal horn. The latter finding represents a previously not known outcome of this surgical repair procedure.

The mechanisms behind the neuroprotective effects provided by the surgical reimplantation of avulsed ventral roots are not well understood. For the present study, it is unclear whether the surgical reimplantation of avulsed ventral roots restored a reduced expression of select primary afferent markers or protected primary afferent projections against structural degeneration. A downregulation of markers associated with transmitter function in the spinal cord is possible after a peripheral injury. Specifically, myelinated primary afferents to laminae III, IV, and IX in the rat spinal cord showed depletion of VGLUT1 IR after a sciatic nerve transection injury (22). Future studies are needed to clarify the effects of VRA injury on the integrity and the mechanisms for the protection of primary afferent marker expressions by root reimplantation.

Functional Aspects

Our morphological findings may be compared with prior pain behavioral studies of sensory thresholds after a lumbosacral VRA injury and ventral root reimplantation in rats. Specifically, the examined spinal cord tissues were obtained from the same animals that developed long-term allodynia in the absence of hyperalgesia within the L5 dermatome after an L6 + S1 VRA injury (6). It is therefore interesting to note that the long-term development of neuropathic pain is associated with decreased IR for VGLUT1 and reduced staining for isolectin IB4 in the L5 dorsal horn, whereas there is normal IR for CGRP, at 8 weeks after a combined L6 + S1 VRA injury. Interestingly, the animals in the surgical treatment group showed gradual amelioration of the neuropathic pain within the L5 dermatome when the VRA injury was followed by an acute ventral root reimplantation (6). The absence of neuropathic pain at 8 weeks postoperatively was associated with normal labeling and staining patterns for VGLUT1, IB4, and CGRP in the L5 dorsal horn. In addition, a VRA injury-associated degeneration of primary afferent collaterals in the spinal dorsal columns was also ameliorated by reimplantation of avulsed ventral roots into the spinal cord of the same rats (33). We conclude that the plasticity for select primary afferent markers in the L5 dorsal horn was closely associated with our previously reported state of allodynia and the normalization of sensory threshold in the VRA injury and surgical root reimplantation groups, respectively.

ETHICS STATEMENT

This study was carried out in accordance with the recommendations of the National Institutes of Health (NIH) Guide for Care and Use of Laboratory Animals and the Chancellor's Animal Research Committee at UCLA. The protocol was approved by the Chancellor's Animal Research Committee at UCLA.

AUTHOR CONTRIBUTIONS

AB and LH designed the study; AB and MA performed experiments; AB, MA, and LH interpreted the data; LH supervised the studies and wrote the manuscript. All authors reviewed and edited the manuscript.

FUNDING

These studies were supported by the National Institutes of Health (NS042719), the Christopher and Dana Reeve Foundation (HA-0704-2), and the Dr. Miriam and Sheldon G. Adelson Medical Research Foundation.

REFERENCES

1. Havton LA, Carlstedt T. Repair and rehabilitation of plexus and root avulsions in animal models and patients. *Curr Opin Neurol* (2009) 22(6):570–4. doi:10.1097/WCO.0b013e328331b63f
2. Carlstedt T, Havton L. The longitudinal spinal cord injury: lessons from intraspinal plexus, cauda equina and medullary conus lesions. *Handb Clin Neurol* (2012) 109:337–54. doi:10.1016/B978-0-444-52137-8.00021-8
3. Li L, Xian CJ, Zhong JH, Zhou XF. Effect of lumbar 5 ventral root transection on pain behaviors: a novel rat model for neuropathic pain without axotomy of primary sensory neurons. *Exp Neurol* (2002) 175(1):23–34. doi:10.1006/exnr.2002.7897
4. Sheth RN, Dorsi MJ, Li Y, Murinson BB, Belzberg AJ, Griffin JW, et al. Mechanical hyperalgesia after an L5 ventral rhizotomy or an L5 ganglionectomy in the rat. *Pain* (2002) 96(1–2):63–72. doi:10.1016/S0304-3959(01)00429-8
5. Obata K, Yamanaka H, Dai Y, Mizushima T, Fukuoka T, Tokunaga A, et al. Contribution of degeneration of motor and sensory fibers to pain behavior and the changes in neurotrophic factors in rat dorsal root ganglion. *Exp Neurol* (2004) 188(1):149–60. doi:10.1016/j.expneurol.2004.03.012
6. Bigbee AJ, Hoang TX, Havton LA. At-level neuropathic pain is induced by lumbosacral ventral root avulsion injury and ameliorated by root reimplantation into the spinal cord. *Exp Neurol* (2007) 204(1):273–82. doi:10.1016/j.expneurol.2006.11.003
7. Hoang TX, Nieto JH, Dobkin BH, Tillakaratne NJ, Havton LA. Acute implantation of an avulsed lumbosacral ventral root into the rat conus medullaris promotes neuroprotection and graft reinnervation by autonomic and motor neurons. *Neuroscience* (2006) 138(4):1149–60. doi:10.1016/j.neuroscience.2005.11.066
8. Hoang TX, Pikov V, Havton LA. Functional reinnervation of the rat lower urinary tract after cauda equina injury and repair. *J Neurosci* (2006) 26(34):8672–9. doi:10.1523/JNEUROSCI.1259-06.2006
9. Alvarez FJ, Villalba RM, Zerda R, Schneider SP. Vesicular glutamate transporters in the spinal cord, with special reference to sensory primary afferent synapses. *J Comp Neurol* (2004) 472(3):257–80. doi:10.1002/cne.20012
10. Persson S, Boulland JL, Aspling M, Larsson M, Fremeau RT Jr, Edwards RH, et al. Distribution of vesicular glutamate transporters 1 and 2 in the rat spinal cord, with a note on the spinocervical tract. *J Comp Neurol* (2006) 497(5):683–701. doi:10.1002/cne.20987
11. Averill S, McMahon SB, Clary DO, Reichardt LF, Priestley JV. Immunocytochemical localization of trkA receptors in chemically identified subgroups of adult rat sensory neurons. *Eur J Neurosci* (1995) 7(7):1484–94. doi:10.1111/j.1460-9568.1995.tb01143.x
12. Molliver DC, Wright DE, Leitner ML, Parsadanian AS, Doster K, Wen D, et al. IB4-binding DRG neurons switch from NGF to GDNF dependence in early postnatal life. *Neuron* (1997) 19(4):849–61. doi:10.1016/S0896-6273(00)80966-6
13. Bennett DL, Michael GJ, Ramachandran N, Munson JB, Averill S, Yan Q, et al. A distinct subgroup of small DRG cells express GDNF receptor components and GDNF is protective for these neurons after nerve injury. *J Neurosci* (1998) 18(8):3059–72.
14. Nieto JH, Hoang TX, Warner EA, Franchini BT, Westerlund U, Havton LA. Titanium mesh implantation – a method to stabilize the spine and protect the spinal cord following a multilevel laminectomy in the adult rat. *J Neurosci Methods* (2005) 147(1):1–7. doi:10.1016/j.jneumeth.2004.09.031
15. Molander C, Wang HF, Rivero-Melián C, Grant G. Early decline and late restoration of spinal cord binding and transganglionic transport of isolectin B4 from Griffonia simplicifolia I after peripheral nerve transection or crush. *Restor Neurol Neurosci* (1996) 10(3):123–33. doi:10.3233/RNN-1996-10301
16. Abercrombie M. Estimation of nuclear population from microtome sections. *Anat Rec* (1946) 94:239–47. doi:10.1002/ar.1090940210
17. Kim SH, Chung JM. An experimental model for peripheral neuropathy produced by segmental spinal nerve ligation in the rat. *Pain* (1992) 50(3):355–63. doi:10.1016/0304-3959(92)90041-9
18. Campbell JN, Meyer RA. Mechanisms of neuropathic pain. *Neuron* (2006) 52(1):77–92. doi:10.1016/j.neuron.2006.09.021
19. Navarro X, Vivó M, Valero-Cabré A. Neural plasticity after peripheral nerve injury and regeneration. *Prog Neurobiol* (2007) 82(4):163–201. doi:10.1016/j.pneurobio.2007.06.005
20. Costigan M, Scholz J, Woolf CJ. Neuropathic pain: a maladaptive response of the nervous system to damage. *Annu Rev Neurosci* (2009) 32:1–32. doi:10.1146/annurev.neuro.051508.135531
21. Molander C, Xu Q, Grant G. The cytoarchitectonic organization of the spinal cord in the rat. I. The lower thoracic and lumbosacral cord. *J Comp Neurol* (1984) 230(1):133–41. doi:10.1002/cne.902300112
22. Hughes DI, Polgár E, Shehab SA, Todd AJ. Peripheral axotomy induces depletion of the vesicular glutamate transporter VGLUT1 in central terminals of myelinated afferent fibres in the rat spinal cord. *Brain Res* (2004) 1017(1–2):69–76. doi:10.1016/j.brainres.2004.05.054
23. Shehab SA. Fifth lumbar spinal nerve injury causes neurochemical changes in corresponding as well as adjacent spinal segments: a possible mechanism underlying neuropathic pain. *J Chem Neuroanat* (2014) 55:38–50. doi:10.1016/j.jchemneu.2013.12.002
24. Tandrup T, Woolf CJ, Coggeshall RE. Delayed loss of small dorsal root ganglion cells after transection of the rat sciatic nerve. *J Comp Neurol* (2000) 422(2):172–80. doi:10.1002/(SICI)1096-9861(20000626)422:2<172::AID-CNE2>3.0.CO;2-H
25. Welin D, Novikova LN, Wiberg M, Kellerth JO, Novikov LN. Effects of *N*-acetyl-cysteine on the survival and regeneration of sural sensory neurons in adult rats. *Brain Res* (2009) 1287:58–66. doi:10.1016/j.brainres.2009.06.038
26. Fowler CJ, Griffiths D, de Groat WC. The neural control of micturition. *Nat Rev Neurosci* (2008) 9(6):453–66. doi:10.1038/nrn2401
27. de Groat WC, Griffiths D, Yoshimura N. Neural control of the lower urinary tract. *Compr Physiol* (2015) 5(1):327–96. doi:10.1002/cphy.c130056
28. Chung K, Lee WT, Park MJ. Spinal projections of pelvic visceral afferents of the rat: a calcitonin gene-related peptide (CGRP) immunohistochemical study. *J Comp Neurol* (1993) 337(1):63–9. doi:10.1002/cne.903370104
29. Hwang SJ, Oh JM, Valtschanoff JG. The majority of bladder sensory afferents to the rat lumbosacral spinal cord are both IB4- and CGRP-positive. *Brain Res* (2005) 1062(1–2):86–91. doi:10.1016/j.brainres.2005.09.026
30. Llewellyn-Smith IJ, Martin CL, Fenwick NM, Dicarlo SE, Lujan HL, Schreihofer AM. VGLUT1 and VGLUT2 innervation in autonomic regions of intact and transected rat spinal cord. *J Comp Neurol* (2007) 503(6):741–67. doi:10.1002/cne.21414
31. Wang HF, Shortland P, Park MJ, Grant G. Retrograde and transganglionic transport of horseradish peroxidase-conjugated cholera toxin B subunit, wheatgerm agglutinin and isolectin B4 from Griffonia simplicifolia I in primary afferent neurons innervating the rat urinary bladder. *Neuroscience* (1998) 87(1):275–88. doi:10.1016/S0306-4522(98)00061-X
32. Wu L, Wu J, Chang HH, Havton LA. Selective plasticity of primary afferent innervation to the dorsal horn and autonomic nuclei following lumbosacral ventral root avulsion and reimplantation in long term studies. *Exp Neurol* (2012) 233(2):758–66. doi:10.1016/j.expneurol.2011.11.034
33. Bigbee AJ, Hoang TX, Havton LA. Reimplantation of avulsed lumbosacral ventral roots in the rat ameliorates injury-induced degeneration of primary

afferent axon collaterals in the spinal dorsal columns. *Neuroscience* (2008) 152(2):338–45. doi:10.1016/j.neuroscience.2007.11.043

Conflict of Interest Statement: The authors declare that the research was conducted in the absence of any commercial or financial relationships that could be construed as a potential conflict of interest.

frontiers in Neurology

ORIGINAL RESEARCH
published: 21 February 2017
doi: 10.3389/fneur.2017.00049

Expression of Semaphorins, Neuropilins, VEGF, and Tenascins in Rat and Human Primary Sensory Neurons after a Dorsal Root Injury

*Tomas Lindholm[1,2], Mårten Risling[1], Thomas Carlstedt[1,3,4,5], Henrik Hammarberg[1,4,5], Wilhelm Wallquist[1,6], Staffan Cullheim[1] and Mattias K. Sköld[1,7]**

[1] Department of Neuroscience, Karolinska Institutet, Stockholm, Sweden, [2] Helsa Företagshälsovård Östermalm, Stockholm, Sweden, [3] Hammersmith Hospital, University College London and Imperial College, London, UK, [4] Department of Hand Surgery, Södersjukhuset, Stockholm, Sweden, [5] Department of Clinical Science and Education, Karolinska Institutet, Södersjukhuset, Stockholm, Sweden, [6] Department of Anesthesiology and Intensive Care, Västerås General Hospital, Västerås, Sweden, [7] Department of Neuroscience, Section of Neurosurgery, Uppsala University, Uppsala, Sweden

Dorsal root injury is a situation not expected to be followed by a strong regenerative growth, or growth of the injured axon into the central nervous system of the spinal cord, if the central axon of the dorsal root is injured but of strong regeneration if subjected to injury to the peripherally projecting axons. The clinical consequence of axonal injury is loss of sensation and may also lead to neuropathic pain. In this study, we have used *in situ* hybridization to examine the distribution of mRNAs for the neural guidance molecules semaphorin 3A (SEMA3A), semaphorin 3F (SEMA3F), and semaphorin 4F (SEMA4F), their receptors neuropilin 1 (NP1) and neuropilin 2 (NP2) but also for the neuropilin ligand vascular endothelial growth factor (VEGF) and Tenascin J1, an extracellular matrix molecule involved in axonal guidance, in rat dorsal root ganglia (DRG) after a unilateral dorsal rhizotomy (DRT) or sciatic nerve transcetion (SNT). The studied survival times were 1–365 days. The different forms of mRNAs were unevenly distributed between the different size classes of sensory nerve cells. The results show that mRNA for SEMA3A was diminished after trauma to the sensory nerve roots in rats. The SEMA3A receptor NP1, and SEMA3F receptor NP2, was significantly upregulated in the DRG neurons after DRT and SNT. SEMA4F was upregulated after a SNT. The expression of mRNA for VEGF in DRG neurons after DRT showed a significant upregulation that was high even a year after the injuries. These data suggest a role for the semaphorins, neuropilins, VEGF, and J1 in the reactions after dorsal root lesions.

Keywords: rhizothomy, DRG, regeneration, semaphorins, neuropilins, VEGF

OPEN ACCESS

Edited by:
Firas H. Kobeissy, University of Florida, USA

Reviewed by:
Shima Shahjouei, Tehran University of Medical Sciences, Iran
Fredrik Clausen, Uppsala University, Sweden

****Correspondence:***
Mattias K. Sköld
mattias.skold@ki.se

Specialty section:
This article was submitted to Neurotrauma, a section of the journal Frontiers in Neurology

Received: *30 October 2016*
Accepted: *02 February 2017*
Published: *21 February 2017*

Citation:
Lindholm T, Risling M, Carlstedt T, Hammarberg H, Wallquist W, Cullheim S and Sköld MK (2017) Expression of Semaphorins, Neuropilins, VEGF, and Tenascins in Rat and Human Primary Sensory Neurons after a Dorsal Root Injury. Front. Neurol. 8:49. doi: 10.3389/fneur.2017.00049

INTRODUCTION

Primary sensory neurons represent a link between the peripheral nervous system (PNS) and the central nervous system (CNS). Among other things, they convey the crucial information needed for feedback and proper function of the motor systems. At spinal levels, the sensory axons enter the spinal cord *via* the dorsal roots, which mainly belong to the PNS. The primary sensory neurons are distributed to the dorsal root ganglions located in the distal part of the dorsal root. Hence,

unlike other neurons in this pathway, they are located in the PNS and are often referred to as dorsal root ganglion neurons (DRG neurons). The DRG neuron have a rather unusual configuration with only one process—an axon that bifurcates and sends one peripheral branch into the peripheral nerve and one central branch to the CNS *via* the dorsal root. The response to injuries in these two axonal branches is highly dissimilar. Injury to peripheral branch initiates a powerful retrograde reaction in the cell body of the affected DRG neuron. This may initiate the death of the neuron, but surviving neurons have a capacity to regrow the peripheral branch. Injury to the central branch in the dorsal root seems to initiate a less vigorous reaction (1, 2). Thus, axon regrowth is possible in the PNS environment of the dorsal root, but the sprouts are typically arrested at the PNS–CNS border (3), and therefore, replantation of avulsed dorsal roots has not been considered to be useful even if recent studies have indicated that this situation can be changed by pharmacological intervention (4) or special procedures, such as removal of the DRG (5, 6). Due to this difference in response to injury, the DRG neurons offer the possibility to study the same neuron after two different kinds of injury where on is followed by regeneration (the peripheral injury) but the other one (central injury) followed by much less regenerative capacity.

In contrast, axons from spinal motoneurons have a high capacity for successful sprouting after lesions in the ventral funiculus of the spinal cord (7). These axons have been shown to penetrate CNS-type scar tissue inside the spinal cord, reenter the ventral root by crossing the CNS-PNS border, and regrow for long distances. This unusual regenerative capability has been employed for more practical use when avulsed ventral roots are replanted into the spinal cord, and this procedure has been shown to be followed by reinnervation of the ventral roots and functional recovery both in experimental animals (8–11) and clinical practice (12, 13).

In previous studies on ventral funiculus lesions or ventral root replantation, we have examined the expression of growth factors and a number of secreted and membrane-associated proteins demonstrated to affect axon steering, fasciculation, branching, or synapse formation through their action as chemorepellents and/or chemoattracants. These studies included members of the semaphorin family, the vascular and neuronal growth factor vascular endothelial growth factor (VEGF) and neuropilin 1 (NP1) and 2 and tenascins (14–16).

The semaphorins (SEMA) are secreted and transmembrane axon guidance molecules (17–19) that mediate axonal guidance in CNS and PNS in various ways including collapsing of growth cones (20) and also regulation of apoptosis (21) and neuroattractant capacities (22).

Semaphorin 3A (SEMA3A) (17), the prototype and founding member of the semaphorin family, has been characterized, besides ephrins, netrins, and slits, to function as a chemorepellent molecule with primarily inhibitory guidance capabilities (19, 23). During development, SEMA3A and its receptor proteins, NP1 (24–26), are known to take part in the regulation of axon fasciculation, axon guidance, and path finding. Another class 3 semaphorin, semaphorin 3F (SEMA3F) (27) has been shown to have widespread expression in adulthood and in sub regions of the CNS during embryogenesis. Neuropilin 2 (NP2) (24), which is the secreted receptor for SEMA3F, acts selectively to mediate repulsive guidance events in discrete populations of neurons and both ligand and receptor are expressed in strikingly complementary patterns during neurodevelopment (28). It has also been shown that a class 4 semaphorin, semaphorin 4F (SEMA4F), may play an important role in preventing growing retinal axons from deviating from their proper paths during development. In contrast to other SEMA, SEMA4F is expressed at the highest levels postnatal, and this might make it a potentially important molecule in nerve system maintenance and repair (29).

After intraspinal injuries to the ventral motoneuron axons, an injury known to be followed by successful regeneration of motoneuron axons (7), we did show increased expression SEMA3A in both injured motoneurons and spinal scar tissue (15), which indicates that SEMA3A expression could have in influence on the observed regenerative capacity of the motoneurons in this particular injury model.

Given this background, it appears logical to examine the expression of the same growth related genes in DRG neurons in a regenerative state (sciatic nerve lesion) or after a dorsal root lesion, which is not followed by functional regeneration.

MATERIALS AND METHODS

Surgery and Collection of Tissues Concerning Animals

Dorsal Rhizotomy (DRT)

Adult female Sprague-Dawley rats (200–250 g) were anesthetized with intraperitonal administration of chloral hydrate (300 mg/kg) (KEBO-Lab, Sweden). A half-sided laminectomy was performed at the lumbar level, approximately at the L4 to S1 segments. The dural sac was cut open, and axotomy of two or three of the central processes of the dorsal roots was made with microsiccors (Fine Science Tools, Heidelberg, Germany). The wound was closed with sutures in multiple layers. The rats were allowed to survive for 1 day ($n = 3$), 3 days ($n = 3$), 5 days ($n = 3$), 7 days ($n = 3$), 14 days ($n = 3$), 21 days ($n = 3$), 42 days ($n = 3$), and 365 days ($n = 3$). Adult rats were deeply reanaesthetized and transcardially perfused with Tyrode's solution. The pertinent tissues were rapidly dissected out and fresh frozen on dry ICE. Tissues from four adult rats were used as controls.

Sciatic Nerve Transection and Crush

Young, adult Sprague-Dawley rats (180–220 g; $n = 3$ per survival time) were anesthetized with chloral hydrate (300 mg/kg). After surgery, the animals were allowed to survive for 1, 3, 7, 14, 21, or 42 days. Tissue from four adult rats was used as controls.

Sciatic Nerve Transection and Resection

A 5–7 mm segment from the sciatic nerve was unilaterally resected below the obturator tendon. The wound was sutured to avoid contact between the proximal and distal ends.

Sciatic Nerve Crush (SNC)

The sciatic nerve was pressed one time with a pair of tweezers for 30 s, just below the obturator tendon. The wound was then inspected under a microscope to ensure that the crush was correctly performed.

The animals were killed with an overdose of pentobarbital (15 mg per 100 g body weight), and the L5–L6 dorsal root ganglions were taken out and frozen on a chuck.

Embryonic Tissue

In addition to tissue from injured and non-injured adult rats, tissue from normal embryonic and new-born rats was used as positive controls due to the high levels of expression of the studied factors in embryonic and new-born tissue. Tissue from normal Sprague-Dawley rat embryos was obtained by killing pregnant female rats by CO2 overdose and collection by cesarean section at embryonic days 16 (E16, $n = 1$) or 18 (E18, $n = 2$). The first sperm-positive day of the dam was considered E0. In addition, new-born rats were anesthetized by hypothermia and killed by decapitation at postnatal day 0.5 (P0.5, $n = 1$) or postnatal day 4.5 (P4.5, $n = 1$). Noon of the day of delivery was considered P0.5. After decapitation the head, spinal cord and ventral root were rapidly fresh frozen as described above.

The use of animals for all experiments was approved by the local ethical committee for animal experimentation (Stockholms Norra Försöksdjursetiska Nämnd, N5/99, N366/01).

Surgery and Collection of Tissues in Clinical Material

Cervical dorsal root ganglia whose roots were avulsed from the spinal cord were obtained in one female and four male patients (age range 18–44 years), all with traumatic injuries to their brachial plexus with delay between injury and collection of tissue at operation ranged between 1 day and 6 weeks. The ganglia were removed as a necessary part of the surgical repair procedure. In all cases, informed personal consent from each individual patient was obtained for tissue collection. Each ganglion was snap frozen in liquid nitrogen.

In Situ Hybridization

Fresh-frozen DRG tissue was cut in an RNAse free environment on a cryostat (Microm HM 500 M, Heidelberg, Germany) in 14-µm-thick transverse sections from *Rattus norvegicus* thawed onto Probe-on object-slides (Fisher Scientific, Pittsburgh, PA, USA) and stored in black, sealed boxes at −70°C until used. Synthetic oligonucleotides were synthesized (CyberGene AB, Huddinge, Sweden). The sequence of the probes was checked in a GeneBank database search to exclude significant homology with other genes. The synthesized oligonucleotides were:

5′ TGG TCT CGC AGC ACT GAC ACC TCC CTC TCC AGC ATC TCG ATT CGG CTC AA 39, complementary to nucleotides 3,274–3,323 of the mRNA encoding *Rattus norvegicus* J1-160/180 mRNA (GenBank Accession No. Z18630);
ACA AAG GCC GGG GCA CTC TCA AGG GAG CAG CAA CAA GTG GAA GCA CAT GC, which is complementary to nucleotides 2,205–2,254 of the Rattus norvegicus mRNA for semaphorin III/collapsin-1 (Genebank accession X95286);
GGG GTC TGG GCT CAG GGG AGG GGA AGT CAC AAA TGC AGC TGC CTT GGC CC, complementary to nucleotides 889–938 of the mRNA for the Rattus norvegicus collapsin response mediator protein (Genebank U52095);
5′ AGC AGA CGA GCC GCG CCT TCA GGA ATG TGC TCC ACT TGT TGA CCA GGC AA 3′ complementary to nucleotides 1,143–1,192 of Homo sapiens SEMA3F, mRNA (Genbank accession HSU38276), which is 97% identical with Mus musculus, semaphorin 3 F;
5′ CAG ATC CTC CAA GAC ACT GAG CTG AGC TCC AAT GCG CAC AGC CCG GTG GA 3′ complementary to nucleotides 1,475–1,524 of Rattus norvegicus (SEMA4F), mRNA (Genbank accession NM_019272.1);
5′ TGG GCC AGG ATG CAC TCT GAG CAG CTC TGG AGA CGG CCA CAG TTG GTT GT 3′ complementary to nucleotides 1,079–1,128 of Homo sapiens semaphorin 4F mRNA (Genbank accession NM_004263.1);
5′ AAC AGG CAC AGT ACA GCA CGA CCC CAC AGA CAG CCC CCA GGA GGA CCC CC 3′ complementary to nucleotides 2,601–2,650 of Homo sapiens NP1 mRNA (Genbank accession XM_005798.2);
GCA CAA CTC CAC AGA CTG CAC CCA GGA GCA CCC CCA GGG CAC TCA TGG CT complementary to nucleotides 2,580–2,629 of Rattus norvegicus neuropilin mRNA (Genebank AF018957);
CCA CGT CTG CGG GCG GAT CCT GAT GAA ACG AGT CAA CAG CGG CGT GTG CA complementary to nucleotides 1,504–1,553 of Rattus norvegicus neuropilin-2 mRNA (Genebank AF016297);
5′ GTC TGT CCA GTC ACA GCC CAG CAC CTC CAG CCG CAT CCC AAT CCC CGC CG 3′ complementary to nucleotides 1,739–1,788 of Homo sapiens NP2 mRNA (Genbank accession XM_002670.2);
5′ CTG GGG CTG GGG GCG GTG TCT GTC TGT CTG TCC GTC AGC GCG ACT GGT CA 3′ complementary to nucleotides 157–206 of Homo sapiens VEGF mRNA (Genbank accession AF022375.1);
5′ TCG ACG GTG ACG ATG GTG GTG TGG TGG TGA CAT GGT TAA TCG GTC TTT CC 3′ complementary to nucleotides 365–414 of the mRNA encoding rat VEGF (GeneBank accession AF062644).

The probes were labeled at the 3′-end with deoxyadenosine-alpha-(thio)triphosphate -35S- (NEN, Boston, MA, USA) by using terminal deoxynucleotidyl transferase (Amersham Pharmacia Biotec, Uppsala, Sweden) and hybridized to the sections, without pretreatment, for 16–18 h at 42°C. The hybridization mixture contained: 50% formamide (G.T. Baker Chemicals B W, Deventer, The Netherlands), 4 × SSC (1 × SSC is 0.15 M NaCl and 0.015 M sodium citrate), 1 × Denhardt's solution (0.02% each of polyvinyl-pyrrolidone, bovine serum albumin and Ficoll), 1% Sarcosyl (*N*-lauroylsarcosine; Sigma-Aldrich), 0.02 M phosphate buffer (pH 7.0), 10% dextran sulfate (Amersham Pharmacia Biotec), 500 µg/ml sheared and heat-denatured salmon sperm DNA (Sigma-Aldrich), and 200 mM

dithiothreitol (DTT; Sigma-Aldrich). Following hybridization, the sections were washed several times in 1 × SSC for 15 min at 60°C, rinsed in distilled water, and dehydrated in ascending concentrations of ethanol. The sections were then coated with NTB2 nuclear track emulsion (Kodak, Rochester, NY, USA). After 3–5 weeks, the sections were developed in D-19 developer (Kodak) for 5 min at room temperature and fixed in AL-4 fixative (Kodak) for 5 min. Finally, the slides were counterstained with cresyl violet (Sigma C5042, USA) and then dehydrated in ascending concentrations of ethanol, mounted in Entellan (Histolab products AB, Göteborg, Sweden), and coverslipped.

Image Analysis

The hybridization signal was recorded with a 40× objective in a Leica DM RBE microscope equipped with a dark-field condenser (Leica, Wetzlar, Germany) and digitized at a final linear magnification of 400× using a Kappa video camera (Mikroskop System, Näsviken, Sweden) and a Perceptics PixelBuffer image grabber card (Parameter AB, Stockholm, Sweden) mounted in an Apple Macintosh computer (Apple Inc., USA). The gray scale of the darkfield image was adjusted and segmented by using the "enhance contrast" and "density slicing" features of the NIH Image software (version 1.55), National Institutes of Health Image software (version 1.55, Bethesda, MD, USA). After that the contour of the cell-soma had been outlined manually, the density of silver grains over neuronal profiles in the dorsal root ganglia could be assessed automatically. Cells having a hybridization signal of three times the background level or higher were considered positive. For each neuron studied, separate recordings of the area of the soma and the area covered by silver grains were obtained. These data allowed for a calculation of labeling intensity (particle density), over each analyzed neuron. Six spinal cord sections, derived from all three of the animals in each experimental group, were analyzed. They were randomly selected, but in a few cases, sections were excluded due to artifacts. Statistical evaluation of the counts was performed using Prism 2.0 (GraphPad Inc., USA) software. Images were sampled directly from the microscope, using a Nikon 950 and 990 digital camera (Bergström Instrument AB, Solna, Sweden). Representative digital images were mounted with Adobe InDesign software (Adobe Systems Inc., USA) and used for illustration.

Statistics

When comparing the density, in series with three or more different animals or humans, of the silver grains located to neurons in the affected sides DRG's, we have used the one-way ANOVA Kruskal–Wallis statistics (Dunn's Multiple Comparison Test). When it has been only two humans we have used the Mann–Whitney's *t*-test.

RESULTS

The embryonic tissue was used as a positive control of the different mRNA probes and expression patterns similar to what has previously described was found (25, 29–32).

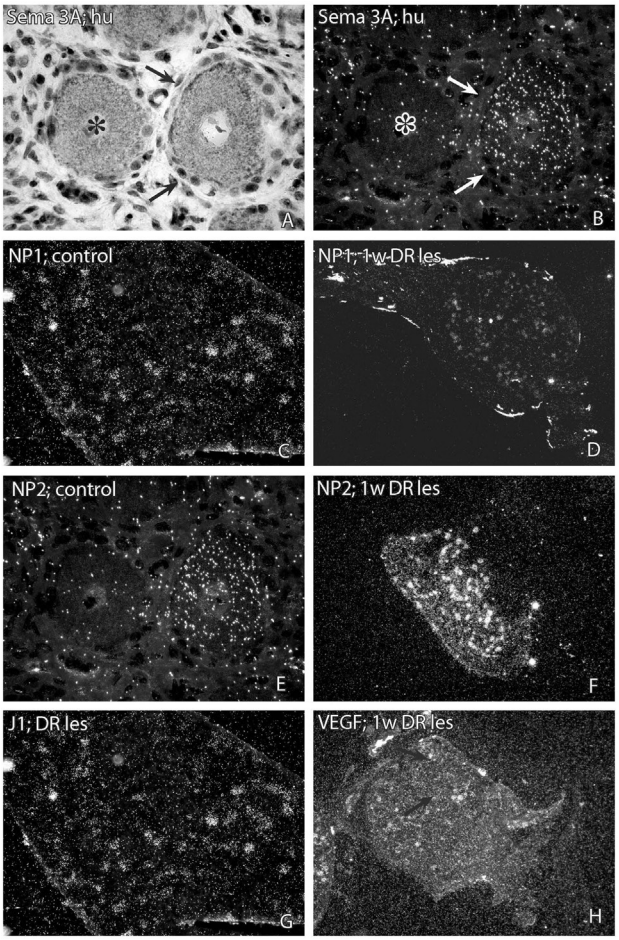

FIGURE 1 | **Photomicrographs showing representative sections from dorsal root ganglia after *in situ* hybridization for detection of semaphorin 3A (SEMA3A) (A,B), neuropilin 1 (NP1) (C,D), neuropilin 2 (NP2) (E,F), J1 (G), or vascular endothelial growth factor (VEGF) mRNA (H)**. **(A)** (=bright field) and **(B)** (=dark field), two neurons in a DRG from a patient treated for root avulsion injury is shown. In dark field illumination it is possible to see that the neuron indicated with arrows has a positive labeling signal for SEMA3A, whereas the neuron indicated by an asterisk is unlabeled. Panel **(C)** is a low magnification micrograph showing a rat DRG hybridized with a NP1 antisense probe. Panel **(D)** shows a section from a DRG one week after dorsal root transection. The labeling signal for NP1 is clearly upregulated in Panel **(D)**. Panels **(E,F)** show DRG from a control rat **(E)** and a rat subjected to dorsal root transection **(F)** after hybridization with a NP2 antisense probe. The labeling signal for NP2 was clearly higher after dorsal root transection **(F)** than in the control DRG **(E)**. The micrograph 1G shows a section from a rat DRG 1 week after dorsal root transection after hybridization with a J1 antisense probe. A number of neurons displayed a positive labeling for J1, although at a similar level as in control rats. The micrograph 1H shows a section from a rat DRG 1 week after dorsal root transection. The small neuron that is indicated by the arrows had a fairly high labeling signal for VEGF mRNA.

Examination of sections incubated with the radiolabeled SEMA3A antisense probe showed that many, but not all, DRG neurons in both rats and humans had a strong labeling signal (**Figure 2**). Image analysis revealed that there was a trend for down regulation of SEMA3A mRNA in the DRG of rats subjected

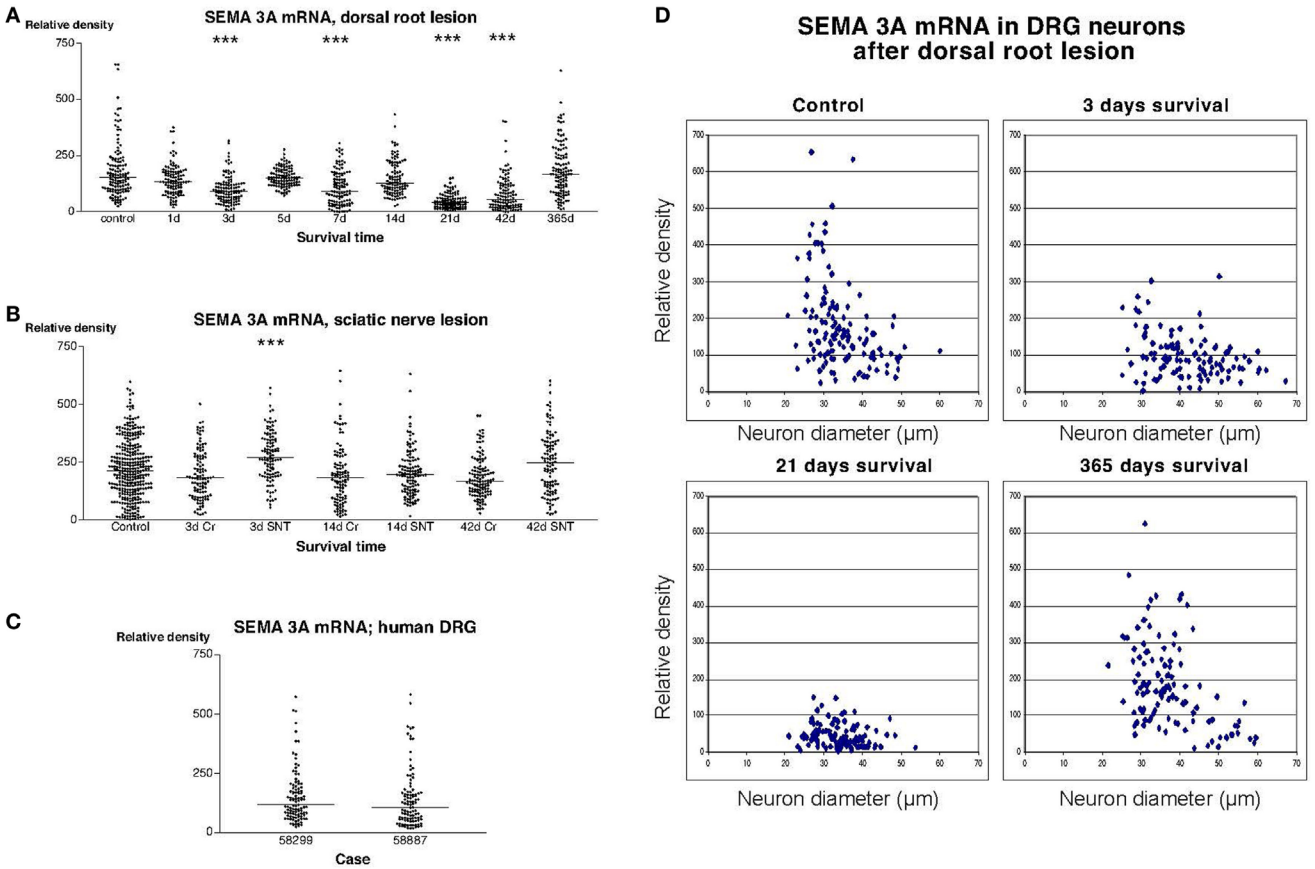

FIGURE 2 | **(A–C)** illustrate the relative density of labeling for semaphorin 3A (SEMA3A) mRNA in dorsal root ganglion neurons at different survival times (expressed in days = d) after dorsal root transection **(A)** or sciatic nerve transection (=SNT) or sciatic nerve crush (=Cr) **(B)**. Each dot represents an analyzed neuron and a horizontal bar indicates the median density at each survival time. The asterisks refer to results obtained with one-way ANOVA Kruskal–Wallis statistics (Dunn's Multiple Comparison Test; ***a difference between controls and the experimental group that is significant according to the test; $P < 0.001$). Panel **(A)** illustrates that there was a transient down regulation in the expression of SEMA3A mRNA after dorsal root transection, whereas the expression of SEMA3A was largely unchanged after sciatic nerve injury **(B)**. Panel **(C)** is a density plot for SEMA3A mRNA in human dorsal root ganglion neurons in two patients who had sustained root avulsion injury. Horizontal bar indicates the median density. **(D)** The diameter (expressed in microns) of the examined dorsal root ganglion neurons (DRG) has been plotted against the labeling density for SEMA3A mRNA in control rat DRG and at different survival times after dorsal root transection. Each examined neuron is represented by a dot in the diagram. In the control diagram is shown that many of the small DRG neurons had a high labeling density. The observed down regulation in SEMA3A after dorsal root transection appeared to affect the small neurons more profoundly than the larger ones. One year after the injury, the size distribution of the labeled neurons was found to be largely restored.

to dorsal rhizotomy. The expression of SEMA3A mRNA reached it lowest level at 21 days after the injury. The mean particle density (i.e., the fraction of the area of the examined DRG neurons that was covered by silver grains) was about 4.6% at this stage, to be compared with 18.5% in control DRG neurons. These values were obtained by recording labeling density in about 100 neurons that were randomly selected in three different rats at each survival time. Although, it may be argued that the measurements are not independent, these recorded values from individual neurons were analyzed using one-way ANOVA Kruskal–Wallis statistics (Dunn's Multiple Comparison Test), which indicated that SEMA3A mRNA was significantly down regulated in the DRG ($P < 0.001$) 3, 7, and 21 days after the dorsal root injury. The labeling was gradually restored and reached a mean value of 18.7% 1 year after the operation. Thus, at 1 year after the trauma, there was no significant difference between control and experimental DRG (**Figure 2A**). This transient down regulation in the labeling intensity was most pronounced in the small DRG neurons (**Figure 2D**). Examination of sections from rats subjected to sciatic nerve transection (SNT) or SNC showed that the labeling signal for SEMA3A in the DRG was largely unaltered after these injuries. Dunn's test indicated a transient upregulation of the SEMA3A signal 3 days after SNT but not after SNC. The signal was normalized 14 days after the injury (**Figure 2B**). The labeling intensity in DRG from patients who had sustained root avulsion injury was similar to what had been observed in rats (**Figures 2A,C**).

In sections from normal rat DRG that had been hybridized with a SEMA3F antisense probe, there was a significant labeling signal in virtually all DRG neurons. We found a trend for down

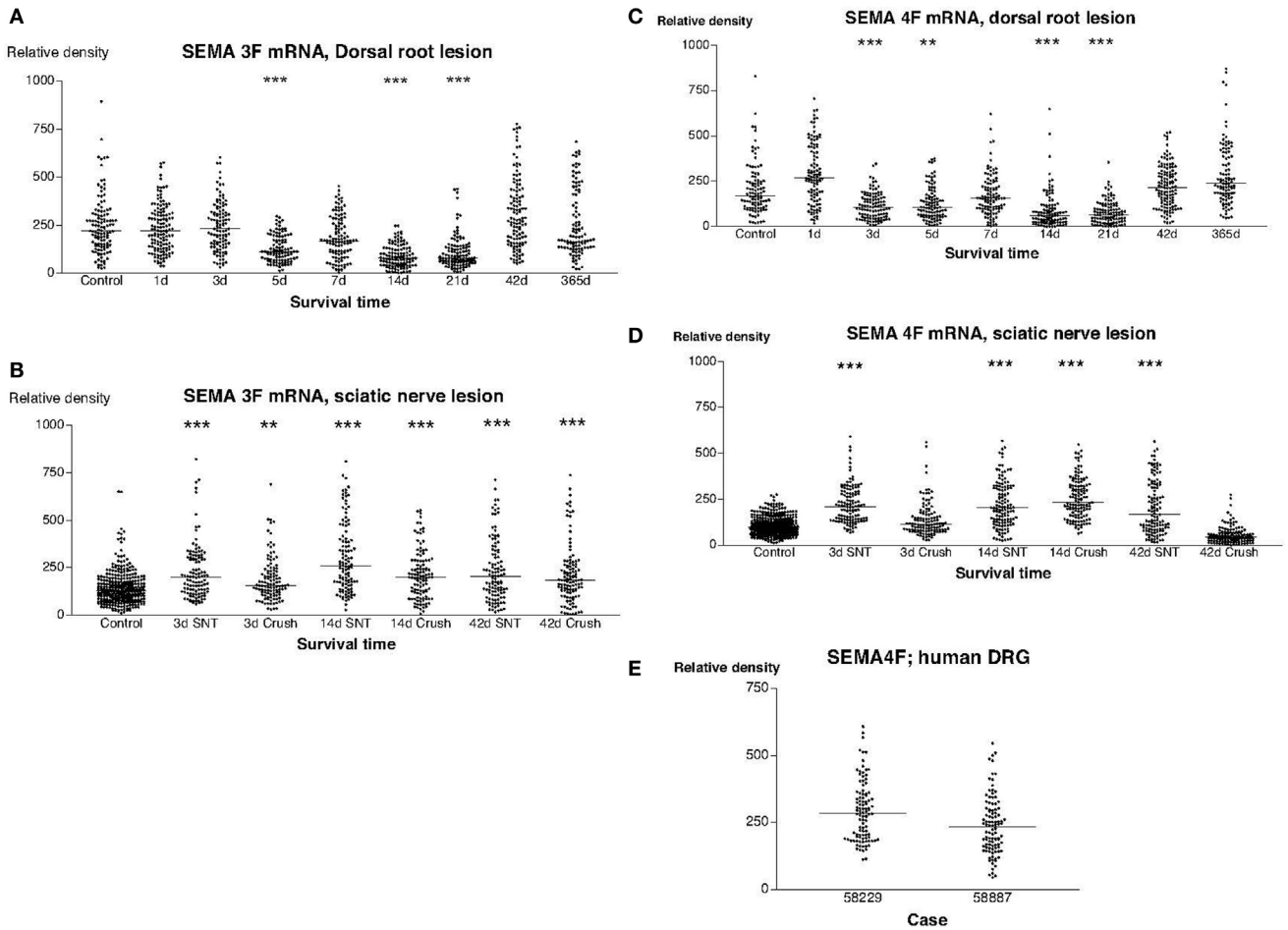

FIGURE 3 | This diagram illustrates the relative density of labeling for semaphorin 3F (SEMA3F) and semaphorin 4F (SEMA4F) mRNA in dorsal root ganglions neuron at different survival times (expressed in days = d) after dorsal root transection (A) or sciatic nerve transection (=SNT) or sciatic nerve crush (SNC) (=Cr) (B). Each dot represents an analyzed neuron and a horizontal bar indicates the median density at each survival time. The asterisks refer to results obtained with one-way ANOVA Kruskal–Wallis statistics (Dunn's Multiple Comparison Test; ***a difference between controls and the experimental group that is significant according to the test; $P < 0.001$). Panel **(A)** illustrates that there was a transient down regulation in the expression of SEMA3F mRNA after dorsal root transection whereas the expression of SEMA3F was significantly upregulated after sciatic nerve injury **(B)**. Panels **(C,D)** illustrate the relative density of labeling for SEMA4F mRNA in dorsal root ganglion neurons at different survival times (expressed in days = d) after dorsal root transection **(C)** or sciatic nerve transection (=SNT) or SNC (=Cr) **(D)**. Each dot represents an analyzed neuron and a horizontal bar indicates the median density at each survival time. The asterisks refer to results obtained with one-way ANOVA Kruskal–Wallis statistics (Dunn's Multiple Comparison Test; ***a difference between controls and the experimental group that is significant according to the test; $P < 0.001$). Panel **(C)** illustrates that there was a transient down regulation in the expression of SEMA4F mRNA after dorsal root transection whereas the expression of SEMA4F showed a transient upregulation after sciatic nerve injury **(D)**. Panel **(E)** is a density plot for SEMA4F mRNA in human dorsal root ganglion neurons in two patients who had sustained root avulsion injury. Horizontal bar indicates the median density.

regulation of labeling with the radiolabeled SEMA3F antisense probe in rats subjected to dorsal root transection (**Figure 3A**). A decrease in mean labeling was observed from day 5 and reached the lowest value at 3 weeks ($P < 0.001$) after the operation. The labeling signal was then gradually restored and was completely restored 1 year after the operation (**Figure 3A**). The labeling for SEMA3F was significantly upregulated in all rats subjected to sciatic nerve lesions (**Figure 3B**). Similar trends were observed in sections hybridized with a SEMA4F antisense probe. Thus, a transient downregultion was observed in rats subjected to dorsal root lesion (**Figure 3C**), whereas a transient upregulation in the labeling signal for SEMA4F could be detected in rats subjected to SNT or SNC (**Figure 3D**). Labeling with the probe for human SEMA4F in sections of DRG from patients after root avulsion seemed to correspond fairly with the findings in rats (**Figures 3C,E**) with regard to intensity and distribution.

In sections from DRG of normal rats incubated with the NP1 antisense probe, there was a detectable labeling signal in many of the DRG neurons (**Figure 1**). This signal was found to be clearly up regulated both after dorsal root lesion (**Figures 1** and **4A**) and after sciatic nerve injury (**Figure 4B**). This upregulation did not seem to be specific for any size-class of DRG neurons (**Figure 4C**). With exception for rats surviving for

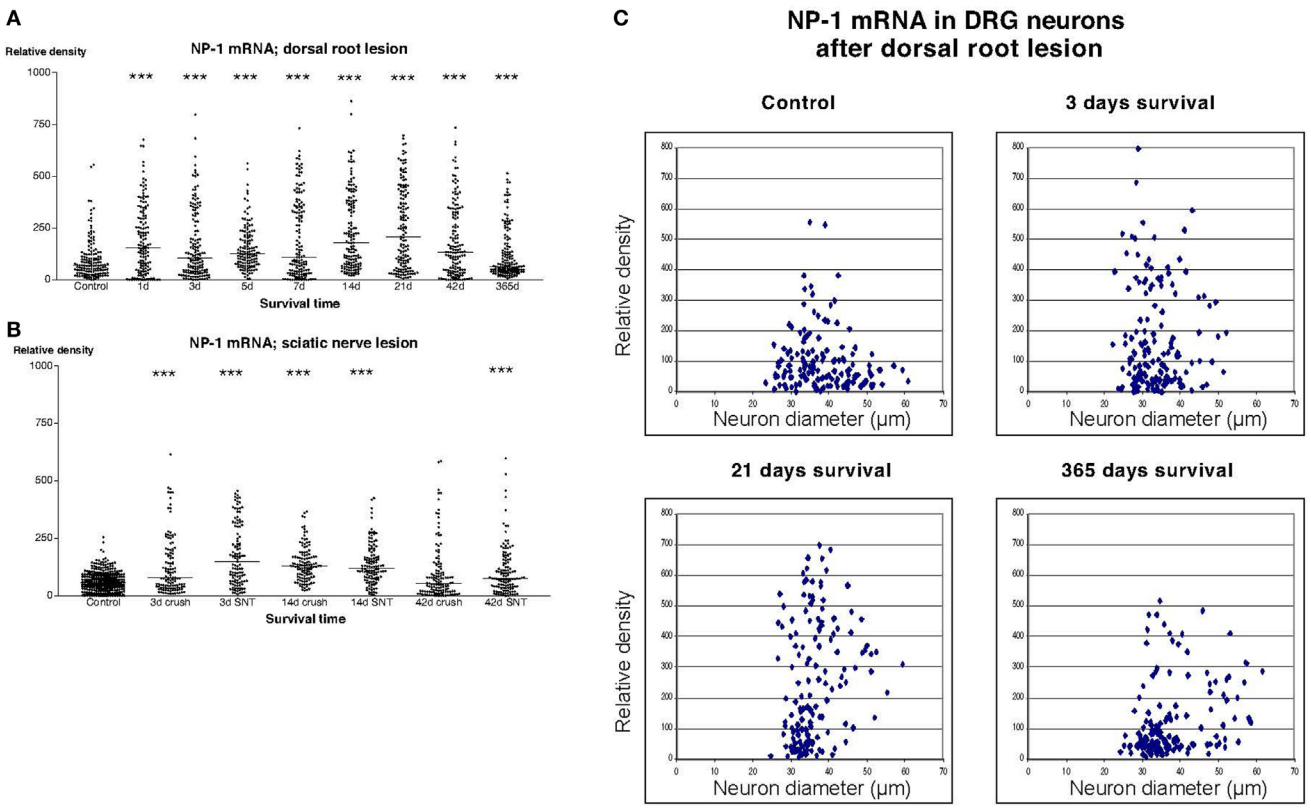

FIGURE 4 | Diagram illustrating the relative density of labeling for neuropilin 1 (NP1) mRNA in dorsal root ganglion neurons at different survival times (expressed in days = d) after dorsal root transection (A) or sciatic nerve transection (=SNT) or sciatic nerve crush (=Cr) (B). Each dot represents an analyzed neuron and a horizontal bar indicates the median density at each survival time. The asterisks refer to results obtained with one-way ANOVA Kruskal–Wallis statistics (Dunn's Multiple Comparison Test; ***a difference between controls and the experimental group that is significant according to the test; $P < 0.001$). There was a transient upregulation in the expression of NP1 mRNA after dorsal root transection [panel **(A)** and after sciatic nerve injury panel **(B)**]. **(C)** The diameter (expressed in microns) of the examined dorsal root ganglion neurons (DRG) has been plotted against the labeling density for NP1 mRNA in control rat DRG and at different survival times after dorsal root transection. Each examined neuron represents a dot in the diagram. The observed upregulation in NP1 after dorsal root transection appeared to affect neurons in all size classes.

42 days after SNC, the difference between normal and operated rats was significant at all survival times according to Dunn's test. Almost identical results were obtained with the probe for NP2. Thus, a large number of the DRG neurons in control rat ganglia had a significant labeling for NP2 (**Figure 1**), and this signal was clearly upregulated in rats subjected to dorsal root transection (**Figure 1**) or sciatic nerve injury. With exception for rats surviving for 42 days after SNC, the labeling signal was elevated at all survival times both after dorsal root lesion and sciatic nerve lesions (**Figures 5A,B**) and the changes did not appear to be size specific (**Figure 5C**).

Also in sections hybridized with the VEGF probe, there was a significant upregulation of the labeling signal at all survival times after dorsal root lesion (**Figure 6A**). Although, still significantly upregulated according to Dunn's test, there seemed to be gradual normalization in the labeling 1 year after the operation. The upregulation of labeling for VEGF affected neurons of all sizes (**Figure 6C**). The labeling for VEGF in DRG of patients treated for avulsion injury (**Figure 6B**) was similar to the findings in rats subjected to dorsal root lesion.

The labeling for J1 mRNA showed two different patterns. With the possible exception for the first postoperative day, there were no detectable changes in the labeling for J1 after dorsal root transection (**Figure 7A**), whereas there was a significant upregulation in the signal for J1 at all examined stages after sciatic nerve injury (**Figure 7B**).

DISCUSSION

In this study, we do investigate the expression of SEMA, neuropilins, and tenascin in different injury models to the dorsal spinal roots. The injuries are either applied to the central axon of the dorsal root (DRT), i.e., the root central to the dorsal root ganglion (DRG), or to the peripheral axon [sciatic nerve transection (SNT) and SNC], the part peripheral to the DRG. These two different injuries to the same neuron results in different regenerative responses, making them interesting models for the study of nerve regeneration and thus for study of nerve guidance molecules, such as SEMA. After an injury to the central axon of DRG neurons, the axons are less able to regenerate

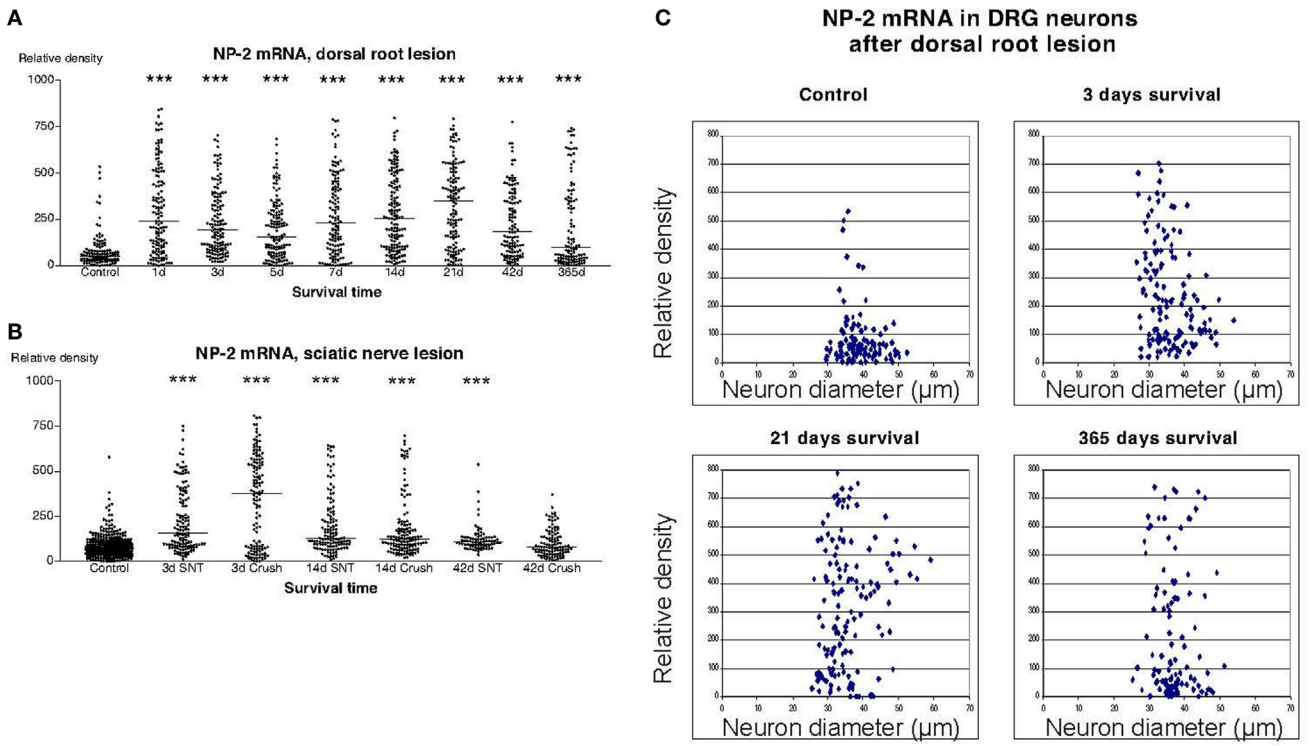

FIGURE 5 | Diagram illustrating the relative density of labeling for neuropilin 2 (NP2) mRNA in dorsal root ganglion neurons at different survival times (expressed in days = d) after dorsal root transection (A) or sciatic nerve transection (=SNT) or sciatic nerve crush (SNC) (=Cr) (B). Each dot represents an analyzed neuron and a horizontal bar indicates the median density at each survival time. The asterisks refer to results obtained with one-way ANOVA Kruskal–Wallis statistics (Dunn's Multiple Comparison Test; ***a difference between controls and the experimental group that is significant according to the test; $P < 0.001$). Panel **(A)** illustrates that there was a transient upregulation in the expression of NP2 mRNA after dorsal root transection. The expression of NP2 in DRG neurons was also found to be increased after sciatic nerve injury **(B)**. **(C)** The diameter (expressed in microns) of the examined dorsal root ganglion neurons (DRG) has been plotted against the labeling density for NP2 mRNA in control rat DRG and at different survival times after dorsal root transection. Each examined neuron represents a dot in the diagram. The observed upregulation in NP2 after dorsal root transection could be observed in neurons of all size classes.

then after injuries to the peripheral axons of the DRG neurons that instead are followed by strong regenerative capacity (1, 2). This interesting difference has been studied in various ways, and it has for example been shown that the growth associated protein GAP-43, a molecular marker for regenerative response after nerve injury (33) is upregulated in DRG neurons after an injury to the peripheral DRG axon but not to the central DRG axon (34). Interestingly, the regeneration of the central DRG axon can be enhanced by concurrent injury to the peripheral DRG axon (2, 35–37), and such injuries do result in cellular responses in DRG neurons typical for a regenerative state, including induction of GAP-43 (34). These kind conditional injuries can also support regeneration of dorsal root axons to enter the spinal cord (3).

Another marker for regenerative responses after nerve injury, activating transcription factor 3 has been studied after injuries to DRG axons and do show a pattern similar to GAP-43 with a strong upregulation in DRG neurons after peripheral axon injury but a much less pronounced expression after central DRG axon injury (38).

We have also previously studied the expression of SEMA and VEGF in an injury model where motoneuron axons are cut in the ventral funiculus within the spinal cord (15, 16, 39). This is an injury model followed by successful regeneration of the injured motoneuron axons through the scar tissue and in to ventral roots (7), which enables us to compare the expression pattern of the SEMA in the present study with the expression of the same factors in a model with successful regeneration.

We show in this study that mRNA for SEMA3A in the DRG neurons was significantly downregulated after a DRT and that its receptor, NP1, showed an instant mRNA upregulation in the DRG following DRT, SNT, and SNC, the latter being opposite to findings from Gavazzi and colleagues who reported an upregulation of NP1 in DRG after SNT but no changes in NP1 mRNA after DRT (40). If considering that DRT is followed by a less vigorous regrowth of axons, it is reasonable to speculate that the down regulation of SEMA3A as shown by us reflects that SEMA3A could be of importance for nerve regrowth in injured DRG. Decreased expression of SEMA3A in motor and sensory neurons during peripheral nerve regeneration has indeed been discussed as a molecular event that is part of the adaptive response related to the success of regenerative neurite outgrowth occurring peripheral nerve injury (41). We have in a previous publication also described increased levels of SEMA3A in both neurons and scar

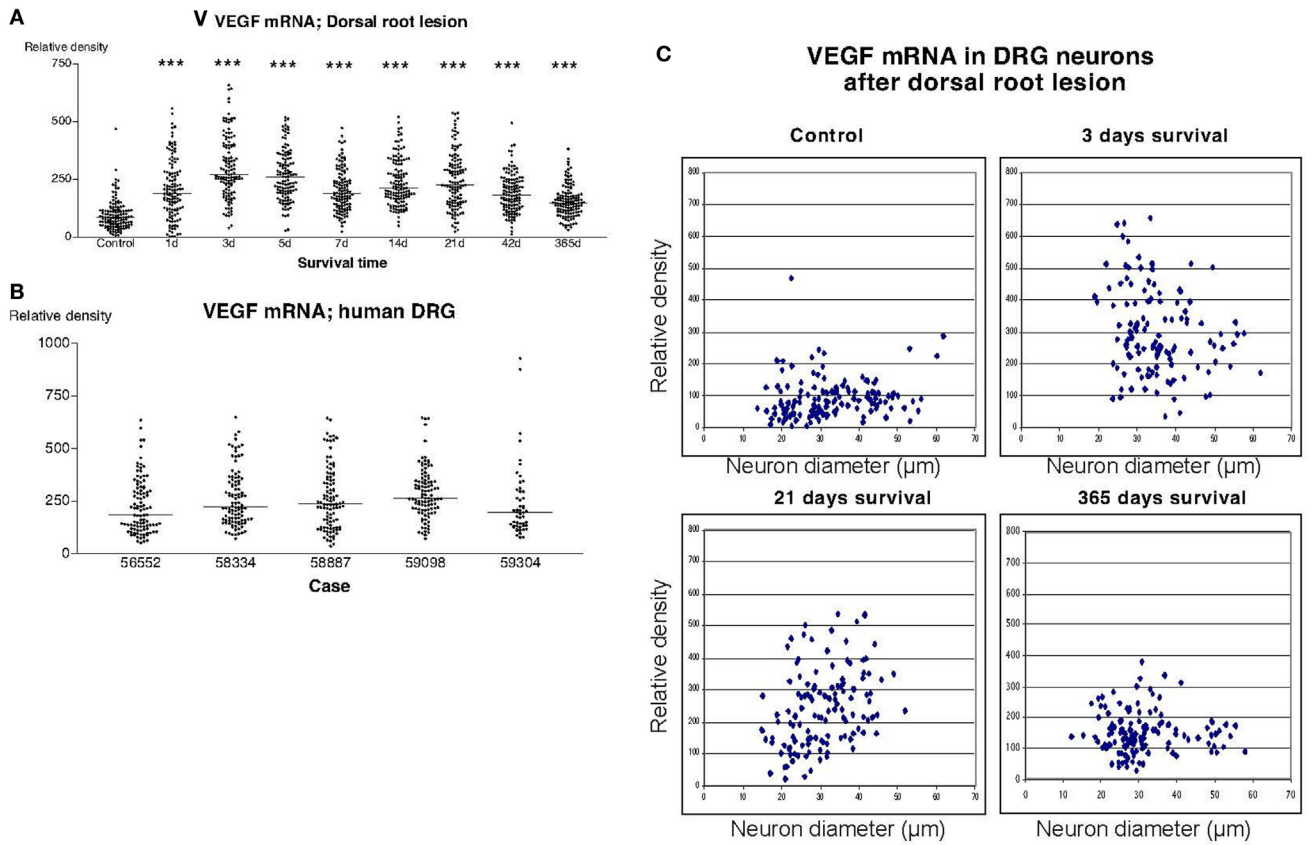

FIGURE 6 | The diagram shown in panel (A) illustrates the relative density of labeling for vascular endothelial growth factor (VEGF) mRNA in dorsal root ganglion neurons at different survival times (expressed in days = d) after dorsal root transection. Each dot represents an analyzed neuron and a horizontal bar indicates the median density at each survival time. The asterisks refer to results obtained with one-way ANOVA Kruskal–Wallis statistics (Dunn's Multiple Comparison Test; ***a difference between controls and the experimental group that is significant according to the test; $P < 0.001$). There was a distinct increase in the expression of VEGF mRNA after dorsal root transection. Panel **(B)** is a density plot for VEGF mRNA in human dorsal root ganglion neurons from five different patients who had sustained root avulsion injury. It can be revealed that the labeling in these patients had a similar intensity as the labeling that was observed in rats subjected to dorsal root transection. **(C)** The diameter (expressed in microns) of the examined dorsal root ganglion neurons (DRG) has been plotted against the labeling density for VEGF mRNA in control rat DRG and at different survival times after dorsal root transection. Each examined neuron is represented by a dot in the diagram. The observed upregulation in VEGF after dorsal root transection appeared to affect neurons of all sizes.

tissue in a model followed by successful nerve regeneration of motoneuron axons (15) making the described down regulation of SEMA3A in a model followed by less successful nerve regeneration interesting. Others have also demonstrated that upregulation of SEMA3A, SEMA3F, NP1, and NP2 are correlated with regrowth in peripheral nerve injuries where expression of these factors were found mainly in Schwann cells distal of the injury (42, 43), again pointing toward possibly positive nerve growth guidance capacities of SEMA3A.

On the other hand, do we in this study not find a consistent upregulation of SEMA3A after SNT and SNC, SNT 3d postoperatively being an exception, see **Figure 2B**, even though these kind of injuries are known to be followed by nerve regeneration (1). SEMA3A is secreted and not membrane bound, which could be of importance for the interpretation of our findings. It might not be that the expression of SEMA3A we find have an impact on the DRG neurons directly but rather on peripheral targets such as the dorsal horn where others have found increased expression of the SEMA3A receptor NP1 after dorsal root rhizotomy (44). In this way, the secreted SEMA3A could possibly interact with NP1 at the dorsal horn and be a part in the well described inhibition of regenerating DRG neuritis over the CNS-PNS border of the dorsal horn (3).

Our findings show a striking trend for downregulation of mRNA for SEMA3F during the examined period after DRT, with a decrease from 42 days and normalization at 1-year post-trauma. On the other hand, did SEMA3F mRNA show an early significant upregulation after SNT. The former finding do correspond to our findings on dorsal root injury and downregulation of SEMA3A as shown in **Figure 2**, while the latter do not correspond to the findings of unchanged SEMA3A levels after sciatic injury. We have previously described that mRNA for SEMA3F has a strong expression in the ventral root on the injured side after a ventral funiculus lesion in adult rats (15), thus in a model followed by

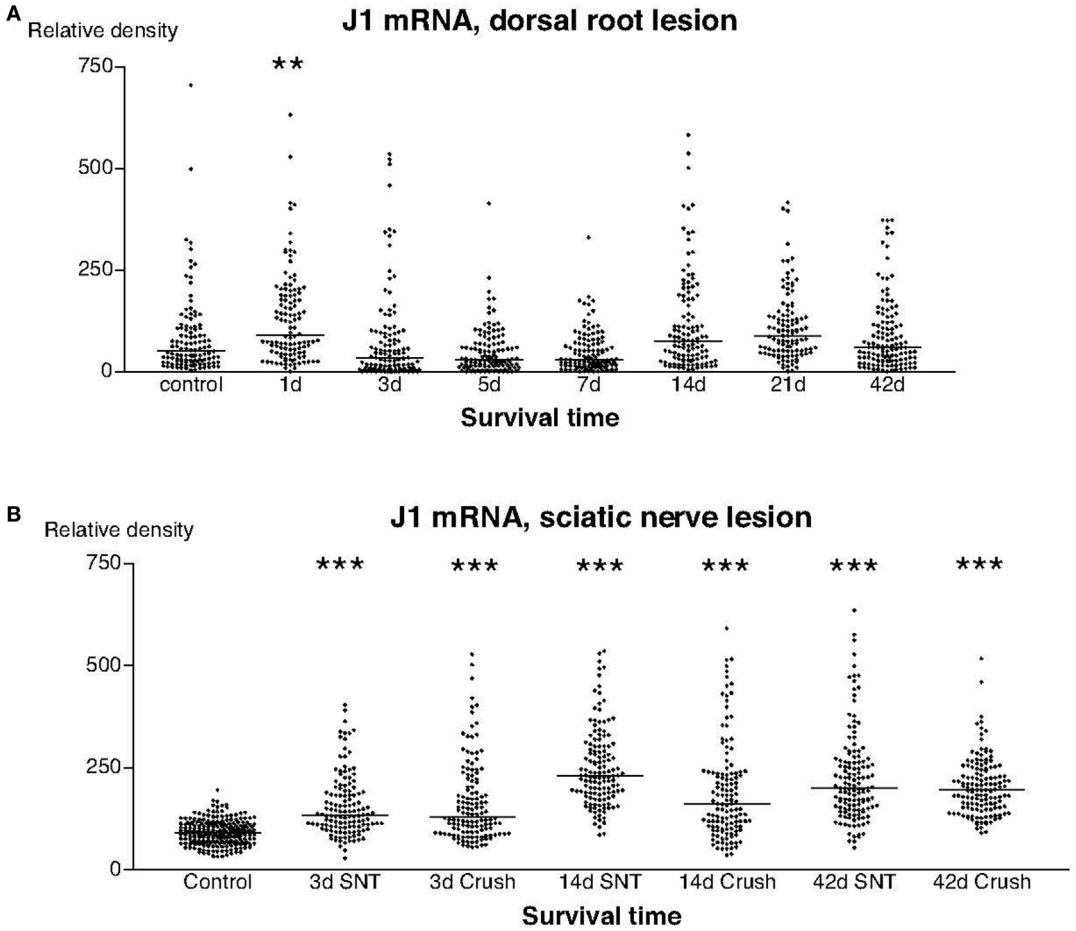

FIGURE 7 | This diagram illustrates the relative density of labeling for J1 mRNA in dorsal root ganglion neurons at different survival times (expressed in days = d) after dorsal root transection (A) or sciatic nerve transection (=SNT) or SNC (=Cr) (B). Each dot represents an analyzed neuron and a horizontal bar indicates the median density at each survival time. The asterisks refer to results obtained with one-way ANOVA Kruskal–Wallis statistics (Dunn's Multiple Comparison Test; ***a difference between controls and the experimental group that is significant according to the test; $P < 0.001$). Panel **(A)** illustrates that the expression of J1 mRNA was largely unchanged after dorsal root transection, whereas the expression of J1 was clearly upregulated after sciatic nerve injury **(B)**.

successful regeneration, which might indicate that the down-regulation shown after DRT reflects the weak regeneration shown after this injury. We observed a significant downregulation of mRNA for SEMA4F in the DRG neurons after a DRT. On the other hand, in the same time, the labeling of mRNA for SEMA4F was instantly higher in the DRG following SNT and SNC. This implicates a role in the post-traumatic regenerative response of adult axotomized DRG neurons.

Vascular endothelial growth factor is a secreted mitogen with importance in regulation of angiogenesis and vascular permeability. Induction of VEGF has been reported both after traumatic spinal cord injuries (16). It has been shown that VEGF do have a direct neurotropic/neuroprotective function (45, 46). For example, Sondell and coworkers have shown that $VEGF_{165}$ could stimulate axon outgrowth from DRG *in vitro* (45). It is known that the neuropilin receptors 1 and 2, NP1 and NP2, are not only receptors for the SEMA but does also function as co-receptors for $VEGF_{165}$ (47) and are as such of importance for the VEGF mediated rearrangement of the actin skeleton in the nerve growth cone (48, 49). Thus, the neuropilins are receptors for two unrelated ligands: SEMA acting as inhibitors of axon growth and VEGF acting as an angiogenic and neurotropic factor. The interplay between VEGF and SEMA are not yet fully understood, but it has been shown that $VEGF_{165}$ and SEMA do compete for the binding sites of NP1 (50). In this work, we did also find a strong upregulation of VEGF mRNA in DRG neurons after dorsal root lesions. We did also find an upregulation of the VEGF co-receptors NP1 and NP2 mRNA that coincide in time with the upregulation of VEGF. In addition, SEM3A mRNA is promptly downregulated during the same time. Since VEGF and SEMA3A both binds to the NP receptors (47), this could imply that there is an interaction between VEGF and SEMA3A *in vivo* in our injury model system and that VEGF could compete with SEMA3A in the binding to the NP receptors. This, in turn, could have a positive impact on the axon growth from DRG neurons after dorsal root lesions. Others

have shown both that VEGF and SEMA do compete for the binding site of NP1 (50) and that $VEGF_{165}$ do inhibit the action of SEMA3A *in vitro.* It has also been shown that DRG neurons in culture could be stimulated to axon growth after addition of $VEGF_{165}$ (45). Our novel findings after dorsal root lesions of VEGF, NP1, and NP2 upregulation and the synchronous downregulation of SEMA3A are, as far as we know, the first possible indications of a VEGF-semaphorin interplay *in vivo*. If our findings of both NP1 and NP2 in combination with VEGF and in association with downregulation of SEMA3A and SEMA3F could reflect a VEGF-NP mediated regenerative machinery cannot be answered within the present study but is an interesting hypothesis.

In this study, we do also present findings on post-traumatic human DRG tissue. The findings might state that the anatomical distribution of SEMA3A, SEMA4F, and VEGF has been detected to have similar patterns in rat and man, and that the mRNA labeling intensity, can be compared to the levels documented in rat sections. One conclusion could be that these systems seem to react in similar ways in both rat and man.

The oligodendrocyte-derived extracellular matrix glycoprotein J1-160/180 (tenascin/J1 or janusin) is a recognition molecule expressed exclusively in the CNS. J1-160/180 has been shown to act as an attractant on astrocytes and repellent toward neurons and growth cones (51). The structural architecture predicted from the amino acid sequence is very similar to that of TN-R (52) and J1 should therefore probably be considered a TN-R isoform (53). Expression of J1 protein in the spinal cord is developmentally regulated, with a peak expression in 2- or 3-week-old animals. We have described the downregulation of mRNA for TN-R and J1 in spinal motoneurons after ventral funiculus lesion (14) and elevated J1 expression in the lesion area, after a cut in the ventral funiculus of the spinal cord (54). In the present study, we report that there were almost no changes in the labeling of mRNA for J1 after DRT compared to SNT and SNC, that both showed significant upregulation during the examined period making it complicated to conclude how J1 can be involved in the different regenerative responses described in these models.

In summary, we do in this study show regulatory patterns of the SEMA/NP-family and VEGF after injuries to the dorsal roots indicating an involvement in regenerative efforts of DRG neurites rather than inhibitory, which is puzzling regarding the supposedly unsuccessful regeneration of injured dorsal root sensory neurons. In addition, recent findings show that the regrowth of nerve roots into the spinal cord and the dorsal root entry zone can be supported under certain circumstances (4). This in summary might indicate that the findings in this study support that injured dorsal roots do have a regenerative capacity and that the regulatory patterns shown in this study is in fact part of the injured dorsal root ganglion cells effort to regenerate.

AUTHOR CONTRIBUTIONS

TL together with MR and MS conducted the main part of the practical laboratory work, surgery, and analysis of the results. HH and WW performed part of the surgery and analysis of sciatic injuries. TC contributed with the clinical material and analysis of the results. SC contributed to analysis of the study. MS supervised the work together with MR.

ACKNOWLEDGMENTS

We gratefully acknowledge Ms. Maria Angeria for excellent technical assistance.

FUNDING

This study was supported by grants from the Swedish Research Council (projects 6815 and 8657), Stiftelsen Marcus and Amalia Wallenbergs Minnesfond and Karolinska Institutet.

REFERENCES

1. Oblinger MM, Lasek RJ. A conditioning lesion of the peripheral axons of dorsal root ganglion cells accelerates regeneration of only their peripheral axons. *J Neurosci* (1984) 4(7):1736–44.
2. Chong MS, Woolf CJ, Turmaine M, Emson PC, Anderson PN. Intrinsic versus extrinsic factors in determining the regeneration of the central processes of rat dorsal root ganglion neurons: the influence of a peripheral nerve graft. *J Comp Neurol* (1996) 370(1):97–104.
3. Chong MS, Woolf CJ, Haque NS, Anderson PN. Axonal regeneration from injured dorsal roots into the spinal cord of adult rats. *J Comp Neurol* (1999) 410(1):42–54.
4. Goncalves MB, Malmqvist T, Clarke E, Hubens CJ, Grist J, Hobbs C, et al. Neuronal RARbeta signaling modulates PTEN activity directly in neurons and via exosome transfer in astrocytes to prevent glial scar formation and induce spinal cord regeneration. *J Neurosci* (2015) 35(47):15731–45. doi:10.1523/JNEUROSCI.1339-15.2015
5. Carlstedt T, Misra VP, Papadaki A, McRobbie D, Anand P. Return of spinal reflex after spinal cord surgery for brachial plexus avulsion injury. *J Neurosurg* (2012) 116(2):414–7. doi:10.3171/2011.7.JNS111106
6. Carlstedt T. New treatments for spinal nerve root avulsion injury. *Front Neurol* (2016) 7:135. doi:10.3389/fneur.2016.00135
7. Risling M, Cullheim S, Hildebrand C. Reinnervation of the ventral root L7 from ventral horn neurons following intramedullary axotomy in adult cats. *Brain Res* (1983) 280(1):15–23.
8. Cullheim S, Carlstedt T, Risling M. Axon regeneration of spinal motoneurons following a lesion at the cord-ventral root interface. *Spinal Cord* (1999) 37(12):811–9.
9. Carlstedt T, Linda H, Cullheim S, Risling M. Reinnervation of hind limb muscles after ventral root avulsion and implantation in the lumbar spinal cord of the adult rat. *Acta Physiol Scand* (1986) 128(4):645–6.
10. Cullheim S, Carlstedt T, Linda H, Risling M, Ulfhake B. Motoneurons reinnervate skeletal muscle after ventral root implantation into the spinal cord of the cat. *Neuroscience* (1989) 29(3):725–33.
11. Hallin RG, Carlstedt T, Nilsson-Remahl I, Risling M. Spinal cord implantation of avulsed ventral roots in primates; correlation between restored motor function and morphology. *Exp Brain Res* (1999) 124(3):304–10.
12. Carlstedt T, Grane P, Hallin RG, Noren G. Return of function after spinal cord implantation of avulsed spinal nerve roots. *Lancet* (1995) 346(8986):1323–5.
13. Carlstedt T, Hultgren T, Nyman T, Hansson T. Cortical activity and hand function restoration in a patient after spinal cord surgery. *Nat Rev Neurol* (2009) 5(10):571–4. doi:10.1038/nrneurol.2009.137
14. Lindholm T, Cullheim S, Carlstedt T, Risling M. Expression of tenascin R and J1 mRNA in motoneurons after a traumatic lesion in the spinal cord. *Neuroreport* (2001) 12(16):3513–7.
15. Lindholm T, Skold MK, Suneson A, Carlstedt T, Cullheim S, Risling M. Semaphorin and neuropilin expression in motoneurons after intraspinal motoneuron axotomy. *Neuroreport* (2004) 15(4):649–54.
16. Sköld M, Cullheim S, Hammarberg H, Piehl F, Suneson A, Lake S, et al. Induction of VEGF and VEGF receptors in the spinal cord after mechanical

spinal injury and prostaglandin administration. *Eur J Neurosci* (2000) 12(10):3675–86.
17. Kolodkin AL, Matthes DJ, Goodman CS. The semaphorin genes encode a family of transmembrane and secreted growth cone guidance molecules. *Cell* (1993) 75(7):1389–99.
18. Nakamura F, Kalb RG, Strittmatter SM. Molecular basis of semaphorin-mediated axon guidance. *J Neurobiol* (2000) 44(2):219–29.
19. Van Battum EY, Brignani S, Pasterkamp RJ. Axon guidance proteins in neurological disorders. *Lancet Neurol* (2015) 14(5):532–46. doi:10.1016/S1474-4422(14)70257-1
20. Behar O, Golden JA, Mashimo H, Schoen FJ, Fishman MC. Semaphorin III is needed for normal patterning and growth of nerves, bones and heart. *Nature* (1996) 383(6600):525–8.
21. Gagliardini V, Fankhauser C. Semaphorin III can induce death in sensory neurons. *Mol Cell Neurosci* (1999) 14(4–5):301–16.
22. Pasterkamp RJ, Peschon JJ, Spriggs MK, Kolodkin AL. Semaphorin 7A promotes axon outgrowth through integrins and MAPKs. *Nature* (2003) 424(6947):398–405. doi:10.1038/nature01790
23. Culotti JG, Kolodkin AL. Functions of netrins and semaphorins in axon guidance. *Curr Opin Neurobiol* (1996) 6(1):81–8.
24. Chen H, Chedotal A, He Z, Goodman CS, Tessier-Lavigne M. Neuropilin-2, a novel member of the neuropilin family, is a high affinity receptor for the semaphorins Sema E and Sema IV but not Sema III. *Neuron* (1997) 19(3):547–59.
25. He Z, Tessier-Lavigne M. Neuropilin is a receptor for the axonal chemorepellent semaphorin III. *Cell* (1997) 90(4):739–51.
26. Kolodkin AL, Levengood DV, Rowe EG, Tai YT, Giger RJ, Ginty DD. Neuropilin is a semaphorin III receptor. *Cell* (1997) 90(4):753–62.
27. Kolk SM, Gunput RA, Tran TS, van den Heuvel DM, Prasad AA, Hellemons AJ, et al. Semaphorin 3F is a bifunctional guidance cue for dopaminergic axons and controls their fasciculation, channeling, rostral growth, and intracortical targeting. *J Neurosci* (2009) 29(40):12542–57. doi:10.1523/JNEUROSCI.2521-09.2009
28. Giger RJ, Pasterkamp RJ, Holtmaat AJ, Verhaagen J. Semaphorin III: role in neuronal development and structural plasticity. *Prog Brain Res* (1998) 117:133–49.
29. Encinas JA, Kikuchi K, Chedotal A, de Castro F, Goodman CS, Kimura T. Cloning, expression, and genetic mapping of Sema W, a member of the semaphorin family. *Proc Natl Acad Sci U S A* (1999) 96(5):2491–6.
30. Skaliora I, Singer W, Betz H, Puschel AW. Differential patterns of semaphorin expression in the developing rat brain. *Eur J Neurosci* (1998) 10(4):1215–29.
31. Giger RJ, Wolfer DP, De Wit GM, Verhaagen J. Anatomy of rat semaphorin III/collapsin-1 mRNA expression and relationship to developing nerve tracts during neuroembryogenesis. *J Comp Neurol* (1996) 375(3):378–92.
32. Carmeliet P, Ferreira V, Breier G, Pollefeyt S, Kieckens L, Gertsenstein M, et al. Abnormal blood vessel development and lethality in embryos lacking a single VEGF allele. *Nature* (1996) 380(6573):435–9.
33. Skene JH, Virag I. Posttranslational membrane attachment and dynamic fatty acylation of a neuronal growth cone protein, GAP-43. *J Cell Biol* (1989) 108(2):613–24.
34. Chong MS, Reynolds ML, Irwin N, Coggeshall RE, Emson PC, Benowitz LI, et al. GAP-43 expression in primary sensory neurons following central axotomy. *J Neurosci* (1994) 14(7):4375–84.
35. Richardson PM, Issa VM. Peripheral injury enhances central regeneration of primary sensory neurones. *Nature* (1984) 309(5971):791–3.
36. Richardson PM, Verge VM. The induction of a regenerative propensity in sensory neurons following peripheral axonal injury. *J Neurocytol* (1986) 15(5):585–94.
37. Lu X, Richardson PM. Inflammation near the nerve cell body enhances axonal regeneration. *J Neurosci* (1991) 11(4):972–8.
38. Linda H, Skold MK, Ochsmann T. Activating transcription factor 3, a useful marker for regenerative response after nerve root injury. *Front Neurol* (2011) 2:30. doi:10.3389/fneur.2011.00030
39. Skold MK, Marti HH, Lindholm T, Linda H, Hammarberg H, Risling M, et al. Induction of HIF1alpha but not HIF2alpha in motoneurons after ventral funiculus axotomy-implication in neuronal survival strategies. *Exp Neurol* (2004) 188(1):20–32. doi:10.1016/j.expneurol.2004.03.024
40. Gavazzi I, Stonehouse J, Sandvig A, Reza JN, Appiah-Kubi LS, Keynes R, et al. Peripheral, but not central, axotomy induces neuropilin-1 mRNA expression in adult large diameter primary sensory neurons. *J Comp Neurol* (2000) 423(3):492–9.
41. Pasterkamp RJ, Giger RJ, Verhaagen J. Regulation of semaphorin III/collapsin-1 gene expression during peripheral nerve regeneration. *Exp Neurol* (1998) 153(2):313–27.
42. Ara J, Bannerman P, Hahn A, Ramirez S, Pleasure D. Modulation of sciatic nerve expression of class 3 semaphorins by nerve injury. *Neurochem Res* (2004) 29(6):1153–9.
43. Scarlato M, Ara J, Bannerman P, Scherer S, Pleasure D. Induction of neuropilins-1 and -2 and their ligands, Sema3A, Sema3F, and VEGF, during Wallerian degeneration in the peripheral nervous system. *Exp Neurol* (2003) 183(2):489–98.
44. Agudo M, Robinson M, Cafferty W, Bradbury EJ, Kilkenny C, Hunt SP, et al. Regulation of neuropilin 1 by spinal cord injury in adult rats. *Mol Cell Neurosci* (2005) 28(3):475–84. doi:10.1016/j.mcn.2004.10.008
45. Sondell M, Sundler F, Kanje M. Vascular endothelial growth factor is a neurotrophic factor which stimulates axonal outgrowth through the flk-1 receptor. *Eur J Neurosci* (2000) 12(12):4243–54.
46. Sondell M, Lundborg G, Kanje M. Vascular endothelial growth factor has neurotrophic activity and stimulates axonal outgrowth, enhancing cell survival and Schwann cell proliferation in the peripheral nervous system. *J Neurosci* (1999) 19(14):5731–40.
47. Soker S, Takashima S, Miao HQ, Neufeld G, Klagsbrun M. Neuropilin-1 is expressed by endothelial and tumor cells as an isoform-specific receptor for vascular endothelial growth factor. *Cell* (1998) 92(6):735–45.
48. Foehring D, Brand-Saberi B, Theiss C. VEGF-induced growth cone enhancement is diminished by inhibiting tyrosine-residue 1214 of VEGFR-2. *Cells Tissues Organs* (2012) 196(3):195–205. doi:10.1159/000334600
49. Olbrich L, Foehring D, Happel P, Brand-Saberi B, Theiss C. Fast rearrangement of the neuronal growth cone's actin cytoskeleton following VEGF stimulation. *Histochem Cell Biol* (2013) 139(3):431–45. doi:10.1007/s00418-012-1036-y
50. Miao HQ, Soker S, Feiner L, Alonso JL, Raper JA, Klagsbrun M. Neuropilin-1 mediates collapsin-1/semaphorin III inhibition of endothelial cell motility: functional competition of collapsin-1 and vascular endothelial growth factor-165. *J Cell Biol* (1999) 146(1):233–42.
51. Schachner M, Taylor J, Bartsch U, Pesheva P. The perplexing multifunctionality of janusin, a tenascin-related molecule. *Perspect Dev Neurobiol* (1994) 2(1):33–41.
52. Fuss B, Wintergerst ES, Bartsch U, Schachner M. Molecular characterization and in situ mRNA localization of the neural recognition molecule J1-160/180: a modular structure similar to tenascin. *J Cell Biol* (1993) 120(5):1237–49.
53. Pesheva P, Probstmeier R. The yin and yang of tenascin-R in CNS development and pathology. *Prog Neurobiol* (2000) 61(5):465–93.
54. Deckner M, Lindholm T, Cullheim S, Risling M. Differential expression of tenascin-C, tenascin-R, tenascin/J1, and tenascin-X in spinal cord scar tissue and in the olfactory system. *Exp Neurol* (2000) 166(2):350–62. doi:10.1006/exnr.2000.7543

Conflict of Interest Statement: The authors declare that the research was conducted in the absence of any commercial or financial relationships that could be construed as a potential conflict of interest.

The reviewer FC declared a shared affiliation, though no other collaboration, with one of the authors MKS to the handling Editor, who ensured that the process nevertheless met the standards of a fair and objective review.

frontiers in Neurology

ORIGINAL RESEARCH
published: 23 December 2016
doi: 10.3389/fneur.2016.00238

A Review of the Segmental Diameter of the Healthy Human Spinal Cord

Arvid Frostell[1], Ramil Hakim[1], Eric Peter Thelin[1], Per Mattsson[1] and Mikael Svensson[1,2]*

[1] *Department of Clinical Neuroscience, Karolinska Institutet, Stockholm, Sweden,* [2] *Department of Neurosurgery, Karolinska University Hospital, Stockholm, Sweden*

Knowledge of the average size and variability of the human spinal cord can be of importance when treating pathological conditions in the spinal cord. Data on healthy human spinal cord morphometrics have been published for more than a century using different techniques of measurements, but unfortunately, comparison of results from different studies is difficult because of the different anatomical landmarks used as reference points along the craniocaudal axis for the measurements. The aim of this review was to compute population estimates of the transverse and anteroposterior diameter of the human spinal cord by comparing and combining previously published data on a normalized craniocaudal axis. We included 11 studies presenting measurements of spinal cord cross-sectional diameters, with a combined sample size ranging from 15 to 488 subjects, depending on spinal cord level. Based on five published studies presenting data on the lengths of the segments of the spinal cord and vertebral column, we calculated the relative positions of all spinal cord neuronal segments and vertebral bony segments and mapped measurements of spinal cord size to a normalized craniocaudal axis. This mapping resulted in better alignment between studies and allowed the calculation of weighted averages and standard deviations (SDs) along the spinal cord. These weighted averages were smoothed using a generalized additive model to yield continuous population estimates for transverse and anteroposterior diameter and associated SDs. The spinal cord had the largest transverse diameter at spinal cord neuronal segment C5 (13.3 ± 2.2), decreased to segment T8 (8.3 ± 2.1), and increased slightly again to 9.4 ± 1.5 at L3. The anteroposterior diameter showed less variation in size along the spinal cord at C5 (7.4 ± 1.6), T8 (6.3 ± 2.0), and L3 (7.5 ± 1.6). All estimates are presented in millimeters ± 2 SDs. We conclude that segmental transverse and anteroposterior diameters of the healthy human spinal cord from different published sources can be combined on a normalized craniocaudal axis and yield meaningful population estimates. These estimates could be useful in routine management of patients with neurodegenerative diseases as well as for clinical research and experimental applications aimed at surgical spinal cord repair.

Keywords: spinal cord, reference point conversion, morphometry, segmental diameter, vertebral segment, neuronal segment

Abbreviations: CT, computed tomography; MRI, magnetic resonance imaging; C, cervical; T, thoracic; L, lumbar; S, sacral.

OPEN ACCESS

Edited by:
Mattias K. Sköld,
Uppsala University, Sweden

Reviewed by:
Claire Wyart,
Brain and Spinal cord Institute (ICM), France
Michael G. Fehlings,
University of Toronto, Canada

****Correspondence:***
Arvid Frostell
arvid.frostell@ki.se

Specialty section:
This article was submitted to Neurotrauma, a section of the journal Frontiers in Neurology

Received: *15 September 2016*
Accepted: *09 December 2016*
Published: *23 December 2016*

Citation:
Frostell A, Hakim R, Thelin EP, Mattsson P and Svensson M (2016) A Review of the Segmental Diameter of the Healthy Human Spinal Cord. Front. Neurol. 7:238. doi: 10.3389/fneur.2016.00238

INTRODUCTION

The spinal cord constitutes the main channel of afferent and efferent signaling between the body and the brain, and pathology in the spinal cord typically leads to significant lifelong functional deficits in afflicted patients, regardless of traumatic or autoimmune etiology (e.g., spinal cord injury and multiple sclerosis).

Knowledge of the average size and variation of the human spinal cord can be of importance when treating pathological conditions in the spinal cord. It is known that patients suffering from multiple sclerosis have a reduced cross-sectional area compared to healthy matched controls (1). These case-control studies typically suffer from low power and without population estimates, it can be difficult to determine whether a specific patient should be considered to have a pathologically small spinal cord. Furthermore, many experimental strategies for the treatment of acute and chronic traumatic spinal cord injuries are in different phases of development (2). In all studies where a premade device, instrumentation, or otherwise physical object needs to be applied to the spinal cord, the population estimates of spinal cord size are of importance because they represent the variation in physical dimensions that will be encountered when operating on patients.

Data on healthy human spinal cord morphometrics have been published for more than a century using different techniques of measurements and different reference points along the craniocaudal axis of the spinal cord. Imaging techniques such as computed tomography (CT) can be used to detect soft-tissue changes and damage to vertebrae, while magnetic resonance imaging (MRI) is most appropriate for defining neuronal tissue (3–5). Voxel-based techniques, implemented on MRI images, are available for spinal cord cross-sectional area measurement as a means for fast and comprehensive assessment of volumetric changes (6). Although these imaging techniques give important information about the existence of damage to vertebrae and/or neuronal tissue, the techniques do not provide an exact methodology for determining the location and morphometries of an affected spinal cord neuronal segment. The main disadvantage with the radiological approaches is inadequate resolution. Therefore, histological studies have also been implemented. However, neuronal tissue does not retain shape postmortem, introducing other technical challenges and possible bias.

The human spinal cord is made up of 30 neuronal segments distributed along the spinal cord in eight cervical, 12 thoracic, 5 lumbar, and 5 sacral segments. The spinal cord is positioned in the vertebral canal of the vertebral column. The vertebral column is made up of 24 segments with 7 cervical, 12 thoracic, and 7 lumbar segments. However, the spinal cord terminates approximately between lumbar vertebrae L1 and L2, and, therefore, the 30 spinal cord neuronal segments are distributed over 20 vertebral bony segments. Most radiological techniques cannot determine spinal cord neuronal segment level, but instead, rely on reporting the vertebral bony segment level. In contrast, postmortem studies commonly rely on the spinal rootlets for determining spinal cord neuronal segmental level. Comparison between and combination of results from different studies are inherently difficult because of the diverse anatomical landmarks used for the measurements.

This review sought to compute population estimates of the transverse and anteroposterior diameter of the entire human spinal cord by comparing and combining previously published data on a normalized craniocaudal axis.

MATERIALS AND METHODS

Studies and Data

Inclusion in the Analysis

We searched PubMed for original research publications reporting morphometric data on the human spinal cord. Studies not found in PubMed but referred to in the included studies were also added. **Table 1** shows the studies presenting cross-sectional measurements of the human spinal cord, while **Table 2** shows the studies presenting longitudinal measurements along the craniocaudal axis of the spinal cord neuronal segments. We also included three studies presenting the length of the vertebral bony segments in **Table 2** (7–9).

Extracting Data from Studies

Most of the studies included did not present the raw data from their measurements; instead, averages and standard deviations (SDs) were provided. Some studies presented their data in graphical instead of numerical format. To ensure correct extraction of data from these studies, we imported images of the graphs into a

TABLE 1 | Studies presenting measurements of the cross-sectional diameter of the human spinal cord included in this review.

Article	Method	Reference point	Segments measured	Number of subjects
Elliot (23)	Postmortem examination	Neuronal	C5, T6, L5	102
Nordqvist (16)	Postmortem X-ray myelography	Vertebral	C2-L1	18
Thijssen et al. (17)	*In vivo* CT myelography	Vertebral	C1-T1	20
Lamont et al. (18)	*In vivo* X-ray myelography	Vertebral	C1-T1	69
Sherman et al. (4)	*In vivo* MRI	Vertebral	C1-T3	66
Kameyama et al. (19)	Postmortem examination	Neuronal	C2-T1	14
Kameyama et al. (19)	Postmortem examination	Neuronal	C7	152
Kameyama et al. (20)	Postmortem examination	Neuronal	C2-S3	12
Fountas et al. (21)	*In vivo* CT myelography	Vertebral	C2-C7	102
Ko et al. (22)	Postmortem examination	Neuronal	C3-S5	15
Zaaroor et al. (5)	*In vivo* MRI	Vertebral	C1-L1	20

C, cervical; T, thoracic; L, lumbar; CT, computed tomography; MRI, magnetic resonance imaging.

TABLE 2 | Studies presenting measurements of the length of the human spinal cord neuronal segments and verebral bony segments included in this review.

Article	Method	Reference point	Segments measured	Number of subjects
Donaldson and Davis (24)	Postmortem examination	Neuronal	C1-S5	4
Panjabi et al. (7–9)	Postmortem examination	Vertebral	C2-L5	12
Ko et al. (22)	Postmortem examination	Neuronal	C3-S5	15
Cadotte et al. (10)	*In vivo* MRI	Neuronal/vertebral	C3-C8/C3-C7	10

C, cervical; L, lumbar; S, sacral.

CAD-program (Rhino 5 for Mac, Robert McNeel & Associates) and used the internal measurements tool to extract the precise values from the graphs.

Relative Lengths of Segments

Calculating Relative Lengths of Spinal Cord Neuronal Segments

Using the data from the studies in **Table 2**, we calculated the relative length of each spinal cord neuronal segment by simply dividing the length of each segment by the total length of the spinal cord. By estimating the segmental diameter, the measurements from the different studies were weighted according to the number of subjects (i.e., individuals) in each study.

Calculating Relative Lengths of Vertebral Bony Segments and Aligning Spinal Cord Neuronal Segments

Using the data from the studies in **Table 2**, we also calculated the relative length of each vertebral bony segment using the same method described above for the neuronal segments. A vertebral bony segment was defined as the vertebra and half of the two adjacent intervertebral disks. The disks were assumed to increase in size proportionally to the vertebrae.

There were no measurements for vertebral segments C1 and C2 in the studies that we found. Their respective ratios were approximated by aligning vertebral bony segments with spinal cord neuronal segments in the cervical region according to Cadotte et al. (10). Specifically, the distance between the midpoint of spinal cord neuronal segment C3 and vertebral bony segment C3 was set to 1.3 times the distance between spinal cord neuronal segments C3 and C4. Finally, we assumed that both the spinal cord and the vertebral column terminated at the same cranial level and divided the distance equally between C1 and C2 vertebral bony segments. Therefore, our calculated relative sizes of C1 and C2 should be considered approximations and interpreted with care.

Relative Positioning of Segments

Relative Positioning and Scaling of Spinal Cord Neuronal Segments and Vertebral Bony Segments

To align the spinal cord neuronal segments with the vertebral bony segments, we multiplied all cumulative percentages for vertebral bony segments by 1.29. This scaling factor was calculated by dividing the cumulative percentage of entire spinal cord (100%) with the cumulative percentage of the vertebral column at vertebral bony segment L1. This new scaling of vertebral bony segments set the caudal end of the L1 vertebral bony segment equal to the caudal end of spinal cord neuronal segment S5. As a result, the positioning depends on knowledge of the positions of the C3 and C4 spinal cord neuronal segments relative to the C3 vertebral bony segment presented by Cadotte et al. (10) and the level of termination of the spinal cord between vertebral bony segments L1 and L2 (11).

Corrected Positioning of Transverse Diameter Measurements of the Human Cervical Spinal Cord

The positions of the segments shown in **Figure 1** were used to find the correct relative positions of each cross-sectional measurement along a normalized craniocaudal axis of the human spinal cord. Each measurement was placed as closely as possible to the anatomical position described by the original authors, with respect to the type of segmental reference used in the study (spinal cord neuronal segment or vertebral bony segment) as well as the positioning on that specific segment (cranial end of segment, midpoint of segment, or caudal end of segment).

Evaluating the Corrected Positioning of Measurements

To estimate the effect of adjusted craniocaudal positions on transverse diameter measurements of the human cervical spinal cord shown in **Figure 2**, we fitted a linear regression model, before and after correction of craniocaudal position:

$$Transverse\ Diameter \sim \beta_1 * Position + \beta_2 * Position^2 + \beta_3 * Study$$

The squared term was added because the cervical spinal cord transverse diameter approximates the shape of a second-degree polynomial, and the dummy term study was added to correct for differences in intercept between the studies. Adjusted R-squared was used as a measure of alignment of the cervical intumescences between studies. Confidence intervals for the adjusted R-squared were estimated using a 1,000 iteration bootstrap.

Weighted Averages

Calculating Weighted Averages and Variances along the Spinal Cord

To combine the cross-sectional measurements of the human spinal cord from all studies into single estimates, we calculated a moving weighted average. First, measurements from all studies were aligned along their correct position on our corrected craniocaudal axis described above and in **Figures 1** and **2**.

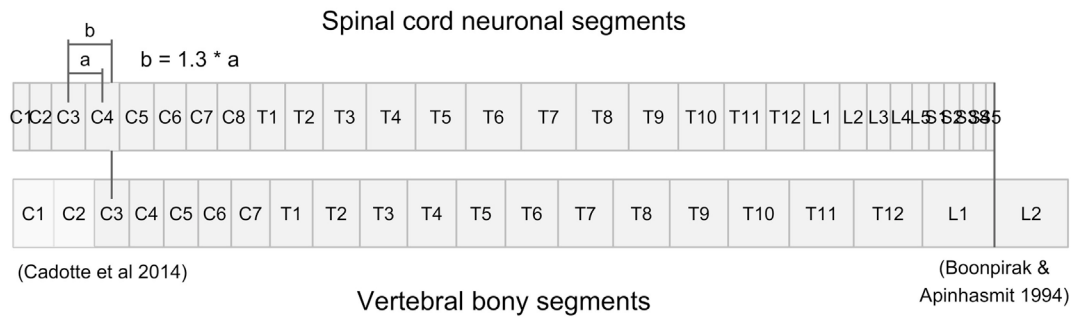

FIGURE 1 | **Figure illustrates the relative positions of each neuronal spinal cord segment and vertebral bony segment in the human spine**. Relative positions were calculated using data from **Tables 3** and **4**, together with relative positions of the C3-vertebral and C3-neuronal segment (10) and the mean spinal cord termination in the spinal canal at L1/L2 (11).

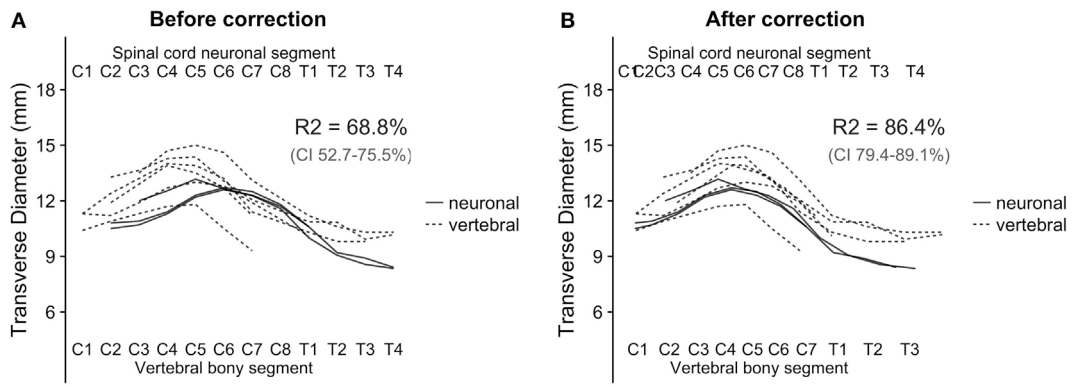

FIGURE 2 | **(A,B)**: with the relative positions of spinal cord neuronal segments and vertebral bony segments illustrated in **Figure 1**, we plotted measurements of the transverse diameter of the cervical spinal cord. In panel **(A)**, the measurement of the transverse diameter of the spinal cord is not corrected for craniocaudal position, and, therefore, the cervical intumescence is misaligned between studies with different reference points. In panel **(B)** (corrected for craniocaudal position), the intumescence appears aligned. The difference in alignment was tested by fitting a second degree polynomial regression to the data points. Bootstrapping confidence intervals for the two estimates of R2 (for corrected and uncorrected, respectively) showed that the confidence intervals were non-overlapping, indicating a substantial improvement of alignment after correction.

Thereafter, starting at the cranial end, four consecutive measurements of spinal cord diameter were combined into a single average, weighted by the number of subjects in the comprising studies for the four included measurements. The average position along the craniocaudal axis of the four measurements was used as the new position for the weighted average. Next, the most cranial of the four measurements was dropped, and the closest measurement caudal to the three remaining measurements was included to create a new group of four measurements, with a new weighted average and a new position along the craniocaudal axis.

Moving weighted variances were calculated using the same method as described for the moving weighted averages. The calculated variances were then converted to weighted SDs.

Population Estimates

Constructing Continuous Population Estimates with a Generalized Additive Model

To construct continuous population estimates and achieve further smoothing, a generalized additive model was used to fit the weighted averages and weighted SDs. We used the smoothing function of ggplot2 (12) in *R* (13) with the formula $y \sim s(x, k = 12)$, allowing a 12° polynomial function to fit the data.

Extracting Point Values of Continuous Population Estimates along the Spinal Cord

To facilitate comparison between our continuous population estimates and other studies, we extracted values for each spinal

cord neuronal segment and vertebral bony segment. The number of subjects measured for a given segment was defined as the total number of subjects included in any study with a calculated craniocaudal position inside the cranial and caudal limits of the segment in question. This was used as an approximation of sample size, as there is no obvious way of calculating exact sample size for different portions of a smoothing function.

Number of Measurements and Relative Contribution of Studies along the Spinal Cord

To present the total number of measurements included at different points along the craniocaudal axis of the spinal cord, we plotted the total number of measurements in each vertebral bony segment in **Figure 6A**. **Figure 6B** shows the relative contribution of each included study along the spinal cord, and **Figure 6C** shows the relative contribution of different methods for obtaining measurements.

Software

Data was gathered in Microsoft Excel and stored as comma-separated values (.csv), all calculations were performed in *R* (13), and graphs were produced with the ggplot2 and cowplot packages (12, 14). Bootstrapping was performed with the boot package (15).

RESULTS

Studies and Data

Studies Included in the Analysis

Data on the diameter of the healthy human spinal cord were available from various published sources, covering more than 100 years of research and various acquisition methodologies (4, 5, 16–24). The published papers differed in terms of methodology of measurement, anatomical reference points, segments measured, and the number of subjects included. Six published papers reported data on the lengths of the spinal cord neuronal and vertebral bony segments (7–9, 22).

All studies reported SDs of measurements, except for the following: Fountas et al. (21), Ko et al. (22), and Nordqvist (16). Donaldson and Davis (24) did not report SDs, but all raw data was presented in the paper, so the SDs could be computed. Raw data for measurements of anteroposterior diameter in Nordqvist (16) was also presented in the paper, but not for transverse diameter. **Tables 1** and **2** give an overview of included studies.

Relative Lengths of Segments

Relative Length of Spinal Cord Neuronal Segments

The longest spinal cord neuronal segments were found in the thoracic spinal cord, and each segment constituted approximately 5% of the whole spinal cord. Multiplying the relative length of a spinal cord neuronal segment in **Table 3** with the average length of the spinal cord yielded segments lengths well above 2 cm in the thoracic spinal cord and around 1.5 cm in the cervical spinal cord. The calculated relative lengths of each spinal cord neuronal segment are presented in **Table 3**.

TABLE 3 | Relative lengths of human neuronal spinal cord segments.

Segment	Percentage of spinal cord	Cumulative percentage of spinal cord
C1	1.6	1.6
C2	2.2	3.9
C3	3.5	7.3
C4	3.5	10.8
C5	3.5	14.3
C6	3.3	17.6
C7	3.2	20.8
C8	3.4	24.1
T1	3.6	27.7
T2	3.9	31.6
T3	4.4	36
T4	5	41
T5	5.1	46.1
T6	5.6	51.8
T7	5.6	57.4
T8	5.4	62.7
T9	5.1	67.8
T10	4.7	72.4
T11	4.3	76.7
T12	3.9	80.6
L1	3.6	84.2
L2	2.8	87
L3	2.4	89.4
L4	2.2	91.6
L5	1.7	93.3
S1	1.5	94.9
S2	1.6	96.4
S3	1.4	97.8
S4	1.3	99.1
S5	0.9	100

*With data from the articles in **Table 2**, we calculated the relative proportions of each spinal cord neuronal segment relative to the length of the whole spinal cord.*
C, cervical; T, thoracic; L, lumbar, S, sacral.

Relative Length of Vertebral Bony Segments

The vertebral bony segments became longer in the caudal direction, with the lumbar vertebrae being the longest. The lumbar vertebrae constitute almost 6% each of the whole vertebral column, or 3.5 cm per segment. The absolute measurement is naturally highly dependent on the length of torso of the individual. The calculated relative length of each vertebral bony segment is presented in **Table 4**.

Relative Positioning of Segments

Effect of Corrected Positioning of Transverse Diameter Measurements of the Human Cervical Spinal Cord—*R*-Squared and Bootstrap

Figure 1 shows the alignment of spinal cord neuronal segments and vertebral bony segments calculated by our method. **Figure 2A** shows a raw positioning using only segment index, and **Figure 2B** shows our best effort to position measurements of the transverse diameter of the human cervical spinal cord correctly along a normalized craniocaudal axis.

To estimate the effect of the adjustment of craniocaudal position of measurements, we set up two second-degree polynomial regression models. The *R*-squared value for Model 1 (uncorrected positioning) was 68.8% and 86.4% for Model 2 (corrected positioning), which was applied to the corrected data shown in

TABLE 4 | Relative lengths of human vertebral bony segments.

Segment	Percentage of vertebral column	Cumulative percentage of vertebral column
C1	3.2[a]	3.2
C2	3.2[a]	6.4
C3	2.8	9.1
C4	2.7	11.9
C5	2.7	14.6
C6	2.6	17.2
C7	3.1	20.2
T1	3.4	23.6
T2	3.7	27.3
T3	3.7	31.1
T4	3.9	34.9
T5	3.9	38.8
T6	4.2	42.9
T7	4.3	47.3
T8	4.5	51.7
T9	4.6	56.3
T10	4.8	61.2
T11	5.1	66.2
T12	5.4	71.7
L1	5.7	77.3
L2	5.8	83.1
L3	5.7	88.8
L4	5.7	94.6
L5	5.5	100

[a]*Approximated.*

With data from Panjabi et al. (7–9), we calculated the relative proportions of each vertebral bony segment relative to the length of the whole vertebral column. One vertebral bony segment was defined as the vertebra and half of both adjacent intervertebral disks. There was no data for segments C1 and C2, and their respective percentages were approximated using the relative positions of C3 and C4 spinal cord neuronal segments and C3 vertebral bony segment from Cadotte et al. (10), with the assumption that the upper end of the C1 spinal cord neuronal segment was aligned with the upper end of the C1 vertebral bony segment and the termination of the spinal cord was located between vertebral bony segments L1 and L2.

C, cervical; T, thoracic; L, lumbar.

Figure 2B. The 95% confidence intervals for the *R*-squared values were non-overlapping, indicating a robust difference.

The numerical results from the models and bootstraps are presented with the underlying data in **Figures 2A,B**.

Weighted Averages

Weighted Averages along the Spinal Cord

To combine the cross-sectional measurements and SDs of the human spinal cord from all studies into single estimates, we calculated weighted averages. **Figure 5** shows the raw weighted averages and SDs along the spinal cord.

Population Estimates

Continuous Population Estimates along the Spinal Cord

To construct continuous population estimates and achieve further smoothing, a generalized additive model was fit to the weighted averages and weighted SDs.

The smoothed continuous population estimates of human spinal cord transverse and anteroposterior diameters are shown in **Figure 3** (cervical spinal cord with original data from the studies), **Figure 4** (whole spinal cord with original data from the studies), and **Figure 5** (whole spinal cord with weighted averages and SDs). The transverse diameter of the spinal cord showed the expected shape with a marked cervical intumescence and a smaller lumbar intumescence. The anteroposterior diameter decreased throughout the spinal cord.

Point Values of Continuous Population Estimates along the Spinal Cord

To facilitate comparison between our continuous population estimates and other studies, we extracted exact values for each spinal cord neuronal segment as well as vertebral bony segment.

Results for each spinal cord neuronal segment are presented in **Table 5** and for vertebral bony segment in **Table 6**.

Number of Measurements and Relative Contribution of Studies along the Spinal Cord

As seen in **Figure 6A**, the number of measurements in the cervical spinal cord is much greater than in the thoracic, lumbar, and sacral parts, with around 10 times the sample sizes. The proportion of *in vivo* methods is also greater in the cervical spinal cord (**Figures 6B,C**).

DISCUSSION

We estimated normal human spinal cord transverse and anteroposterior diameter from previously published data. To compare and combine these different studies, we created and analyzed a conversion method to place measurements correctly along a standardized craniocaudal axis. We created weighted averages of measurements and combined them with a generalized additive model to create a final continuous population estimate of transverse and anteroposterior diameter, as well as the associated SDs along the craniocaudal axis of the entire human spinal cord.

Studies and Data

Studies Included in the Analysis

We included a variety of studies from different eras of research using different methodologies. We deemed this necessary because of the small number of studies available overall and the incomplete coverage of the spinal cord in these studies.

Quality of Original Data Included in the Analysis

The reliability of the estimated segmental spinal cord diameters presented is based on the quality of the reported data in the studies included. These reported data were based on either radiology or postmortem examination of the healthy human spinal cord. When implementing a radiological approach for segmental measurements, the delimitation of the cord is vital in order to achieve accurate measurements (18). Lamont et al. found it challenging to delimit the nerve root from the actual spinal cord, which prompted them to measure the whole width of both the cord and the root and to conduct the measurements at the mid-vertebral level only (18). Single reference points

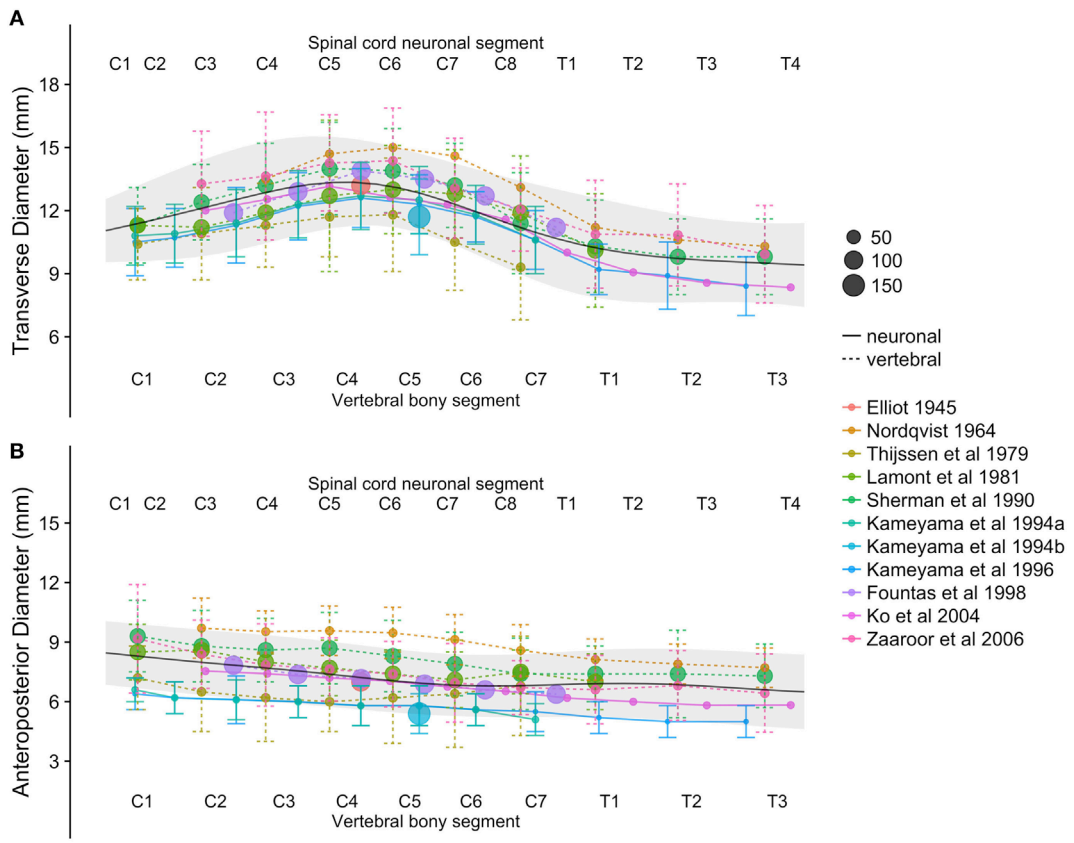

FIGURE 3 | **(A,B)**: figure illustrates measurements of the human cervical spinal cord transverse [panel **(A)**] and anteroposterior diameter [panel **(B)**] from different published studies. The size of the dots represents the number of subjects included in each study. The full black line shows the continuous population estimate from the general additive model, and the gray ribbon represents the population estimate ± 2 standard deviations (SDs) (based on the SDs of the studies).

imply error consistency throughout the spinal cord but are likely to reduce the quality of the estimate and aggravate the comparison between previously published data. Sherman et al. used a more rigorous approach in obtaining between 10 and 110 samples from each cord level (4). Techniques such as computed myelography allow sectioning down to 13 mm thickness, which is significantly thicker than what is achievable through post-mortem studies (17). However, both Thijssen et al. and Sherman et al. emphasized the need for axial radiological sectioning perpendicular to the cord to avoid elongation of the sections (4, 17). Other elements which might influence the quality of radiological measurement are: window settings, concentration of contrast media like computed tomographic myelography (20, 25), and window level and pulse sequence for MRI (20, 26). Finally, cranial parts of the cervical spinal cord are especially difficult to measure using the radiological approach, as overlap with the base of the skull, incisor teeth, and maxilla greatly obstructs vision (18).

Despite the potential for differences in quality between studies, we did not weigh the different studies based on their perceived quality.

Relative Lengths of Segments

Relative Length of Spinal Cord Neuronal Segments

Delimitation of the segments is vital when calculating the length of spinal cord neuronal segments. Donaldson and Davis measured the distance between the uppermost fila of successive nerves in four subjects on the dorsal and ventral aspect of the cord (24). However, Ko et al. measured the distance between the lowermost filament of the just proximal segment and the lowermost filament within each root, based on a sample consisting of 13 males and 2 females (22).

Relative Length of Vertebral Bony Segments

We have included three studies from the same research group reporting data on vertebral length (7–9). The sample size included in the respective publications was 15 or lower, and additional studies and/or more subjects would have been an advantage. When estimating the height of the vertebral body, the points of measurement are important. Panjabi et al. measured the posterior vertebral body height of cervical vertebras in the

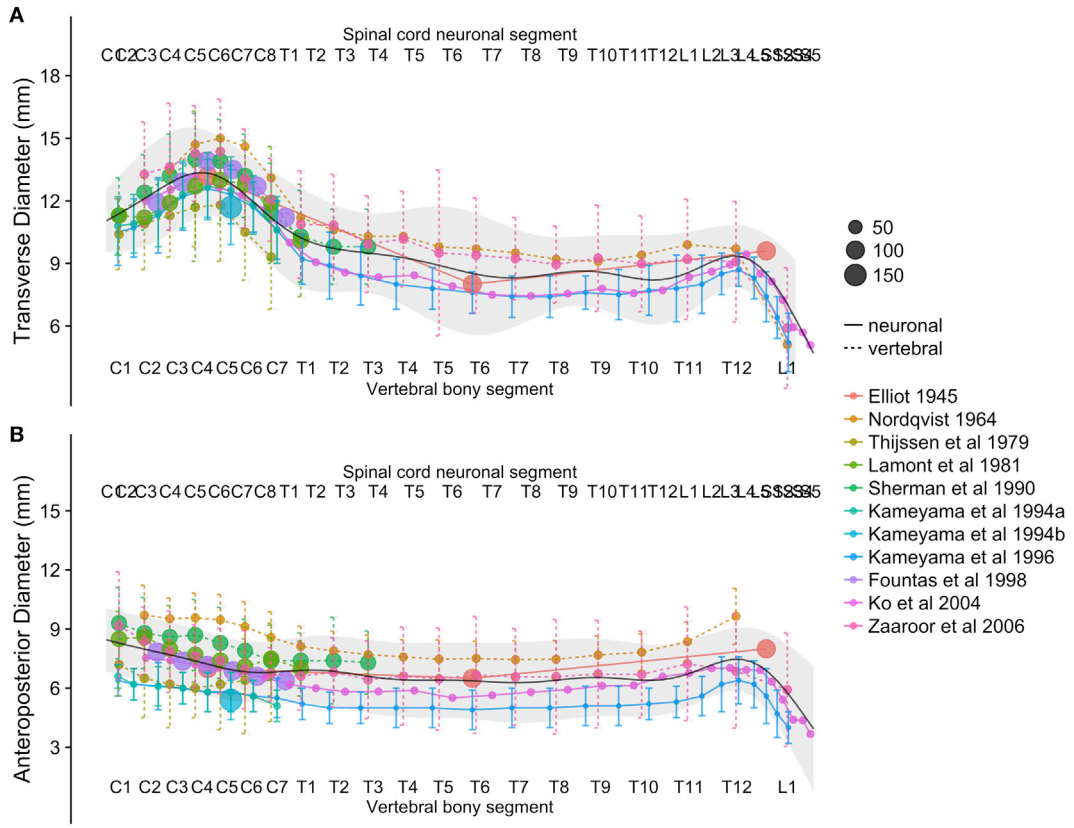

FIGURE 4 | **(A,B)**: figure illustrates measurements of the human spinal cord transverse [panel **(A)**] and anteroposterior diameter [panel **(B)**] from different published studies. The size of the dots represents the number of subjects included in each study. The full black line shows the continuous population estimate from the general additive model, and the gray ribbon represents the population estimate ± 2 standard deviations (SDs) (based on the SDs of the studies).

midsagittal plane (7). The authors reported that this resulted in an average underestimation of the height of each vertebral body by approximately 2 mm, when comparing to previously reported data (7, 27, 28). The same research group (8) found that the posterior thoracic vertebral body height was consistently one to 2 mm less than that reported by Berry et al. and Scoles et al. (29, 30) but in line with data reported by Cotterill et al. (31). The same applied for lumbar vertebral body posterior height (27, 29, 30). Since we used relative vertebral size rather absolute measurements, a systematic error in measurement is of minor importance. Panjabi et al. did not report the lengths of the C1 and C2 vertebrae. Therefore, we calculated approximate percentages for these vertebrae by using previously published relative positions of segments in the cervical spinal cord (10), termination of the spinal cord between lumbar vertebral bony segments L1 and L2 (11), and the assumption that the upper end of the C1 vertebrae is aligned with the upper end of the C1 neuronal segment. Therefore, the relative proportions of segments C1 and C2 in our model should be interpreted with care.

Because we defined a vertebral bony segment as the vertebra and half of both the adjacent intervertebral disks, our model assumes that intervertebral disks increase in thickness along the craniocaudal axis by same proportion as the vertebrae. This is not an unreasonable assumption, but one that was not backed with any data.

Relative Positioning of Segments

Effect of Corrected Measurement Positioning of the Transverse Diameter of the Human Cervical Spinal Cord—*R*-Squared and Bootstrap

Despite the complexity and shortcomings of our model, with scarce data and reliance on a number of assumptions, the strategy to create a normalized craniocaudal axis for comparison of cross-sectional measurements of the human spinal cord was successful. Success was indicated by the increase in adjusted *R*-squared from 68.8 to 86.4% when comparing the raw positioning using only segment index and our best effort to place measurements based on their calculated position. The increase in adjusted *R*-squared was robust, as shown by the non-overlapping 95% confidence intervals achieved by bootstrapping the adjusted *R*-squared for the two models. The relative positioning of segments along the spinal cord relies heavily on the studies by Cadotte et al. (10) and Boonpirak and Apinhasmit (11).

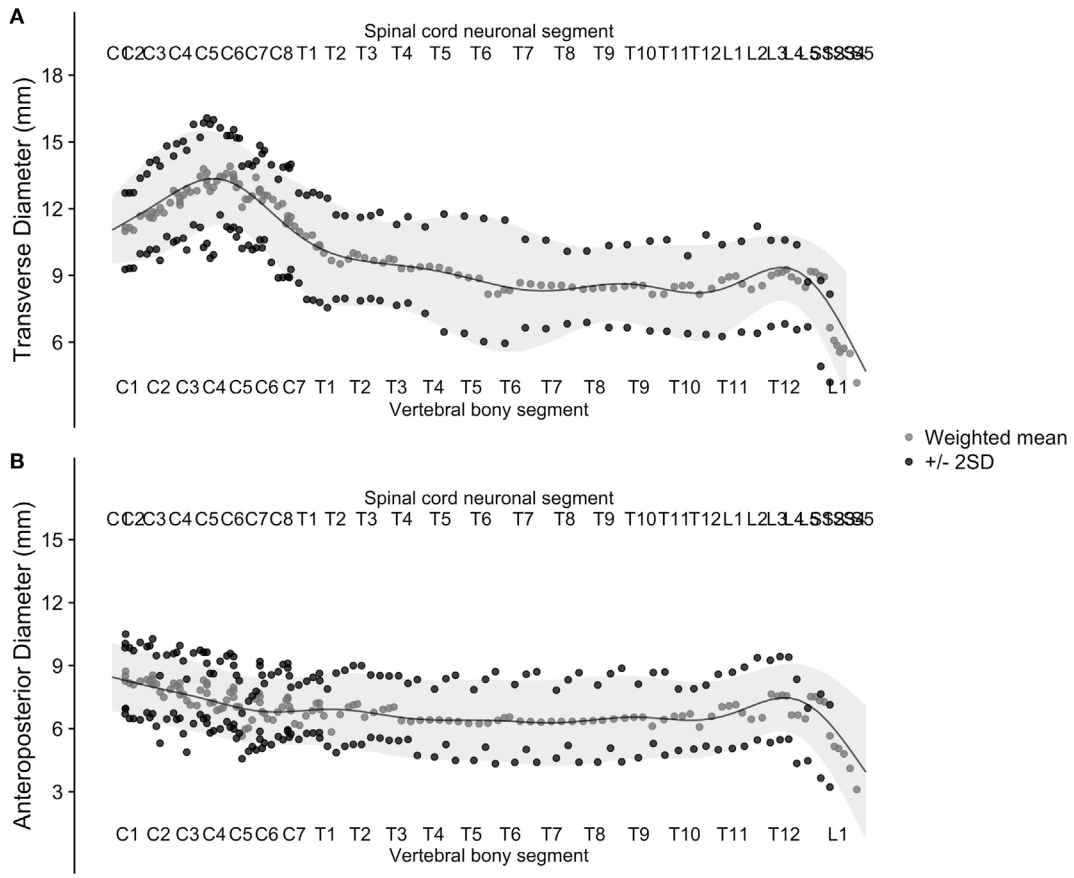

FIGURE 5 | **(A,B)**: figure illustrates the weighted averages of the human spinal cord transverse [panel **(A)**] and anteroposterior diameter [panel **(B)**] from different published studies. The full black line shows the continuous population estimate from the general additive model, and the gray ribbon shows two standard deviations (SDs) from the population estimate based on the SDs of the studies.

Weighted Averages

Weighted Averages along the Spinal Cord

The weighted averages were calculated by combining four adjacent measurements. This step was necessary to normalize the number of measurements along the spinal cord before fitting the generalized additive model to decrease problems where sample sizes changed suddenly along the spinal cord.

The number four was reached empirically by the authors and can therefore be questioned. We argue that it combined measurements to a reasonable degree without losing frequency response in the signal. In the measurements of anteroposterior diameter, the small number of measurements resulted in periodical oscillations of the weighted averages in the cervical spinal cord (**Figure 5B**). This was ameliorated in the next step by fitting the generalized additive model.

Weighted SDs along the Spinal Cord

The weighted SDs were calculated by squaring the known SDs to become variances and computing the weighted average variances. Taking the square root of the weighted average variances yielded the weighted SDs. This approach assumes that samples were drawn from the same population, which is probably not entirely true but represented the only practical way of estimating aggregated SDs known to us without the original data.

Population Estimates

Weighted Averages along the Spinal Cord

The continuous population estimates of the transverse and anteroposterior diameter resulting from the combination of the included studies (**Figures 3–5**) were consistent with the expected shape of the spinal cord (e.g., cervical and lumbar intumescence). The population SDs enclosed almost all data points when plotted as two SDs, giving further confidence that these data were combined with some accuracy.

The choice of parameters for the generalized additive model was reached empirically just like the weighted average. When choosing parameters that accurately described the data, we chose the lowest possible order polynomial that would follow the

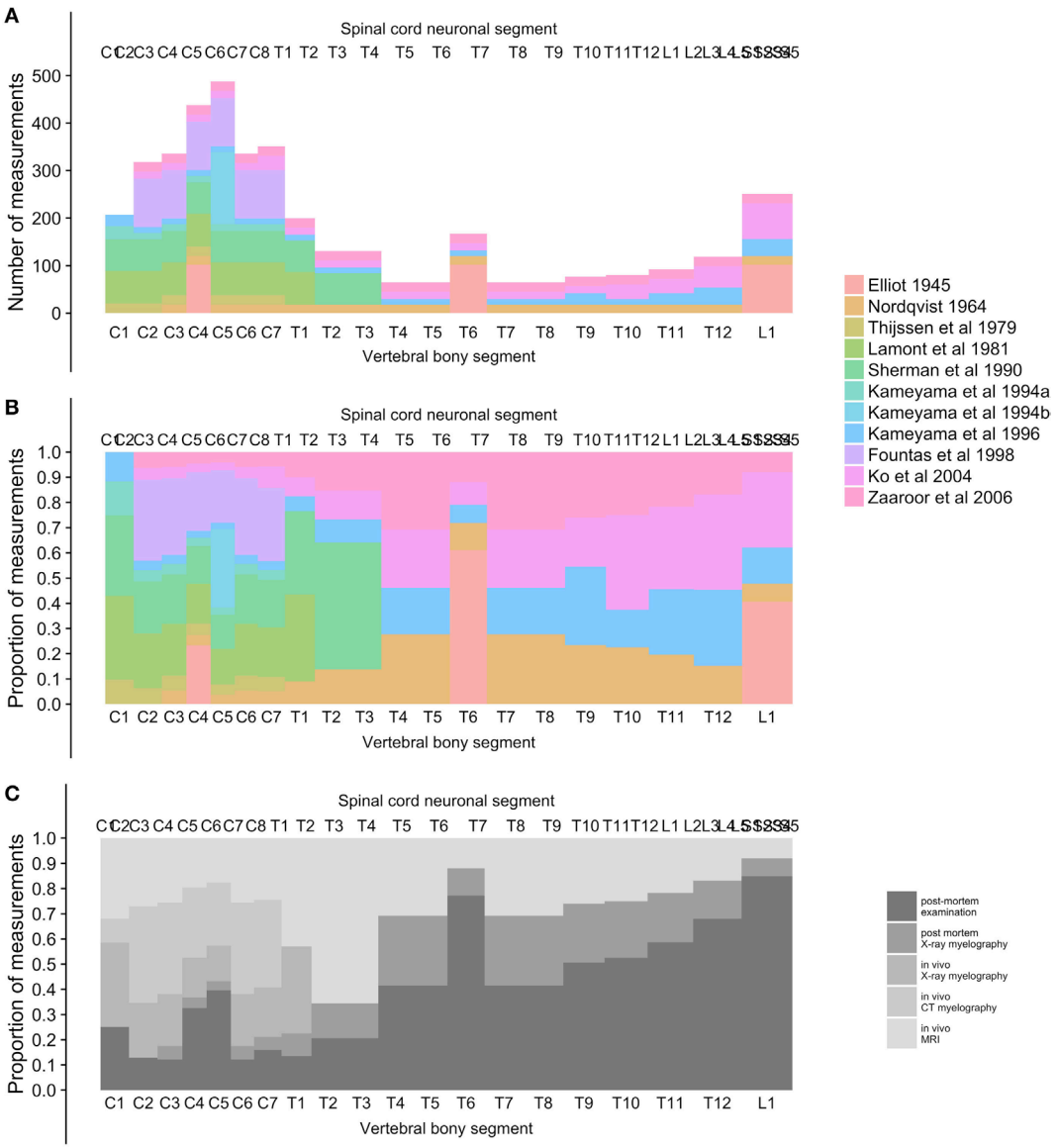

FIGURE 6 | **(A–C)**: figure demonstrates the total number of individual measurements contributed from each study at different points along the craniocaudal axis [panel **(A)**] and the proportional contribution of studies [panel **(B)**] and methods [panel **(C)**] used to measure the diameters of the human spinal cord.

perceived shape of the spinal cord with some accuracy. This was only evaluated visually and represents a weakness of the approach.

Correlation between Spinal Cord Size and Other Morphometrics

It is reasonable to discuss the impact of morphometrics defining body size, such as gender, height and body weight. Sherman et al. confirmed the previously established (32) lack of correlation between body weight, age, and spinal cord size, and that these parameters do not have to be adjusted (4). Kameyama et al. (20) also confirmed that the size of the spinal cord has no correlation with age, height, or body weight by concluding that the relative ratio of the cross-sectional area of each cervical, thoracic, and lumbar segment to that of the C3 are similar between individuals, even with a large interindividual variation in spinal cord size. However, some contradictory results were presented by Kameyama et al. (19), who reported that differences between genders seem to include not only spinal cord length (11) but also the cross-sectional area. They found that the cross-sectional area for C7 was significantly smaller in females when compared to males, hypothesizing

TABLE 5 | Estimated spinal cord diameters—spinal cord neuronal segment reference.

Spinal cord segment	Transverse diameter	Anteroposterior diameter	Number of subjects
C1	11.3 ± 1.7	8.3 ± 1.6	26
C2	11.5 ± 1.9	8.2 ± 1.6	181
C3	12 ± 2.3	8 ± 1.6	318
C4	12.8 ± 2.4	7.7 ± 1.7	362
C5	13.3 ± 2.2	7.4 ± 1.6	234
C6	13.1 ± 1.9	7 ± 1.6	438
C7	12.5 ± 1.9	6.9 ± 1.6	488
C8	11.3 ± 2.2	6.8 ± 1.6	336
T1	10.7 ± 2.3	6.9 ± 1.6	316
T2	10 ± 2.3	6.9 ± 1.7	27
T3	9.6 ± 2	6.8 ± 1.8	131
T4	9.5 ± 1.9	6.6 ± 1.9	131
T5	9.2 ± 2.4	6.4 ± 1.9	65
T6	8.7 ± 3	6.4 ± 1.9	65
T7	8.4 ± 2.7	6.3 ± 2	167
T8	8.3 ± 2.1	6.3 ± 2	77
T9	8.6 ± 1.7	6.5 ± 2	65
T10	8.6 ± 1.8	6.5 ± 2	65
T11	8.3 ± 2.1	6.4 ± 1.9	65
T12	8.2 ± 2.1	6.4 ± 1.8	27
L1	8.6 ± 1.9	6.7 ± 1.7	65
L2	9.1 ± 1.6	7.2 ± 1.6	27
L3	9.4 ± 1.5	7.5 ± 1.6	77
L4	9.3 ± 1.5	7.5 ± 1.6	27
L5	8.8 ± 1.7	7.1 ± 1.8	27
S1	8.4 ± 1.9	6.8 ± 2	129
S2	7.1 ± 2.5	5.8 ± 2.4	65
S3	6.3 ± 2.8	5.2 ± 2.7	27
S4	5.5 ± 3.2	4.6 ± 2.9	15
S5	4.7 ± 3.5	3.9 ± 3.2	15

*Point values of population estimates shown in **Figures 3** and **4** are depicted here in numerical format at the craniocaudal position of the middle of each spinal cord neuronal segment. "Number of subjects" indicates the number of measurements found within the craniocaudal limits of each segment and should not be interpreted as an exact "n" for statistical calculations, but rather as an approximation of the amount of data available along the spinal cord.*
C, cervical; T, thoracic; L, lumbar; S, sacral.

TABLE 6 | Estimated spinal cord diameters—vertebral column bony segment reference.

Vertebral column segment	Transverse diameter	Anteroposterior diameter	Number of subjects
C1	11.5 ± 1.9	8.2 ± 1.6	207
C2	12.3 ± 2.4	7.9 ± 1.6	318
C3	13.1 ± 2.4	7.6 ± 1.7	336
C4	13.3 ± 2.1	7.3 ± 1.6	438
C5	13.1 ± 1.9	7 ± 1.6	488
C6	12.1 ± 2	6.8 ± 1.6	336
C7	11 ± 2.3	6.8 ± 1.6	351
T1	10.2 ± 2.4	6.9 ± 1.7	200
T2	9.7 ± 2	6.8 ± 1.8	131
T3	9.5 ± 1.9	6.6 ± 1.9	131
T4	9.2 ± 2.4	6.4 ± 1.9	65
T5	8.8 ± 2.9	6.4 ± 1.9	65
T6	8.4 ± 2.9	6.3 ± 2	167
T7	8.3 ± 2.3	6.3 ± 2	65
T8	8.6 ± 1.7	6.4 ± 2	65
T9	8.6 ± 1.8	6.5 ± 2	77
T10	8.2 ± 2.1	6.4 ± 1.8	80
T11	8.6 ± 1.9	6.7 ± 1.7	92
T12	9.4 ± 1.5	7.5 ± 1.6	119
L1	7.1 ± 2.5	5.8 ± 2.4	251

*Point values of population estimates shown in **Figures 3** and **4** are shown here in numerical format at the craniocaudal position of the middle of each vertebral bony segment. "Number of subjects" indicates the number of measurements found within the craniocaudal limits of each segment and should not be interpreted as an exact "n" for statistical calculations, but rather as an approximation of the amount of data available along the spinal cord.*
C, cervical; T, thoracic; L, lumbar; S, sacral.

that the difference in size of the spinal cord between sexes may be partly explained by the variation in height. However, they could not find any correlation between spinal cord size and body weight.

Individual variation in cord size was substantial between individuals with equal height and resulted in significant positive correlation to cross-sectional area, transverse diameter, and sagittal diameter (19). However, Kameyama et al. found that body weight had no significant correlation to cross-sectional area, diameter, or sagittal diameter. The authors report that age had a slight negative correlation to cross-sectional area and sagittal diameter at C7, but not for transverse diameter at the same level. They hypothesize that age-related degenerative changes may explain the flattening of the cervical spinal cord with age, confirming previously published data (16, 19, 33). We observed that many of the included studies tended to include more males than females, which could have affected our analysis.

In summary, some contradictions seem to exist between the impact of body type characteristics on spinal cord size, but most previous studies have been underpowered to detect all but very strong correlations. Because our present study lacks the raw data, further investigation of predictors for spinal cord size was not possible. An interesting expansion of this study would be to gather all raw data and analyze predictors of size in a larger sample.

Clinical Implications

Clinical Implications of Population Estimates

Continuous population estimates of the transverse and anteroposterior diameters of the spinal cord could be useful in diagnosing and monitoring patients with neurodegenerative and neuroinflammatory diseases. It is known, for example, that patients suffering from multiple sclerosis have a reduced cross-sectional area compared to healthy matched controls (1), but these studies have low power. Without population estimates, it can be difficult to determine whether a specific patient should be considered to have a pathologically small or large spinal cord.

Clinical Implications of Model for Relative Segmental Positions

In the future, the model of spinal cord neuronal segment relation to vertebral bony segment could be used to achieve a better understanding of visible localized pathology on MRI in the spinal cord in situations where identification of spinal cord neuronal segments is challenging. This would require a validating study in patients in whom a well-defined pathology

of the spinal cord is present and can be correlated to a segmental symptom such as the motor or sensory level of a patient with a spinal cord injury. Such a study is currently being planned in our research group.

Clinical Research Implications

Multiple experimental studies for treatment of acute and chronic human spinal cord injuries are in different phases of development (2). In all studies where a premade device, instrumentation, or otherwise physical object needs to be applied to the spinal cord, the population estimates are of importance because they represent the variation in physical dimensions that will be encountered in patients.

Our research group is involved in a clinical trial exploring surgical repair of the human spinal cord (http://ClinicalTrials.gov Identifier: NCT02490501). During the design of the biodegradable device used in the study, knowing population estimates of the human spinal cord was a necessity, and, therefore, we believe that this work can be useful for other groups in similar projects.

CONCLUSION

We conclude that segmental transverse and anteroposterior diameters of the healthy human spinal cord from different published sources can be combined on a normalized craniocaudal axis and yield meaningful population estimates with reasonable sample sizes. These estimates could be useful for the routine management of patients with neurodegenerative diseases as well as for clinical research and experimental applications involving surgical spinal cord repair.

ETHICS STATEMENT

This review was based solely on published papers and their reported data. We did not conduct any radiological or postmortem examinations by ourselves. Hence, this review itself is exempt from ethical approval but relies on the ethics of the included studies, which we have found no reason to question.

AUTHOR CONTRIBUTIONS

Substantial contributions to the conception or design of the work (AF); or the acquisition (AF), analysis (AF, RH, ET, PM, and MS), or interpretation (AF, RH, ET, PM, and MS) of data for the work. Drafting the work or revising it critically for important intellectual content (AF, RH, ET, PM, and MS). Final approval of the version to be published (AF, RH, ET, PM, and MS). Agreement to be accountable for all aspects of the work in ensuring that questions related to the accuracy or integrity of any part of the work are appropriately investigated and resolved (AF, RH, ET, PM, and MS).

ACKNOWLEDGMENTS

We would like to acknowledge the contributions of all personnel at the neurosurgical research laboratory (R2:02), Department of Clinical Neuroscience, located at Neurocentrum, Karolinska University Hospital, Stockholm, Sweden.

FUNDING

This study was supported by the Torsten and Ragnar Söderberg Foundation, the Swedish Research Council, The Swedish Society of Medicine, and Karolinska Institutet.

REFERENCES

1. Kearney H, Miller DH, Ciccarelli O. Spinal cord MRI in multiple sclerosis – diagnostic, prognostic and clinical value. *Nat Rev Neurol* (2015) 11(6):327–38. doi:10.1038/nrneurol.2015.80
2. Ahuja CS, Fehlings M. Concise review: bridging the gap: novel neuroregenerative and neuroprotective strategies in spinal cord injury. *Stem Cells Transl Med* (2016) 5(7):914–24. doi:10.5966/sctm.2015-0381
3. McDonald JW, Sadowsky C. Spinal-cord injury. *Lancet* (2002) 359(9304):417–25. doi:10.1016/S0140-6736(02)07603-1
4. Sherman JL, Nassaux PY, Citrin CM. Measurements of the normal cervical spinal cord on MR imaging. *AJNR Am J Neuroradiol* (1990) 11(2):369–72.
5. Zaaroor M, Kósa G, Peri-Eran A, Maharil I, Shoham M, Goldsher D. Morphological study of the spinal canal content for subarachnoid endoscopy. *Minim Invasive Neurosurg* (2006) 49(4):220–6. doi:10.1055/s-2006-948000
6. Freund PA, Dalton C, Wheeler-Kingshott CA, Glensman J, Bradbury D, Thompson AJ, et al. Method for simultaneous voxel-based morphometry of the brain and cervical spinal cord area measurements using 3D-MDEFT. *J Magn Reson Imaging* (2010) 32(5):1242–7. doi:10.1002/jmri.22340
7. Panjabi MM, Duranceau J, Goel V, Oxland T, Takata K. Cervical human vertebrae. Quantitative three-dimensional anatomy of the middle and lower regions. *Spine (Phila Pa 1976)* (1991) 16(8):861–9. doi:10.1097/00007632-199108000-00001
8. Panjabi MM, Takata K, Goel V, Federico D, Oxland T, Duranceau J, et al. Thoracic human vertebrae. Quantitative three-dimensional anatomy. *Spine (Phila Pa 1976)* (1991) 16(8):888–901. doi:10.1097/00007632-199108000-00001
9. Panjabi MM, Goel V, Oxland T, Takata K, Duranceau J, Krag M, et al. Human lumbar vertebrae. Quantitative three-dimensional anatomy. *Spine (Phila Pa 1976)* (1992) 17(3):299–306. doi:10.1097/00007632-199203000-00010
10. Cadotte DW, Cadotte A, Cohen-Adad J, Fleet D, Livne M, Wilson JR, et al. Characterizing the location of spinal and vertebral levels in the human cervical spinal cord. *AJNR Am J Neuroradiol* (2015) 36(4):803–10. doi:10.3174/ajnr.A4192
11. Boonpirak N, Apinhasmit W. Length and caudal level of termination of the spinal cord in Thai adults. *Acta Anat (Basel)* (1994) 149(1):74–8. doi:10.1159/000147558
12. Wickham H. In: Use R, editor. *SpringerLink (Online Service): ggplot2 Elegant Graphics for Data Analysis*. New York, NY: Springer (2009).
13. R Core Team. *R: A Language and Environment for Statistical Computing*. Vienna, Austria: R Foundation for Statistical Computing (2016). Available from: http://www.r-project.org/
14. Wilke CO. *Cowplot: Streamlined Plot Theme and Plot Annotations for 'ggplot2.' R Package Version 0.6.0*. (2015).
15. Canty A, Ripley B. *boot: Bootstrap R (S-Plus) Functions. R package version 1.3–18*. (2016).
16. Nordqvist L. The sagittal diameter of the spinal cord and subarachnoid space in different age groups. A Roentgenographic post-mortem study. *Acta Radiol Diagn (Stockh)* (1964) 227(Suppl):1–96.
17. Thijssen HO, Keyser A, Horstink MW, Meijer E. Morphology of the cervical spinal cord on computed myelography. *Neuroradiology* (1979) 18(2):57–62. doi:10.1007/BF00344822
18. Lamont AC, Zachary J, Sheldon PW. Cervical cord size in metrizamide myelography. *Clin Radiol* (1981) 32(4):409–12. doi:10.1016/S0009-9260(81)80284-X

19. Kameyama T, Hashizume Y, Ando T, Takahashi A. Morphometry of the normal cadaveric cervical spinal cord. *Spine (Phila Pa 1976)* (1994) 19(18):2077–81. doi:10.1097/00007632-199409150-00013
20. Kameyama T, Hashizume Y, Sobue G. Morphologic features of the normal human cadaveric spinal cord. *Spine (Phila Pa 1976)* (1996) 21(11):1285–90. doi:10.1097/00007632-199606010-00001
21. Fountas KN, Kapsalaki EZ, Jackson J, Vogel RL, Robinson JS. Cervical spinal cord – smaller than considered? *Spine (Phila Pa 1976)* (1998) 23(14):1513–6. doi:10.1097/00007632-199807150-00001
22. Ko HY, Park JH, Shin YB, Baek SY. Gross quantitative measurements of spinal cord segments in human. *Spinal Cord* (2004) 42(1):35–40. doi:10.1038/sj.sc.3101538
23. Elliott HC. Cross-sectional diameters and areas of the human spinal cord. *Anat Rec* (1945) 93:287–93. doi:10.1002/ar.1090930306
24. Donaldson HH, Davis DJ. A description of charts showing the areas of the cross sections of the human spinal cord at the level of each spinal nerve. *J Comp Neurol* (1903) 13(1):19–40. doi:10.1002/cne.910130104
25. Seibert CE, Barnes JE, Dreisbach JN, Swanson WB, Heck RJ. Accurate CT measurement of the spinal cord using metrizamide: physical factors. *AJR Am J Roentgenol* (1981) 136(4):777–80. doi:10.2214/ajr.136.4.777
26. Miyasaka K. [MR imaging of the spinal cord – with special emphasis on the factors influencing spinal cord measurement]. *No To Shinkei* (1992) 44(3):241–7.
27. Nissan M, Gilad I. The cervical and lumbar vertebrae – an anthropometric model. *Eng Med* (1984) 13(3):111–4. doi:10.1243/EMED_JOUR_1984_013_030_02
28. Francis CC. Dimensions of the cervical vertebrae. *Anat Rec* (1955) 122(4):603–9. doi:10.1002/ar.1091220409
29. Berry JL, Moran JM, Berg WS, Steffee AD. A morphometric study of human lumbar and selected thoracic vertebrae. *Spine (Phila Pa 1976)* (1987) 12(4):362–7. doi:10.1097/00007632-198705000-00010
30. Scoles PV, Linton AE, Latimer B, Levy ME, Digiovanni BF. Vertebral body and posterior element morphology: the normal spine in middle life. *Spine (Phila Pa 1976)* (1988) 13(10):1082–6. doi:10.1097/00007632-198810000-00002
31. Cotterill PC, Kostuik JP, D'Angelo G, Fernie GR, Maki BE. An anatomical comparison of the human and bovine thoracolumbar spine. *J Orthop Res* (1986) 4(3):298–303. doi:10.1002/jor.1100040306
32. Yu YL, du Boulay GH, Stevens JM, Kendall BE. Morphology and measurements of the cervical spinal cord in computer-assisted myelography. *Neuroradiology* (1985) 27(5):399–402. doi:10.1007/BF00327602
33. Tanaka Y. [Morphological changes of the cervical spinal canal and cord due to aging]. *Nihon Seikeigeka Gakkai Zasshi* (1984) 58(9):873–86.

Conflict of Interest Statement: The authors declare that the research was conducted in the absence of any commercial or financial relationships that could be construed as a potential conflict of interest.

frontiers in Neurology

CASE REPORT
published: 03 March 2017
doi: 10.3389/fneur.2017.00072

Rehabilitation, Using Guided Cerebral Plasticity, of a Brachial Plexus Injury Treated with Intercostal and Phrenic Nerve Transfers

Lars B. Dahlin[1,2], Gert Andersson[3,4], Clas Backman[5,6], Hampus Svensson[1] and Anders Björkman[1]*

[1] Department of Hand Surgery, Skåne University Hospital, Malmö, Sweden, [2] Department of Translational Medicine – Hand Surgery, Lund University, Malmö, Sweden, [3] Department of Clinical Neurophysiology, Skåne University Hospital, Malmö, Sweden, [4] Department of Clinical Sciences in Lund – Neurophysiology, Lund University, Lund, Sweden, [5] Department of Hand Surgery, University Hospital of Northern Sweden, Umeå University, Umeå, Sweden, [6] Department of Surgical and Perioperative Sciences, Section for Hand and Plastic Surgery, Umeå University, Umeå, Sweden

Recovery after surgical reconstruction of a brachial plexus injury using nerve grafting and nerve transfer procedures is a function of peripheral nerve regeneration and cerebral reorganization. A 15-year-old boy, with traumatic avulsion of nerve roots C5–C7 and a non-rupture of C8–T1, was operated 3 weeks after the injury with nerve transfers: (a) terminal part of the accessory nerve to the suprascapular nerve, (b) the second and third intercostal nerves to the axillary nerve, and (c) the fourth to sixth intercostal nerves to the musculocutaneous nerve. A second operation—free contralateral gracilis muscle transfer directly innervated by the phrenic nerve—was done after 2 years due to insufficient recovery of the biceps muscle function. One year later, electromyography showed activation of the biceps muscle essentially with coughing through the intercostal nerves, and of the transferred gracilis muscle by deep breathing through the phrenic nerve. Voluntary flexion of the elbow elicited clear activity in the biceps/gracilis muscles with decreasing activity in intercostal muscles distal to the transferred intercostal nerves (i.e., corresponding to eighth intercostal), indicating cerebral plasticity, where neural control of elbow flexion is gradually separated from control of breathing. To restore voluntary elbow function after nerve transfers, the rehabilitation of patients operated with intercostal nerve transfers should concentrate on transferring coughing function, while patients with phrenic nerve transfers should focus on transferring deep breathing function.

Keywords: brachial plexus injury, nerve transfer, intercostal nerve, phrenic nerve, electromyography, cerebral plasticity, guided plasticity, rehabilitation

OPEN ACCESS

Edited by:
Mattias K. Sköld, Uppsala University, Sweden

Reviewed by:
Manish Singh Sharma, Mayo Clinic Health System, USA
Robert Jay Spinner, Mayo Clinic, USA

****Correspondence:***
Lars B. Dahlin
lars.dahlin@med.lu.se

Specialty section:
This article was submitted to Neurotrauma, a section of the journal Frontiers in Neurology

Received: *25 August 2016*
Accepted: *16 February 2017*
Published: *03 March 2017*

Citation:
Dahlin LB, Andersson G, Backman C, Svensson H and Björkman A (2017) Rehabilitation, Using Guided Cerebral Plasticity, of a Brachial Plexus Injury Treated with Intercostal and Phrenic Nerve Transfers. Front. Neurol. 8:72. doi: 10.3389/fneur.2017.00072

INTRODUCTION AND BACKGROUND

A brachial plexus injury (BPI) is a devastating injury, which can result in severe and permanent neurologic impairment and disability of the upper extremity. Recovery after surgical reconstruction using nerve grafting and nerve transfer procedures for BPI is a function of peripheral nerve regeneration and adaptations within the central nervous system, i.e., plasticity. The plastic capacity of the brain opens possibilities, where plasticity can be guided to substitute or improve functions that have

been damaged or lost, i.e., guided plasticity (1). Nerve, muscle, or tendon transfers are procedures that require a plasticity to function, and this is important to take into consideration during rehabilitation after such a procedure (2–4).

Intercostal nerves are commonly used to reinnervate muscles after a BPI with avulsion of spinal nerve roots (5–7); where two intercostal nerves should be enough for reinnervation of a muscle (8). Intercostal nerves can be harvested without any residual problems, e.g., pulmonary dysfunction (9). In contrast, the phrenic nerve, innervating the diaphragm, should only be used as a second alternative as a nerve transfer for muscle reinnervation because of potential pulmonary dysfunction (9–11). An important question is how patients with these two nerve transfers should be rehabilitated to transfer control of the original nerve function to a new function, for example, elbow flexion. Here, we describe a patient with a BPI, who was initially treated with a transfer of intercostal nerves to the musculocutaneous nerve to acquire elbow flexion, but due to insufficient regain of active elbow flexion a second procedure, i.e., a free gracilis muscle transfer reinnervated by a phrenic nerve transfer, was performed.

Our aim is to visualize, through electromyography (EMG), the different activation patterns of the biceps and gracilis muscles by coughing and deep breathing, respectively; observations that are relevant for how patients with such nerve transfers can be rehabilitated after surgery.

CASE REPORT

A 15-year-old boy sustained a severe BPI with a complete loss of motor and sensory function corresponding to the brachial plexus in the dominant, right, arm after a motorcycle accident. There was no blunt trauma to the patient's chest according to the history of the patient, and the results from the trauma-computer tomography (CT) just after the accident did not indicate any injury to the chest wall or to the lungs. The patient also had a Horner syndrome. The extent of the BPI was confirmed after a week by magnetic resonance imaging (MRI) and CT-myelography as well as at surgical exploration 3 weeks post-injury; showing avulsion of nerve roots C5–C7 and injuries to the spinal roots C8–T1 (i.e., intraoperatively not ruptured, but in continuity). No further action was done concerning the two lower roots. At the surgical reconstruction, 3 weeks after the injury multiple nerve transfers, focusing on restoring shoulder and elbow function, were done: (a) the terminal part of the accessory nerve was transferred to the suprascapular nerve, (b) the second and third intercostal nerves transferred (the upper intercostal *via* two radial nerve grafts) to the axillary nerve, and (c) the fourth to sixth intercostal nerves were transferred (the two lower *via* three radial nerve grafts) to the musculocutaneous nerve. Postoperatively, he trained under the supervision of a physiotherapist with experience in rehabilitation of patients with BPI.

Twenty-one months after surgery, he had voluntary activation in the infra- and supraspinatus muscles [Medical Research Council (MRC) grade 3], but insufficient function in the biceps muscle (i.e., M1–2). Therefore, the contralateral gracilis muscle was transferred, as a free muscle graft and attached to the coracoid process and to the distal parts of the biceps tendon 25 months after the first procedure. The gracilis muscle was directly reinnervated, through end-to-end repair to the distal part of the specific nerve branch originally innervating the transferred gracilis muscle, using the phrenic nerve that was harvested *via* an open thoracotomy. The patient had postoperative complications with pneumonia on the left side (X-ray examination; spiral-CT also to exclude pulmonary emboli) and a delayed wound healing in the upper part of the incision on the right upper arm, which was treated with antibiotics, revisions with split skin graft, and vacuum-assisted closure therapy, where after these conditions were completely healed. Ultrasound investigations with color-laser-Doppler at 6 and 8 weeks showed a viable gracilis muscle with detectable blood vessels. Postoperative training was initiated 6 weeks after the operation.

Examination with EMG after clinical signs of reinnervation, i.e., 1 year after surgery, showed extensive denervation activity in the biceps muscle with few neurogenic altered activated motor units in the muscle through activation of the intercostal nerves (i.e., essentially with coughing but also with deep expiration, **Figure 1**), although still suboptimal strength (M1–2). The transferred gracilis muscle, innervated by the phrenic nerve, showed no denervation activity, but was rhythmically activated (a large number of motor units) during the inspiration phase of deep breathing (not with coughing; **Figure 2**), and by voluntary elbow flexion (weak M3). Voluntary flexion of the elbow (weak M3; up to 30 degrees of flexion) elicited clear activity in the biceps/gracilis muscles, with minor activity in intercostal muscles (shown for biceps in **Figure 3**). The intercostal muscles showed activation during coughing, while the modulation during normal breathing was hardly detectable with surface electrodes. At the final follow-up, there was no muscular activity at all, observed or palpated, in the brachioradialis muscle (M0), i.e., the elbow function was entirely caused by the biceps and gracilis muscles. He had no supination induced by activity in the supinator muscle, but supination (M3) was observed to be performed by the biceps/gracilis muscles as one would expect due to their insertion at the tuberosity of the proximal part of the radius. No function was observed in the pronator muscle to compensate for the supination. Clinical examination also revealed some finger (i.e., flexor digitorum superficialis/profundus muscles) and thumb (i.e., flexor pollicis longus muscle) activity [i.e., M3–4(−)], but without any real function in activity of daily living. No further surgery was performed. Rehabilitation was terminated in agreement with the patient 2.5 years after the latest surgical procedure, although he still did not show optimal elbow function.

DISCUSSION

In the present case, the initial procedures, after careful preoperative evaluation of the injury with MRI and CT-myelography (12), included different nerve transfers to improve/restore shoulder and elbow function (13). The preoperative investigations, as well as intraoperative findings, indicated continuity of the C8 and Th1 and lower trunk, but without clinical function, and no further action was taken concerning this part of the brachial plexus, including attention to elbow extension. Some finger and thumb function, although not functional in daily activity, had returned

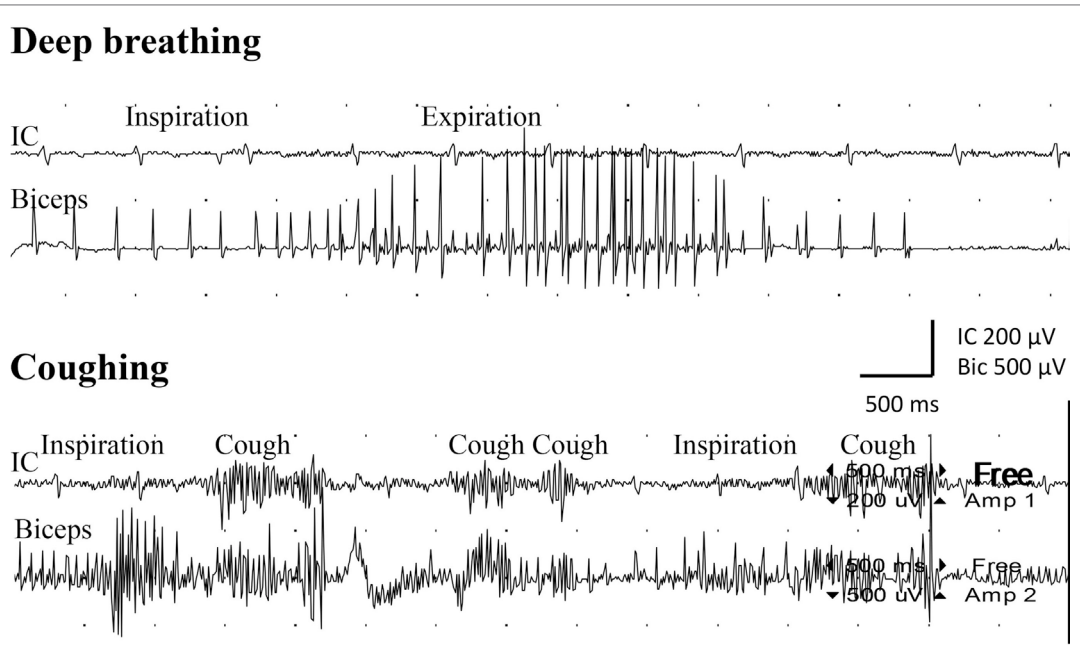

FIGURE 1 | **Electromyogram recorded from the intercostal muscles (IC), distal to level of the transferred intercostal nerves (i.e., around eighth costal level; surface electrodes), as well as from the biceps muscle (biceps; needle electrode) after the second surgery**. Recordings were done during deep breathing (upper panel) and during coughing (lower panel).

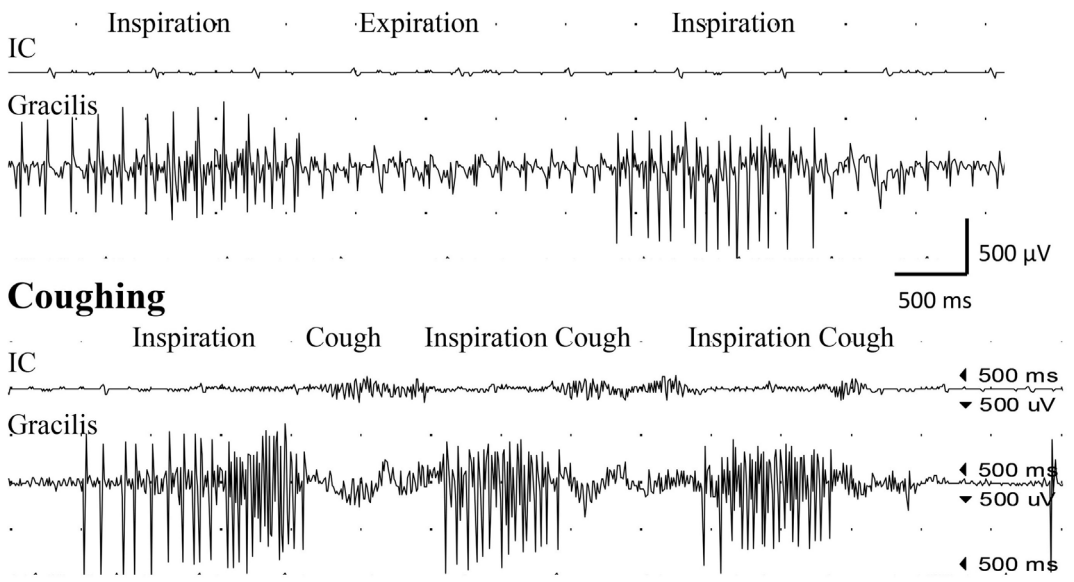

FIGURE 2 | **Electromyogram recorded from the intercostal muscles (IC), distal to the transferred intercostal nerves (i.e., around eighth costal level; surface electrodes), as well as from the gracilis muscle (gracilis; needle electrode) after the second surgery, where the gracilis muscle was transferred as a free muscle graft and reinnervated by the phrenic nerve**. Recordings were done during deep breathing (upper panel) and during coughing (lower panel).

at the final follow-up, indicating that C8 and Th1 roots were indeed not avulsed at injury. We cannot explain the presence of the Horner syndrome in spite of the lack of avulsed C8 and Th1.

Stabilization of the shoulder was achieved with the first two mentioned transfers at the initial procedure, while the conventional transfer of three intercostal nerves to the biceps brachii

FIGURE 3 | Electromyogram recorded from the intercostal muscles (intercostal), distal to the transferred intercostal nerves (i.e., around eighth costal level; surface electrodes), as well as from the biceps muscle (biceps; needle electrode) after the second surgery. Recordings were done during voluntary elbow flexion (arrow indicates start of the voluntary flexion).

muscle was insufficient to restore elbow function (M1–2) in the present case (8). In the second procedure, it was necessary to do a free gracilis muscle transfer with the intention to improve elbow flexion (14–16). Because the intercostal nerves had been used in the first surgical procedure, we chose to reinnervate the transferred gracilis muscle through the phrenic nerve (17, 18), which can be done without affecting pulmonary function although intercostal nerves previously have been used (19). The phrenic nerve was harvested and transected close to the diaphragm through an open thoracotomy. The possibility of a contralateral C7 transfer was discussed (20), but declined for several reasons, including the patient's own opinion. The phrenic nerve was sutured directly end-to-end to the distal nerve supplying the gracilis muscle with the intention to have a short distance for the regenerating nerve and thus a more rapid reinnervation of the muscle (9). In this way, it was also possible to avoid nerve grafts, although considered to be not necessary in phrenic nerve transfer to musculocutaneous nerve (21). The intrathoracic part of the phrenic nerve is rather thin and by relocating the phrenic nerve extensively, as was done in the present case, there may be a risk that the intraneural blood supply can be jeopardized. However, it is known that nerve grafts, and also a thin phrenic nerve, can survive through diffusion before revascularization. This was obviously the case here since the results from the EMG showed that the axons survived and had grown into the gracilis muscle with functional reinnervation. The reinnervation of the present transferred gracilis muscle, noted clinically and by EMG, is in agreement with an earlier report examining gracilis muscle transfers in a large population, where those patients were reconstructed with a similar surgical delay as well as had a similar postoperative follow-up and time for reinnervation (22). Interestingly, around 35% of their patients had a similar recovery (i.e., M3), based on MRC scale, as the present patient, while only 26% had M4 (22). In the present case, the intercostal nerves and the phrenic nerve were used to restore elbow function at two different time points with the purpose to reinnervate the elbow flexors through the musculocutaneous nerve and through the branch innervating the transferred gracilis muscle; thus, a synergistic function could be achieved, which is an advantage in view of the acting cerebral plasticity. Previous data indicate that the two nerves should not be used simultaneously to restore elbow extension and flexion, respectively; thus, with an antagonistically intended function (19).

The clinical outcome following complex brachial plexus reconstructions, like the present one, is not only dependent on regeneration of nerve fibers into the target muscle, but also highly dependent on adaptations within the central nervous system, i.e., plasticity. This was observed in the present case since the patient also could independently, without coughing or deep breathing (i.e., "respiratory standstill"), activate both the biceps and the gracilis muscles by voluntary elbow flexion although it was not functional [i.e., only weak M3 (3)]. Thus, an initial coughing and deep breathing function of the intercostal and phrenic nerves, respectively, had been transferred to voluntary elbow flexion through cerebral plasticity.

A nerve transfer will always induce a cerebral reorganization as well as alteration of respiratory spinal descending inputs to thoracic motoneurons (23). We did not investigate the influence of trunk flexion in the rehabilitation process. Trunk flexion can activate the biceps muscle through the intercostal nerves as presented by Chalidapong et al. in a larger study (24). Higher amplitude was measured in the reinnervated elbow flexor muscles at EMG in that study, but only 6/32 patients preferred trunk flexion to activate flexor muscles of the elbow; most of the patients preferred other techniques alone or in combination to flex the elbow (24). It is imperative that the team treating patients with BPI reconstructed with muscle and/or nerve transfers has a good knowledge in neuroscience in order to understand the cerebral changes caused by the injury and by the surgical reconstruction. With this knowledge at hand, it is possible to individually tailor the rehabilitation and physical therapy protocols using guided plasticity in order to achieve the best possible clinical outcome (1).

Limitations of the Study

During normal breathing, expiration is a passive process. Thus, one would not expect any activation during expiration in a muscle where a nerve is transferred. However, in deep breathing, the expiratory phase can be an active process with the purpose to speed up such a phase. Hence, some EMG activation can be expected during deep breathing, which was observed in the biceps muscle as indicated in **Figure 1**. In the present case, we observed little activity during normal and deep breathing, with EMG, from the intercostal muscles, when one would expect that the quiet and passive expiration would not result in any activity at all. We have no explanation for this observation, but during coughing, bursts of EMG activity were recorded from the intercostal muscles as expected. The intercostal muscles showed activation during coughing, while the modulation during normal breathing was hardly detectable with surface electrodes.

CONCLUDING REMARKS

The present data indicate that intercostal nerves, which was used in the first surgical procedure since there were no concomitant chest trauma (25), support important function as coughing, while the phrenic nerve is crucial for deep breathing. We suggest that the training of patients, in whom transfer of intercostal nerves has been performed, should concentrate to transfer coughing function to the biceps brachii muscle, which is in contrast to a previous study, suggesting trunk flexion during training of the new function in order to facilitate elbow flexion (24). In contrast, patients with a phrenic nerve transfer, which can be performed through harvesting the phrenic nerve *via* a thoracotomy for direct end-to-end attachment to the distal nerve end of the target muscle, should focus on transferring deep breathing function to the reinnervated muscle.

ETHICS STATEMENT

The patient was treated with conventional clinical procedures in the health care sector not requiring any ethical approval. We have informed consent from the patient to publish the history and treatment, which is stated in the patient journal folder.

AUTHOR CONTRIBUTIONS

LD: overall responsible for diagnosis and clinical treatment of the patient; concept of message, draft, and revision and finalization of the manuscript; GA: responsible for neurophysiological examination and draft of the manuscript; CB: responsible for treatment of the patient and draft of the manuscript; HS: draft of the manuscript; AB: draft and finalization of the manuscript.

ACKNOWLEDGMENTS

The authors thank Tina Folker for help with preparation of the manuscript.

FUNDING

Research related to the present study was supported by Swedish Research Council (Medicine), Skåne University Hospital, Region Skåne, and Lund University.

REFERENCES

1. Duffau H. Brain plasticity: from pathophysiological mechanisms to therapeutic applications. *J Clin Neurosci* (2006) 13(9):885–97. doi:10.1016/j.jocn.2005.11.045
2. Dahlin LB, Coster M, Bjorkman A, Backman C. Axillary nerve injury in young adults – an overlooked diagnosis? Early results of nerve reconstruction and nerve transfers. *J Plast Surg Hand Surg* (2012) 46(3–4):257–61. doi:10.3109/2000656X.2012.698415
3. Malessy MJ, Bakker D, Dekker AJ, Van Duk JG, Thomeer RT. Functional magnetic resonance imaging and control over the biceps muscle after intercostal-musculocutaneous nerve transfer. *J Neurosurg* (2003) 98(2):261–8. doi:10.3171/jns.2003.98.2.0261
4. Malessy MJ, Thomeer RT, van Dijk JG. Changing central nervous system control following intercostal nerve transfer. *J Neurosurg* (1998) 89(4):568–74. doi:10.3171/jns.1998.89.4.0568
5. Cho AB, Iamaguchi RB, Silva GB, Paulos RG, Kiyohara LY, Sorrenti L, et al. Intercostal nerve transfer to the biceps motor branch in complete traumatic brachial plexus injuries. *Microsurgery* (2015) 35(6):428–31. doi:10.1002/micr.22453
6. Merrell GA, Barrie KA, Katz DL, Wolfe SW. Results of nerve transfer techniques for restoration of shoulder and elbow function in the context of a meta-analysis of the English literature. *J Hand Surg Am* (2001) 26(2):303–14. doi:10.1053/jhsu.2001.21518
7. Giddins GE, Kakkar N, Alltree J, Birch R. The effect of unilateral intercostal nerve transfer upon lung function. *J Hand Surg Br* (1995) 20(5):675–6. doi:10.1016/S0266-7681(05)80133-0
8. Xiao C, Lao J, Wang T, Zhao X, Liu J, Gu Y. Intercostal nerve transfer to neurotize the musculocutaneous nerve after traumatic brachial plexus avulsion: a comparison of two, three, and four nerve transfers. *J Reconstr Microsurg* (2014) 30(5):297–304. doi:10.1055/s-0033-1361840
9. Chalidapong P, Sananpanich K, Kraisarin J, Bumroongkit C. Pulmonary and biceps function after intercostal and phrenic nerve transfer for brachial plexus injuries. *J Hand Surg Br* (2004) 29(1):8–11. doi:10.1016/S0266-7681(03)00210-9
10. Liu Y, Lao J, Zhao X. Comparative study of phrenic and intercostal nerve transfers for elbow flexion after global brachial plexus injury. *Injury* (2015) 46(4):671–5. doi:10.1016/j.injury.2014.11.034
11. de Mendonca Cardoso M, Gepp R, Correa JF. Outcome following phrenic nerve transfer to musculocutaneous nerve in patients with traumatic brachial palsy: a qualitative systematic review. *Acta Neurochir (Wien)* (2016) 158(9):1793–800. doi:10.1007/s00701-016-2855-8
12. Abul-Kasim K, Backman C, Bjorkman A, Dahlin LB. Advanced radiological work-up as an adjunct to decision in early reconstructive surgery in brachial plexus injuries. *J Brachial Plex Peripher Nerve Inj* (2010) 5:14. doi:10.1186/1749-7221-5-14
13. Sun G, Wu Z, Wang X, Tan X, Gu Y. Nerve transfer helps repair brachial plexus injury by increasing cerebral cortical plasticity. *Neural Regen Res* (2014) 9(23):2111–4. doi:10.4103/1673-5374.147939
14. Kay S, Pinder R, Wiper J, Hart A, Jones F, Yates A. Microvascular free functioning gracilis transfer with nerve transfer to establish elbow flexion. *J Plast Reconstr Aesthet Surg* (2010) 63(7):1142–9. doi:10.1016/j.bjps.2009.05.021
15. Barrie KA, Steinmann SP, Shin AY, Spinner RJ, Bishop AT. Gracilis free muscle transfer for restoration of function after complete brachial plexus avulsion. *Neurosurg Focus* (2004) 16(5):E8. doi:10.3171/foc.2004.16.5.9
16. Yang Y, Yang JT, Fu G, Li XM, Qin BG, Hou Y, et al. Functioning free gracilis transfer to reconstruct elbow flexion and quality of life in global brachial plexus injured patients. *Sci Rep* (2016) 6:22479. doi:10.1038/srep22479

17. Chuang ML, Chuang DC, Lin IF, Vintch JR, Ker JJ, Tsao TC. Ventilation and exercise performance after phrenic nerve and multiple intercostal nerve transfers for avulsed brachial plexus injury. *Chest* (2005) 128(5):3434–9. doi:10.1378/chest.128.5.3434
18. Zheng MX, Qiu YQ, Xu WD, Xu JG. Long-term observation of respiratory function after unilateral phrenic nerve and multiple intercostal nerve transfer for avulsed brachial plexus injury. *Neurosurgery* (2012) 70(4):796–801; discussion801. doi:10.1227/NEU.0b013e3181f74139
19. Zheng MX, Xu WD, Qiu YQ, Xu JG, Gu YD. Phrenic nerve transfer for elbow flexion and intercostal nerve transfer for elbow extension. *J Hand Surg Am* (2010) 35(8):1304–9. doi:10.1016/j.jhsa.2010.04.006
20. Li XM, Yang JT, Hou Y, Yang Y, Qin BG, Fu G, et al. Donor-side morbidity after contralateral C-7 nerve transfer: results at a minimum of 6 months after surgery. *J Neurosurg* (2016) 124(5):1434–41. doi:10.3171/2015.3.JNS142213
21. Liu Y, Lao J, Gao K, Gu Y, Zhao X. Comparative study of phrenic nerve transfers with and without nerve graft for elbow flexion after global brachial plexus injury. *Injury* (2014) 45(1):227–31. doi:10.1016/j.injury.2012.12.013
22. Kazamel M, Sorenson EJ. Electromyographic findings in gracilis muscle grafts used to augment elbow flexion in traumatic brachial plexopathy. *J Clin Neurophysiol* (2016) 33(6):549–53. doi:10.1097/WNP.0000000000000289
23. Sakuta N, Sasaki S, Ochiai N. Analysis of activity of motor units in the biceps brachii muscle after intercostal-musculocutaneous nerve transfer. *Neurosci Res* (2005) 51(4):359–69. doi:10.1016/j.neures.2004.12.011
24. Chalidapong P, Sananpanich K, Klaphajone J. Electromyographic comparison of various exercises to improve elbow flexion following intercostal nerve transfer. *J Bone Joint Surg Br* (2006) 88(5):620–2. doi:10.1302/0301-620X.88B5.17360
25. Kovachevich R, Kircher MF, Wood CM, Spinner RJ, Bishop AT, Shin AY. Complications of intercostal nerve transfer for brachial plexus reconstruction. *J Hand Surg Am* (2010) 35(12):1995–2000. doi:10.1016/j.jhsa.2010.09.013

Conflict of Interest Statement: The authors declare that the research was conducted in the absence of any commercial or financial relationships that could be construed as a potential conflict of interest.

frontiers in Neurology

ORIGINAL RESEARCH
published: 23 December 2016
doi: 10.3389/fneur.2016.00240

Cerebral Reorganization in Patients with Brachial Plexus Birth Injury and Residual Shoulder Problems

Anders Björkman[1], Andreas Weibull[2], Hampus Svensson[1] and Lars Dahlin[1,3]*

[1] Department of Hand Surgery, Skåne University Hospital, Malmö, Sweden, [2] Department of Radiation Physics, Skåne University Hospital, Malmö, Sweden, [3] Department of Translational Medicine – Hand Surgery, Lund University, Malmö, Sweden

The functional outcome after a brachial plexus birth injury (BPBI) is based on changes in the peripheral nerve and in the central nervous system. Most patients with a BPBI recover, but residual deficits in shoulder function are not uncommon. The aim of this study was to determine cerebral activation patterns in patients with BPBI and also residual symptoms from the shoulder. In seven patients (six females and one male, aged 17–23 years) with a BPBI and residual shoulder problems (Mallet score IV or lower), the cerebral response to active movement of the shoulder and elbow of the injured and healthy arm was monitored using functional magnetic resonance imaging at 3 T. Movements, i.e., shoulder rotation or elbow flexion and extension, of the injured side resulted in a more pronounced and more extended activation of the contralateral primary sensorimotor cortex compared to the activation seen after moving the healthy shoulder and elbow. In addition, moving the shoulder or elbow on the injured side resulted in increased activation in ipsilateral primary sensorimotor areas an also increased activation in associated sensorimotor areas, in both hemispheres, located further posterior in the parietal lobe, which are known to be important for integration of motor tasks and spatial aspects of motor control. Thus, in this preliminary study based on a small cohort, patients with BPBI and residual shoulder problems show reorganization in sensorimotor areas in both hemispheres of the brain. The increased activation in ipsilateral sensorimotor areas and in areas that deal with both integration of motor tasks and spatial aspects of motor control in both hemispheres indicates altered dynamics between the hemispheres, which may be a cerebral compensation for the injury.

Keywords: brain, reorganization, brachial plexus, brachial plexus birth injury, nerve, children

OPEN ACCESS

Edited by:
Mattias K. Sköld, Uppsala University, Sweden

Reviewed by:
Peter John Shortland, Western Sydney University, Australia
Aleksandar Beric, New York University, USA

****Correspondence:***
Anders Björkman
anders.bjorkman@med.lu.se

Specialty section:
This article was submitted to Neurotrauma, a section of the journal Frontiers in Neurology

Received: *25 August 2016*
Accepted: *12 December 2016*
Published: *23 December 2016*

Citation:
Björkman A, Weibull A, Svensson H and Dahlin L (2016) Cerebral Reorganization in Patients with Brachial Plexus Birth Injury and Residual Shoulder Problems. Front. Neurol. 7:240. doi: 10.3389/fneur.2016.00240

INTRODUCTION

Brachial plexus birth injury [BPBI; incidence 0.4–5.0 per 1,000 births (1, 2)] is caused by stretching or tearing of the brachial plexus, usually during vaginal delivery. High birth weight and shoulder dystocia are the most important risk factors (2, 3). Most children with BPBI recover spontaneously, but up to 30% may suffer from permanent disability (2, 4), and the number of patients with spontaneous recovery may have been overestimated (5). Following a BPBI, a cascade of processes in the peripheral nerve culminate in target muscle reinnervation (6). However, in cases with a severe injury, successful

nerve regeneration may not be possible at all (7). In patients in whom regenerating axons reach the target muscles, there are still significant barriers to an optimal functional outcome, and the outcome is most often an incomplete reinnervation with a reduced number of functional motor units (8). In patients with residual symptoms after a BPBI, a pattern of recovery is often noted, but deficits are often seen in C5- to C7-innervated muscles. The degree of recovery of external rotation of the shoulder, elbow flexion, and supination at 3 months can be used as a predictor of which infants will retain functional deficits (9). Although external rotation of the shoulder and forearm supination are most affected and recover last, elbow flexion and shoulder abduction are the functional movements that often prove most challenging in patients with severe BPBI (9). Depending of the type of residual problems, surgical muscle transfer and osteotomy can improve function in patients with permanent disability (10). Even so, a number of patients have residual shoulder problems that restrict their daily life.

Evidence is accumulating to suggest that adaptations within the central nervous system are relevant for the clinical recovery following BPI in adults (8, 11–13). Some previous studies, using EMG, in patents with BPBI and residual symptoms has shown partial muscle reinnervation but poor clinical function—a condition termed developmental apraxia (14). This indicates a maladaptation of the cerebral motor network early in infancy following BPBI (15, 16). Thus, beyond peripheral nerve regeneration, plasticity in the central nervous system is involved in determining whether there is successful or failed functional recovery in patients with BPBI.

Our aim was to investigate cerebral activation patterns following activation of muscles controlling shoulder rotation and elbow flexion in young adults with BPBI and subjective shoulder problems.

MATERIALS AND METHODS

Patients

All patients treated for BPBI at the Department of Hand Surgery, Skåne University Hospital, Malmö, Sweden between 2010 and 2011 were asked to participate. Inclusion criteria were as follows: (1) unilateral BPBI; (2) age between 15 and 25 years; (3) no previous reconstructive nerve surgery, i.e., neurolysis, nerve grafting, or neurotisation; (4) residual symptoms from the shoulder with a suboptimal Mallet score (17) (IV or lower) in one or more of the following variables: shoulder abduction, shoulder rotation, and hand to mouth; and (5) a minimum of 36 months since operation in patients operated with reconstruction to improve shoulder function. Exclusion criteria were as follows: (1) a history of neurological disease other than BPBI; (2) psychiatric disorders; and (3) contraindications to investigation by MRI.

Ten patients (eight females and two males) were identified, but one had moved abroad, and two did not want to undergo MRI investigation. Thus, seven patients (six females and one male) between 17 and 23 years of age were included in the study (**Table 1**). All patients had been meticulously followed since birth by specialists from the Departments of Paediatrics and Hand Surgery. At birth, they all had a normal hand function and a rapid initial recovery of some function in the biceps muscle, which indicates a nerve injury at trunk level. The probability of an avulsion injury of one or two of the nerve roots corresponding to the upper trunk seems to be low, which is also supported by the facts that none of the patients had a breech delivery.

Six participants had been operated with reconstructive surgery in some form, although not nerve surgery, to improve shoulder function. None of the patients had been operated to improve elbow function. All the participants were classified according to the Narakas score at birth (18) and according to the Mallet score at the time of surgery and at follow-up (**Table 1**).

The study was approved by the ethical committee of Lund University (number 269/2008, 2009/728, additional approval 2011/23) and was conducted according to the tenets of the Declaration of Helsinki. All the participants gave written consent.

Imaging

Functional magnetic resonance imaging (fMRI) was performed 36–200 months (mean 110 months) after surgery in six patients who were operated with reconstruction to improve shoulder function and in one additional patient with residual shoulder problems who had not been operated.

Functional magnetic resonance imaging was used to investigate cortical activation following active movement

TABLE 1 | Patient characteristics, Narakas group at birth, and Mallet score before and after reconstructive surgery in patients with brachial plexus birth injury.

Patient no.	Gender	Age at functional magnetic resonance imaging (fMRI), years	Affected side	Narakas group	Mallet score before operation[a]	Age at surgery, years	Type of operation	Mallet score after operation[a] (months after op.)
1	F	17	L	I	V/II/IV[b]	n/a	n/a	n/a
2	F	23	R	I	V/II/III	12	A, B, D	V/IV/V (130)
3	F	18	R	II	V/I/II	14	C, D	V/IV/V (46)
4	M	21	L	I	V/I/V	13	A, B, C	V/II/V (90)
5	F	23	L	I	IV/II/V	9	B, D	IV/IV/V (160)
6	F	17	L	I	IV/II/III	14	A, B, C, D	V/IV/V (36)
7	F	23	R	I	III/I/III	5 and 6	B, D	III/IV/IV (200)

[a]*Mallet score for shoulder abduction, external rotation of the shoulder, and hand to mouth.*

A, resection of the coracoid process; B, lengthening of subscapular muscle; C, rotational osteotomy of humerus; D, transfer of latissimus dorsi muscle; n/a, not applicable.

[b]*Patient not operated. Mallet score at the time of fMRI investigation.*

of the shoulder and elbow in a whole-body 3 T MR scanner (Tim-TRIO; Siemens Medical Solutions, Erlangen, Germany) equipped with a 12-channel head matrix coil. Initially, a high-resolution 3D anatomical scan was acquired with transversal slices oriented to form a plane through the anterior and posterior commissures.

Each patient was instructed to perform repetitive flexion/extension of the elbow joint or shoulder rotation (internal/external) at a constant pace during four 30-s periods interspersed with four 30-s periods of "rest."

Sessions of motor activation were alternated with rest conditions of no stimuli in a block design. Each block was 30 s in length, and the experiment started with a rest condition. The same procedure was followed in the injured arm and uninjured arm in a pseudo-randomized order to avoid temporal bias, such as habituation effects and fatigue.

Blood oxygen level-dependent imaging was performed using a gradient echo–echo planar pulse sequence with an echo time of 30 ms, a repetition time of 2,000 ms, and a voxel resolution of 3 mm × 3 mm × 3 mm. After the scanning session, each patient was asked whether any complications had occurred, in order to ensure the use of proper data and to allow data to be excluded on reasonable grounds.

Analysis

Evaluation of the fMRI data was performed using BrainVoyager QX 2.6 software (Brain Innovation B.V., Maastricht, the Netherlands). The functional data series was motion-corrected and spatially smoothed using a smoothing kernel width of 6 mm. The data series was then normalized to Talairach space (19) by co-registration to Talairach-processed anatomical data. Furthermore, low-frequency modulation below two cycles per session was suppressed. Activation maps were created by modeling of mixed effects using the general linear model. Resulting activation maps were visually inspected at a statistical threshold of $p < 0.05$, corrected for multiple comparisons by controlling the false discovery rate (20). Activation present at this threshold was subsequently evaluated at a statistical threshold of $p < 0.01$, uncorrected for multiple comparisons, to avoid cluster size bias when comparing different sessions. Statistical comparisons between groups were performed at $p < 0.05$, uncorrected. Activation clusters were located using Talairach coordinate standardization, and the corresponding Brodmann area (BA) (defined as the BA within 3 mm of the most significant voxel of each cluster) was defined using the Talairach client (21, 22) in applicable cases. This automated classification resulted in some clusters being located in BAs not generally considered to be part of the motor network.

When performing group analysis, the activation maps of patients with a left-side injury were flipped in the left-to-right direction to prevent substantial loss of power, a strategy that has already been used (23). Since the hemispheres in a single subject are neither functional nor anatomically equal, the spatial noise is likely to increase. The contribution of spatial noise is, however, minimized—as the data are smoothed both individually and in group analysis.

RESULTS

The characteristics of the patients and the Narakas group at birth and Mallet score before and after any reconstructive surgery are presented in **Table 1**. All seven patients showed activation of the contralateral primary sensorimotor cortex during elbow movement and shoulder rotation of both the injured arm and the healthy arm. However, moving the injured arm, elbow flexion and extension, or shoulder rotation resulted in a more pronounced and more extended activation of the contralateral primary sensorimotor cortex and also the ipsilateral primary sensorimotor cortex than when moving the healthy arm (**Figure 1**). Furthermore, compared to when moving the healthy arm, moving the injured arm resulted in increased activation in associated sensorimotor areas, in both hemispheres, located further posterior in the parietal lobe. These areas are known to be important for integration of motor tasks and spatial aspects of motor control. In addition, increased activation was also seen in other regions, such as the supplementary motor area, secondary somatosensory cortex, the ipsilateral insula, and the cerebellum.

In the case of elbow movement, these differences were statistically significant ($p < 0.05$, uncorrected) when comparing the injured and healthy arms (**Figure 1**, right-hand side). During shoulder rotation, differences were less evident than changes seen during elbow movement, and they were not statistically significant at $p < 0.05$ (uncorrected) (**Figure 1**, right-hand side).

DISCUSSION

Patients suffering from unilateral BPBI and residual symptoms from the shoulder show increased activation in the primary sensorimotor cortex bilaterally and in associated sensorimotor areas, in both hemispheres, located further posterior in the parietal lobe which are known to be important for integration of motor tasks and spatial aspects of motor control, when using the injured arm compared to when using the healthy arm.

Normal use of the hands is highly dependent on interhemispheric control of motor and sensory areas in both brain hemispheres (24). In adults, a peripheral nerve injury in the forearm or a brachial plexus injury is known to result in substantial reorganization in sensorimotor areas in both brain hemispheres—and also in changes in functional connectivity between sensorimotor areas (11, 25). In addition, the return of sensory and motor functions after these injuries is often poor (26).

Interestingly, the cerebral response and clinical outcome after peripheral nerve injury have been shown to be highly dependent on age at injury (27, 28). The consequences of a neonatal peripheral nerve injury, such as BPBI, on the central nervous system in humans are largely unknown. However, studies on peripheral nerve injuries in neonatal rodents have shown that within days after injury most functional synapses turn into "silent synapses." This is followed by a period of new synapse formation, i.e., reactive synaptogenesis, where new synapses are formed to support the damaged function (29). It is difficult to transform these findings to newborn humans with a BPBI, but a peripheral nerve injury, operated with nerve suture, in the forearm in children less than 13 years of age

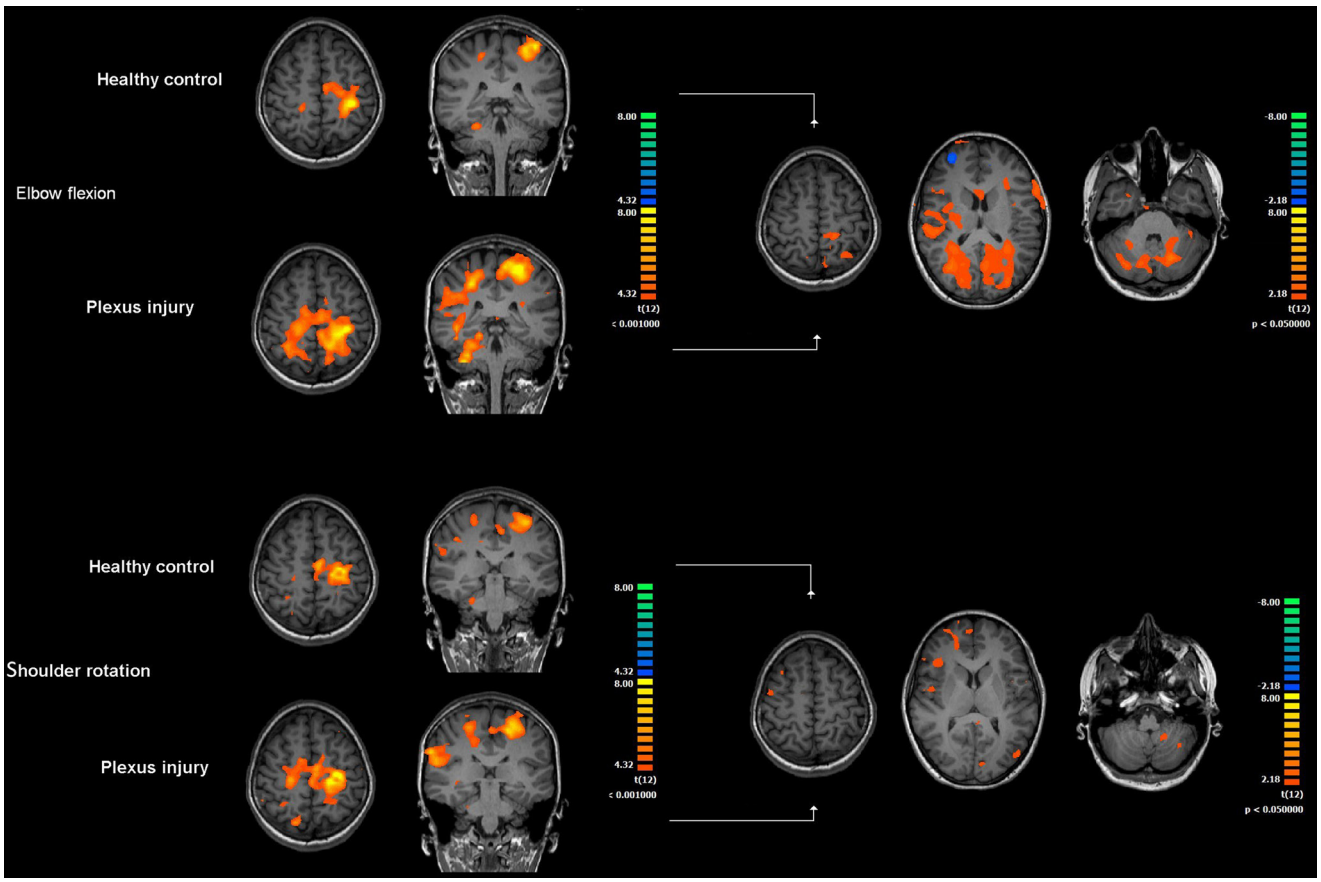

FIGURE 1 | **Cerebral activation during motor stimulation in patients with brachial plexus birth injury**. The left-hand side of the figure shows brain activation during elbow flexion and extension and shoulder rotation compared to rest using the injured and healthy (control) arm, respectively. Activation patterns represent group results, and individual data have been shifted in the right–left direction so that the contralateral hemisphere in respect to motor stimulation is always the left hemisphere (conventionally to the right in radiological images). The right-hand side of the figure shows statistically significant differences ($p < 0.05$, uncorrected for multiple comparisons) in the activation pattern in the injured arm compared to the healthy arm. Elbow flexion resulted in significantly increased activation in the primary sensorimotor cortex in the contralateral hemisphere and in the ispilateral hemisphere compared to when moving the healthy arm ($p < 0.05$). Shoulder rotation on the injured side also resulted in increased activation in the primary sensorimotor cortex bilaterally, but this was not statistically significant.

results in a cerebral activation in sensorimotor areas identical to that in healthy controls, in combination with an excellent return of sensory and motor function. On the other hand, a peripheral nerve injury in children older than 13 years results in a cerebral response similar to that seen in adults and a poor clinical outcome regarding return of sensory and motor functions (27). Given the fact that peripheral nerve injuries sustained at a young age have an excellent clinical outcome, patients with BPBI should have a good possibility of regaining function, and many patients with BPBI do have a complete functional recovery. Those who do not recover—as with the participants in the present study who had residual symptoms from their shoulder—probably have a more severe injury with extensive changes in afferent and efferent nerve signaling. This is supported by the present study, where fMRI showed cerebral changes that were more similar to what is seen in adults with peripheral nerve injuries, where activation in sensorimotor areas in both brain hemispheres is changed. Previous studies on adults with BPI have suggested altered interhemispheric dynamics, resulting in loss of the deactivation normally seen in ipsilateral sensorimotor areas (25). These results have been corroborated here in patients with BPBI and residual shoulder problems, who showed an increased activation in the primary sensorimotor cortex in the ipsilateral hemisphere. Furthermore, patients with BPBI also showed an increased activation in areas in the posterior parietal cortex in both hemispheres, which are known to be important for integration of motor tasks and spatial aspects of motor control. The mechanisms behind the change in neural activity in the ipsilateral primary sensorimotor cortex and the in associated sensorimotor areas found in this study are not clear. Previous studies in healthy humans have suggested a functional interhemispheric inhibition between the primary somatosensory cortices (30, 31), most likely mediated by transcallosal activation of inhibitory GABAergic interneurons (32). Thus, the changes in the ipsilateral hemisphere seen in our study could be driven by changes contralaterally, or they

could be due to an altered balance between homologous parts of sensorimotor areas in both hemispheres. Furthermore, the increased activation seen in posterior parietal areas known to be important for spatial aspects of motor control and motor task integration also suggest that there may be a cerebral compensatory mechanism whereby more neurons are recruited to compensate for the impaired function in the arm.

All but one participant had Narakas I at birth, indicating shoulder and elbow problems. Over time, however, all the participants had improved spontaneously, and none of them had been operated to improve elbow function. At follow-up, none of them experienced any subjective problems from the elbow. On the other hand, all but one participant had been operated to improve shoulder function, and those who were operated also had an improved Mallet score although they still experienced problems from their shoulder to some extent. Interestingly, both shoulder rotation and elbow flexion of the injured arm resulted in cerebral changes in both brain hemispheres. However, these differences were only significant, compared to when using the healthy arm, after flexion and extension of the elbow. Keeping the small number of patients in mind, one possible explanation for this intriguing difference may be found in the dynamic capacity of the brain. Directly after the BPBI, there is a cerebral plasticity trying to compensate for the injury. The difference in clinical recovery in flexion and extension of the elbow and shoulder rotation in the patients may indicate a more severe injury to nerves supplying the shoulder. Six out of the seven patients underwent surgical reconstruction, at a later stage in life, to improve shoulder function, and even if they did not have nerve reconstructions, the surgical procedures performed are likely to result in a new period of cerebral plasticity where the neurons supplying the shoulder muscles adopt to the reconstructions done. This neural process can be detected as a clinical improvement in shoulder function. Thus, in the present study group, plasticity in neurons controlling elbow flexion and extension mainly take place at a very young age whereas the operative reconstructions to the shoulder are done at an older age where the dynamic capacity of the brain is diminished compared to what is the case in the period immediately after birth. This may result in a "smaller" reorganization, which is insufficient to improve shoulder rotation to a normal state.

Furthermore, the increased use of the hemisphere ipsilateral to the injury as well as areas in the posterior part of the parietal cortex bilaterally suggests that neurons in these areas have a more important role in the cerebral recovery processes in patients with BPBI than previously realized.

Our results were limited by the number of patients being examined. However, BPBI is rare, and there have been no previous studies focusing on cerebral changes in patients with BPBI and residual shoulder problems. Considering the long follow-up in this study, we believe that evaluation of seven patients can give valuable information, despite the small number. However, a study involving more patients who are randomized to different operative reconstructions is required to help answer two important questions: (1) is there a correlation between the cerebral changes, clinical deficits experienced by the patients, and the type of surgical reconstruction? and (2) does age at reconstruction affect clinical outcome and cerebral changes? Studies in neonatal rodents have shown that there is a critical time window for reactive, compensatory, synaptogenesis following a neonatal peripheral nerve injury (29). This time window is not known in humans; but since nerve repair before the age of 13 years results in perfect restitution of nerve function, reconstructive surgery for residual shoulder problems should, at least in theory, be done before the age of 13 years in order to optimize clinical outcome. These are important questions requiring further attention.

Many rehabilitation programs for patients with BPBI are purely empirical and are not based on current knowledge in neuroscience. The dynamic capacity of the nervous system creates possibilities, and recent studies have suggested the possibility of using specific interventions to accelerate axon regeneration and CNS plasticity, i.e., guided plasticity (33–35). It has been proposed that rehabilitation programs should be tailored individually according to the nerve injury and the functional problems experienced by the individual patient, to maximize the effects of guided plasticity (36). Further studies are needed to better understand the cerebral response to BPBI and to explore the potential therapeutic approach of guided plasticity in patients with BPBI.

AUTHOR CONTRIBUTIONS

AB and LD designed the study. AB, AW, HS, and LD assessed the patients and created a study database. AB, HS, and AW evaluated all fMRIs. AB, LD, and AW analyzed the results and wrote the manuscript. All the authors contributed to discussion of the results and read and approved the final version of the manuscript.

FUNDING

The institution of the authors has received funding from Lund University, Region Skåne and Funds from the Skåne University Hospital Malmö, Sweden.

REFERENCES

1. Andersen J, Watt J, Olson J, Van Aerde J. Perinatal brachial plexus palsy. *Paediatr Child Health* (2006) 11(2):93–100.
2. Lindqvist PG, Erichs K, Molnar C, Gudmundsson S, Dahlin LB. Characteristics and outcome of brachial plexus birth palsy in neonates. *Acta Paediatr* (2012) 101(6):579–82. doi:10.1111/j.1651-2227.2012.02620.x
3. Sibinski M, Synder M. Obstetric brachial plexus palsy – risk factors and predictors. *Ortop Traumatol Rehabil* (2007) 9(6):569–76.
4. Foad SL, Mehlman CT, Foad MB, Lippert WC. Prognosis following neonatal brachial plexus palsy: an evidence-based review. *J Child Orthop* (2009) 3(6):459–63. doi:10.1007/s11832-009-0208-3
5. Pondaag W, Malessy MJ, van Dijk JG, Thomeer RT. Natural history of obstetric brachial plexus palsy: a systematic review. *Dev Med Child Neurol* (2004) 46(2):138–44. doi:10.1111/j.1469-8749.2004.tb00463.x
6. Fu SY, Gordon T. The cellular and molecular basis of peripheral nerve regeneration. *Mol Neurobiol* (1997) 14(1–2):67–116. doi:10.1007/BF02740621

7. Simon NG, Spinner RJ, Kline DG, Kliot M. Advances in the neurological and neurosurgical management of peripheral nerve trauma. *J Neurol Neurosurg Psychiatry* (2016) 87(2):198–208. doi:10.1136/jnnp-2014-310175
8. Navarro X, Vivo M, Valero-Cabre A. Neural plasticity after peripheral nerve injury and regeneration. *Prog Neurobiol* (2007) 82(4):163–201. doi:10.1016/j.pneurobio.2007.06.005
9. Lagerkvist AL, Johansson U, Johansson A, Bager B, Uvebrant P. Obstetric brachial plexus palsy: a prospective, population-based study of incidence, recovery, and residual impairment at 18 months of age. *Dev Med Child Neurol* (2010) 52(6):529–34. doi:10.1111/j.1469-8749.2009.03479.x
10. Hultgren T, Jonsson K, Roos F, Jarnbert-Pettersson H, Hammarberg H. Surgical correction of shoulder rotation deformity in brachial plexus birth palsy: long-term results in 118 patients. *Bone Joint J* (2014) 96-B(10):1411–8. doi:10.1302/0301-620X.96B10.33813
11. Taylor KS, Anastakis DJ, Davis KD. Cutting your nerve changes your brain. *Brain* (2009) 132(Pt 11):3122–33. doi:10.1093/brain/awp231
12. Li T, Hua XY, Zheng MX, Wang WW, Xu JG, Gu YD, et al. Different cerebral plasticity of intrinsic and extrinsic hand muscles after peripheral neurotization in a patient with brachial plexus injury: a TMS and fMRI study. *Neurosci Lett* (2015) 604:140–4. doi:10.1016/j.neulet.2015.07.015
13. Feng JT, Liu HQ, Xu JG, Gu YD, Shen YD. Differences in brain adaptive functional reorganization in right and left total brachial plexus injury patients. *World Neurosurg* (2015) 84(3):702–8. doi:10.1016/j.wneu.2015.04.046
14. Scarfone H, McComas AJ, Pape K, Newberry R. Denervation and reinnervation in congenital brachial palsy. *Muscle Nerve* (1999) 22(5):600–7. doi:10.1002/(SICI)1097-4598(199905)22:5<600::AID-MUS8>3.0.CO;2-B
15. Brown T, Cupido C, Scarfone H, Pape K, Galea V, McComas A. Developmental apraxia arising from neonatal brachial plexus palsy. *Neurology* (2000) 55(1):24–30. doi:10.1212/WNL.55.1.24
16. Colon AJ, Vredeveld JW, Blaauw G. Motor evoked potentials after transcranial magnetic stimulation support hypothesis of coexisting central mechanism in obstetric brachial palsy. *J Clin Neurophysiol* (2007) 24(1):48–51. doi:10.1097/01.wnp.0000237075.85689.33
17. Mallet J. [Obstetrical paralysis of the brachial plexus. 3. Conclusions]. *Rev Chir Orthop Reparatrice Appar Mot* (1972) 58(Suppl 1):201–4.
18. Al-Qattan MM, El-Sayed AA, Al-Zahrani AY, Al-Mutairi SA, Al-Harbi MS, Al-Mutairi AM, et al. Narakas classification of obstetric brachial plexus palsy revisited. *J Hand Surg Eur Vol* (2009) 34(6):788–91. doi:10.1177/1753193409348185
19. Talairach J, Tournoux P. *Co-Planar Stereotaxic Atlas of the Human Brain*. Stuttgart: Thieme (1988).
20. Chumbley J, Worsley K, Flandin G, Friston K. Topological FDR for neuroimaging. *Neuroimage* (2010) 49(4):3057–64. doi:10.1016/j.neuroimage.2009.10.090
21. Lancaster JL, Woldorff MG, Parsons LM, Liotti M, Freitas CS, Rainey L, et al. Automated Talairach atlas labels for functional brain mapping. *Hum Brain Mapp* (2000) 10(3):120–31. doi:10.1002/1097-0193(200007)10:3<120::AID-HBM30>3.0.CO;2-8
22. Lancaster JL, Rainey LH, Summerlin JL, Freitas CS, Fox PT, Evans AC, et al. Automated labeling of the human brain: a preliminary report on the development and evaluation of a forward-transform method. *Hum Brain Mapp* (1997) 5(4):238–42. doi:10.1002/(SICI)1097-0193(1997)5:4
23. Buhmann C, Glauche V, Sturenburg HJ, Oechsner M, Weiller C, Buchel C. Pharmacologically modulated fMRI – cortical responsiveness to levodopa in drug-naive hemiparkinsonian patients. *Brain* (2003) 126(Pt 2):451–61. doi:10.1093/brain/awg033
24. Wolpert DM, Diedrichsen J, Flanagan JR. Principles of sensorimotor learning. *Nat Rev Neurosci* (2011) 12(12):739–51. doi:10.1038/nrn3112
25. Liu B, Li T, Tang WJ, Zhang JH, Sun HP, Xu WD, et al. Changes of inter-hemispheric functional connectivity between motor cortices after brachial plexuses injury: a resting-state fMRI study. *Neuroscience* (2013) 243:33–9. doi:10.1016/j.neuroscience.2013.03.048
26. Lundborg G, Richard P. Bunge memorial lecture. Nerve injury and repair – a challenge to the plastic brain. *J Peripher Nerv Syst* (2003) 8(4):209–26. doi:10.1111/j.1085-9489.2003.03027.x
27. Chemnitz A, Weibull A, Rosen B, Andersson G, Dahlin LB, Bjorkman A. Normalized activation in the somatosensory cortex 30 years following nerve repair in children: an fMRI study. *Eur J Neurosci* (2015) 42(4):2022–7. doi:10.1111/ejn.12917
28. Chemnitz A, Bjorkman A, Dahlin LB, Rosen B. Functional outcome thirty years after median and ulnar nerve repair in childhood and adolescence. *J Bone Joint Surg Am* (2013) 95(4):329–37. doi:10.2106/JBJS.L.00074
29. Lo FS, Erzurumlu RS. Neonatal sensory nerve injury-induced synaptic plasticity in the trigeminal principal sensory nucleus. *Exp Neurol* (2016) 275(Pt 2):245–52. doi:10.1016/j.expneurol.2015.04.022
30. Ragert P, Nierhaus T, Cohen LG, Villringer A. Interhemispheric interactions between the human primary somatosensory cortices. *PLoS One* (2011) 6(2):e16150. doi:10.1371/journal.pone.0016150
31. Schafer K, Blankenburg F, Kupers R, Gruner JM, Law I, Lauritzen M, et al. Negative BOLD signal changes in ipsilateral primary somatosensory cortex are associated with perfusion decreases and behavioral evidence for functional inhibition. *Neuroimage* (2012) 59(4):3119–27. doi:10.1016/j.neuroimage.2011.11.085
32. Cauli B, Hamel E. Revisiting the role of neurons in neurovascular coupling. *Front Neuroenergetics* (2010) 2:9. doi:10.3389/fnene.2010.00009
33. Gordon T, English AW. Strategies to promote peripheral nerve regeneration: electrical stimulation and/or exercise. *Eur J Neurosci* (2016) 43(3):336–50. doi:10.1111/ejn.13005
34. Udina E, Cobianchi S, Allodi I, Navarro X. Effects of activity-dependent strategies on regeneration and plasticity after peripheral nerve injuries. *Ann Anat* (2011) 193(4):347–53. doi:10.1016/j.aanat.2011.02.012
35. Duffau H. Brain plasticity: from pathophysiological mechanisms to therapeutic applications. *J Clin Neurosci* (2006) 13(9):885–97. doi:10.1016/j.jocn.2005.11.045
36. Rosenkranz K, Rothwell JC. Differences between the effects of three plasticity inducing protocols on the organization of the human motor cortex. *Eur J Neurosci* (2006) 23(3):822–9. doi:10.1111/j.1460-9568.2006.04605.x

Conflict of Interest Statement: The research was conducted in the absence of any commercial or financial relationship that could be construed as a potential conflict of interest.

frontiers in Neurology

ORIGINAL RESEARCH
published: 20 January 2017
doi: 10.3389/fneur.2017.00008

Hand-to-Face Remapping But No Differences in Temporal Discrimination Observed on the Intact Hand Following Unilateral Upper Limb Amputation

*Kassondra L. Collins[1,2], Danielle L. McKean[1], Katherine Huff[1], Mark Tommerdahl[3], Oleg Vyacheslavovich Favorov[3], Robert S. Waters[2] and Jack W. Tsao[1,2,4]**

[1] Department of Neurology, University of Tennessee Health Science Center, Memphis, TN, USA, [2] Department of Anatomy and Neurobiology, University of Tennessee Health Science Center, Memphis, TN, USA, [3] Department of Biomedical Engineering, University of North Carolina at Chapel Hill, Chapel Hill, NC, USA, [4] Children's Foundation Research Institute, Le Bonheur Children's Hospital, Memphis, TN, USA

OPEN ACCESS

Edited by:
Mattias K. Sköld, Uppsala University, Sweden

Reviewed by:
Antonino F. Germanò, University of Messina, Italy
Ralph George Depalma, Department of Veterans Affairs Office of Research and Development, USA

***Correspondence:**
Jack W. Tsao
jtsao@uthsc.edu

Specialty section:
This article was submitted to Neurotrauma, a section of the journal Frontiers in Neurology

Received: *18 October 2016*
Accepted: *06 January 2017*
Published: *20 January 2017*

Citation:
Collins KL, McKean DL, Huff K, Tommerdahl M, Favorov OV, Waters RS and Tsao JW (2017) Hand-to-Face Remapping But No Differences in Temporal Discrimination Observed on the Intact Hand Following Unilateral Upper Limb Amputation. Front. Neurol. 8:8. doi: 10.3389/fneur.2017.00008

Unilateral major limb amputation causes changes in sensory perception. Changes may occur within not only the residual limb but also the intact limb as well as the brain. We tested the hypothesis that limb amputation may result in the detection of hand sensation during stimulation of a non-limb-related body region. We further investigated the responses of unilateral upper limb amputees and individuals with all limbs intact to temporally based sensory tactile testing of the fingertips to test the hypothesis that changes in sensory perception also have an effect on the intact limb. Upper extremity amputees were assessed for the presence of referred sensations (RSs)—experiencing feelings in the missing limb when a different body region is stimulated, to determine changes within the brain that occur due to an amputation. Eight of 19 amputees (42.1%) experienced RS in the phantom limb with manual tactile mapping on various regions of the face. There was no correlation between whether someone had phantom sensations or phantom limb pain and where RS was found. Six of the amputees had either phantom sensation or pain in addition to RS induced by facial stimulation. Results from the tactile testing showed that there were no significant differences in the accuracy of participants in the temporal order judgment tasks ($p = 0.702$), whereby participants selected the digit that was tapped first by a tracking paradigm that resulted in correct answers leading to shorter interstimulus intervals (ISIs) and incorrect answers increasing the ISI. There were also no significant differences in timing perception, i.e., the threshold accuracy of the duration discrimination task ($p = 0.727$), in which participants tracked which of the two digits received a longer stimulus. We conclude that many, but not all, unilateral upper limb amputees experience phantom hand sensation and/or pain with stimulation of the face, suggesting that there could be postamputation changes in neuronal circuitry in somatosensory cortex. However, major unilateral limb amputation does not lead to changes in temporal order judgment or timing perception tasks administered *via* the tactile modality of the intact hand in upper limb amputees.

Keywords: amputation, tactile discrimination, referred sensation, phantom limb, reorganization, somatosensory

INTRODUCTION

Great debate ensues regarding the etiology of phantom limb sensations (PLSs) and associated pain. Almost all amputees experience PLSs (1, 2). The minority that tends not to experience any phantom sensations typically includes congenital amputees (3, 4), although one study has identified such experiences in this population (5). More than 80% of all amputees will also experience phantom limb pain (PLP), characterized by electric shock, stabbing, and cramping sensations (6). PLP is a debilitating condition for many amputees. Unfortunately, the mechanisms that create phantom experiences, including sensation and pain, are not understood. When an amputation occurs, the peripheral limb is removed from the body causing drastic changes not only in the peripheral but also in the central nervous systems. Muscles and nerves attempt to forge new connections in place of lost ones, causing reorganization within the residual limb and the brain (7). Several imaging studies have shown that, after an amputation, cortical representations of adjacent remaining body parts take over the cortical area that once responded to the now amputated region. In particular, the face-representing somatosensory cortical region expands and takes over the arm area in upper extremity amputees (3, 8–11).

Determining the mechanisms and specific pathways within the brain that are affected by an amputation will lead to further insight regarding the experience of PLS and pain. This study aimed to investigate the changes that occur within the brain of upper extremity amputees, testing the hypothesis that upper extremity amputees will experience hand-to-face remapping. Through the utilization of temporally based tactile stimulation, we also examined potential sensory perception changes that could occur within pathways controlling the intact limb. This study aimed to confirm previous studies on hand-to-face remapping while also determining other factors that may play a role in such experiences.

PARTICIPANTS AND METHODS

Participants

Participants for this study included 19 unilateral upper extremity amputees (**Table 1**) and 27 normal control participants. Control participants were recruited through the University of Tennessee Health Science Center from July 2015 through July 2016, and amputee participants were recruited at the National Amputee Coalition conferences in Tucson, AZ (July 2015) and Greensboro, NC (June 2016). The Institutional Review Board at the University of Tennessee Health Science Center gave approval for the study, and all participants provided written informed consent. Inclusion criteria, except for the presence of an amputation, were the same for all groups and included being between the ages of 18 and 65, not having brain injury, able to follow instructions, and normal or corrected-to-normal vision. Exclusion criteria included evidence or the history of a major medical, neurological, or psychiatric illness, any traumatic brain injury, a learning disability, and drug or alcohol abuse/dependence within the last 3 months, except nicotine, taking prescription drugs or supplements that might affect brain function, and having serious vision or hearing problems.

TABLE 1 | Unilateral upper extremity amputee participant information.

Participant #	Amputation	Cause	RS	PLS	PLP
1	RAE	Trauma	Yes	Yes	Yes
2	RBE	Trauma	Yes[b]	No	No
3	RBE	Trauma	No	No	No
4	RBE	Trauma	No	Yes	No
5	LBE	Congenital	Yes	Yes	No
6	LBE	Trauma	Yes	Yes	No
7	LBE	Congenital	No	Yes	No
8	LAE	Trauma	Yes	Yes	Yes
9	LBE	Congenital	No	Yes[a]	No
10	LAE	Trauma	No	Yes	Yes
11	RBE	Trauma	Yes[b]	No	No
12	LBE	Trauma	No	Yes	Yes
13	RAE	Trauma	No	Yes	Yes
14	RBE	Trauma	No	Yes	Yes
15	RBE	Trauma	Yes	Yes	Yes
16	LBE	Trauma	No	Yes	No
17	RAE	Cancer	Yes	Yes	Yes
18	RBE	Compartment syndrome	No	Yes	Yes
19	RAE	Trauma	No	Yes	Yes

Data include participant number, location of the amputation (R, right; L, left; AE, above elbow; BE, below elbow), cause of the amputation, whether or not they experienced referred sensation (RS), phantom limb sensation (PLS), and/or phantom limb pain (PLP).

[a]*Reported feeling a "fizzy" sensation in the missing limb.*

[b]*Phantom sensation only brought on by mislocalization of touch.*

Hand-to-Face Remapping

Amputees were asked to complete a series of questions regarding their amputation and phantom experiences. Information regarding the time since the amputation, the experience of phantom sensations, and the experience of PLP were investigated. Nineteen upper extremity amputees participated in facial mapping in order to determine how the brain reorganizes sensations as a result of amputation. The facial responses experienced by each amputee were mapped by using a stimulus consisting of a Q-tip brushed over different areas of the face. Testing began over the forehead with short smooth brushes and then moved around the eye, down the cheek, and over the chin. Brushing was completed both contralateral and ipsilateral to the side of amputation. As the investigator was brushing the face, the amputee was instructed to verbally express where the location of the brushing was felt. If facial mapping caused sensations within the phantom limb, repeat testing with a Q-tip dipped in cold water was performed. Finally, participants attempted to map the sensations on their own. All verbal reports of sensation felt within the phantom limb were recorded and the location(s) identified.

Tactile Testing

Tactile stimuli were delivered to two fingers with a custom-built tactile stimulator (Cortical Metrics, Carrboro, NC, USA). Control participants underwent a battery of testing conducted on the index and middle fingers of both right and left hands. Upper extremity amputees completed the testing with *the intact hand*. Testing included temporal order judgment and duration discrimination tasks. During the testing session, the participants were situated with their arm (right then left for controls, intact arm for amputees) on a wrist support and fingers positioned appropriately over

the tactile stimulator. Mechanical stimulation was applied to the tips of the index and middle fingers. A computerized procedure guided participants through a series of questions, answered *via* verbal report and recorded by a research member, relating to what the participants perceived on the tips of each finger. In both of the tasks described below, a simple tracking paradigm was used to determine each participant's difference limen, the amount that the stimulus must be changed in order for differences between finger perceptions to be detected. Visual cues on the computer screen informed participants about appropriate times to provide their response. Practice trials were performed before each test to allow the participants to become familiar with the test, and three consecutive correct responses to the training trials were required before data acquisition began. The participant was not provided with feedback or knowledge or response accuracy during data collection trials.

Temporal Order Judgment

To assess temporal order judgment, two taps were delivered sequentially, one to each finger, with an initial interstimulus interval (ISI) of 150 ms. Participants were queried as to which of the two stimuli came first. Subsequently, as the result of the subjects' response, the ISI was altered between each trial. The tracking paradigm employed resulted in correct answers leading to shorter ISIs and incorrect answers increasing the ISI. For each trial, the finger that received the first of the two pulses was chosen randomly. Subjects were required to report which finger was tapped first.

Duration Discrimination

Duration discrimination is the minimal difference in durations of two stimuli at which an individual can successfully identify the stimulus that has a longer duration. Sequential stimulus vibrations of varying durations were delivered, one to each finger. Subjects were asked to report which of the two fingers received the longer stimulus duration. The "standard" stimulus lasted 500 ms and at the start the "test" stimulus lasted 750 ms. Discrimination threshold determination was assessed using the same tracking paradigm, which reduced the duration of the test stimulus when subjects answered correctly and increased the duration of the test stimulus when the responses were incorrect. The finger and order of the stimuli were chosen at random for each trial.

Data Analysis

ANOVA was used to analyze results of tactile testing comparing between upper extremity subject groups and controls. Analyses conducted on the experience of referred sensation (RS) and the presence of PLP were also completed utilizing direct participant verbal reports, a 2 × 2 factorial ANOVA test and a Pearson's correlation test. Significance was determined by a p value <0.05.

RESULTS

Hand-to-Face Remapping

Eight out of 19 (42.1%) upper extremity amputees, including one congenital participant, experienced a mislocalization of touch when an area of their face was brushed. Similar to the results reported by Ramachandran and Rogers-Ramachandran (10), points on the face of each participant who reported elicited sensations within the phantom limb were documented and marked on a forelimb and face diagram, indicating the appropriate body region (**Figure 1**). The cheek area evoked the greatest number of RSs. Two participants experienced the feeling of their little finger when the cheek was brushed. Two participants also reported feeling the first finger when the cheek was stimulated. In addition, amputees reported feeling the thumb, back of hand, underside of the arm, and elbow through cheek stimulation. Three participants reported mislocalization of touch when the forehead was stimulated, expressing feelings within the third finger, palm, and thumb. When the chin was brushed, two participants experienced RSs of the thumb and palm. Four of the participants only experienced phantom sensations in the amputated limb when the ipsilateral side of the face to the amputation was stimulated. Two participants experienced sensations in the amputated limb when either side of the face was stimulated, and one felt sensations when more of the center of the face was stimulated.

After the identification of prominent mislocalization of touch, investigators attempted to remap the experiences with a Q-tip dipped in cold water. Only one participant felt that the sensations were more intense with the cold water, all other participants reported the same experiences as felt with the dry Q-tip. Once the cold-water test was completed, the subjects were then asked to conduct the facial mapping on themselves. Two participants reported being able to still feel RSs, while six participants no longer felt any RSs.

In addition to obtaining reports of the mislocalization of touch, investigators also asked participants to report the time since amputation and their experiences with phantom sensation or PLP. Statistical analysis conducted on the time since amputation and the presence of RS showed no correlation, with the average time since amputation being 211.26 months ($p = 0.507$). A 2 × 2 factorial ANOVA determined that there was no significant correlation between any of the experiences and the presence of RS ($p = 0.134$). A Pearson's correlation test confirmed these results as well ($p = 0.134$). Out of the eight upper extremity amputees who experienced RS, four had PLP and four reported no PLP. In addition, six regularly experienced phantom sensations prior to testing and only two did not. Also, 6 of the 11 amputees who did not experience RSs also experienced PLP, and 10 experienced PLS, with only 1 not experiencing the presence of the missing limb.

Amputees who do not experience PLSs tend to be congenital amputees (those born without a limb) (3, 4). Three congenital amputees completed the hand-to-face remapping study and reported their experiences with phantom sensations and PLP. Initially, all three congenital upper extremity amputees self-reported no RSs, no phantom sensations, and no PLP. However, two of the three participants, when asked to graphically depict their phantom limb on a piece of a paper, completed the task, suggesting that they do, in fact, feel the presence of a phantom limb. The one congenital amputee who was unable to trace the phantom limb reported that they did not have phantom

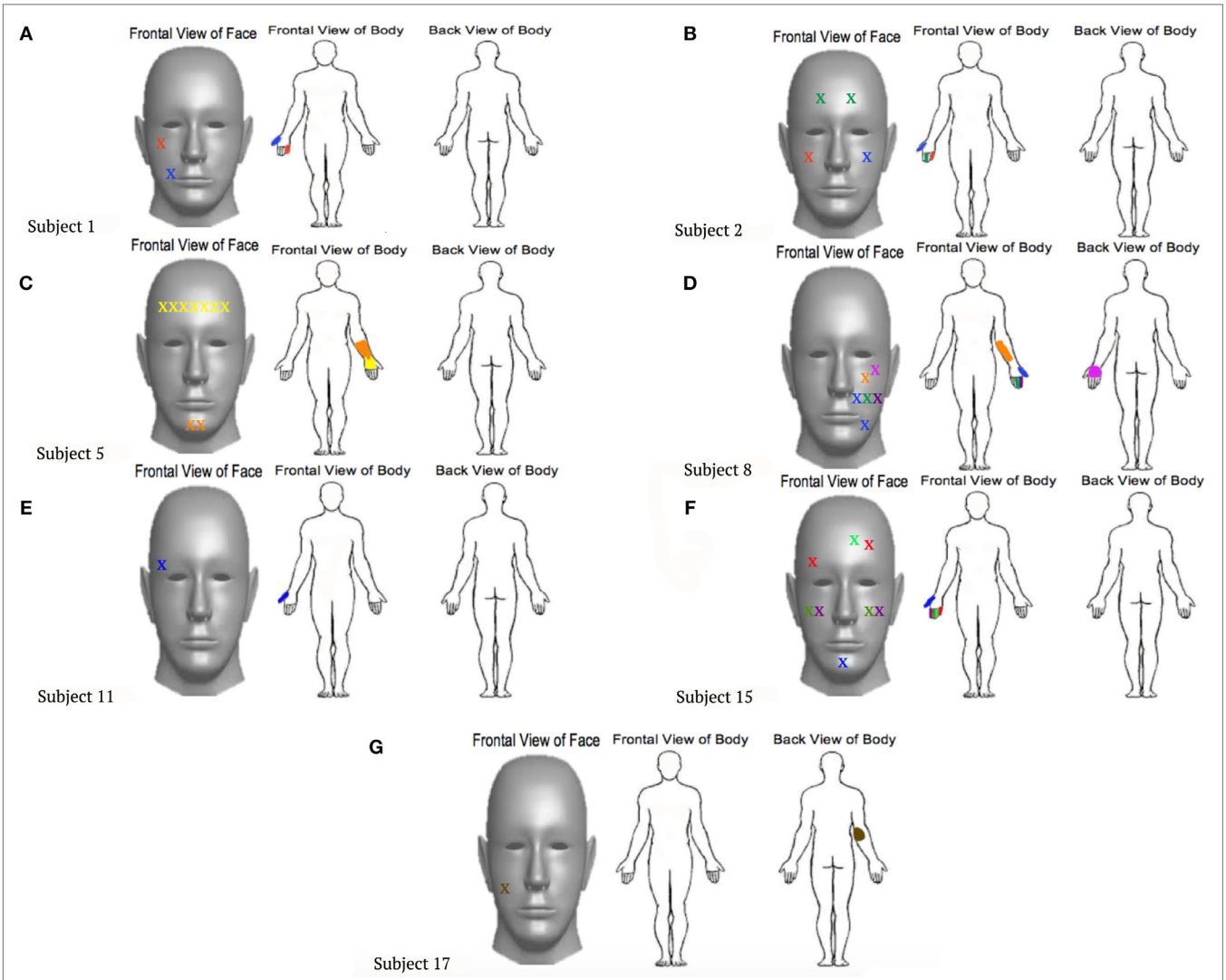

FIGURE 1 | Locations touched on the faces that were reported to also elicit sensations within the phantom limb. Each point marked by an "X" on the face corresponds to a location that was felt on the phantom limb, represented in the same color. **(A)**–**(G)** represent the individual experiences felt by different participants, labeled by subject numbers that correspond to **Table 1**.

sensation, just a "fizzy" feeling, again implying the feeling of sensation within the missing limb. Additionally, while conducting the hand-to-face remapping task, one of the congenital amputees who was able to depict their phantom limb felt the brushing sensation within the palm of the phantom limb when the forehead and chin were stimulated. This information is important to note, considering the rarity of phantom sensation reported by congenital amputees.

Temporal Order Judgment

In the temporal order judgment task, in which the participant was instructed to determine which digit experienced a test tap stimulus first, the mean threshold scores were 31.4 ± 19.5 and 34 ± 22.8 ms for the control and upper extremity amputees, respectively ($p = 0.702$). Additional analysis was conducted to determine correlations between threshold scores and whether the left or right arm was amputated. When compared to controls, neither right nor left-arm amputees differed in the temporal order judgment task ($p = 0.668$).

Duration Discrimination

The threshold accuracy of the duration discrimination task was determined to investigate the potential changes in the accuracy of timing perception for upper extremity amputees. In the duration discrimination task, participants were asked to identify which digit received a longer stimulus. The mean threshold scores were 66 ± 25.5 and 69.1 ± 28.3 ms for control and upper extremity amputees, respectively ($p = 0.727$). When the amputees were separated based on the side of their amputation, results showed no significant difference in the scores obtained on the duration discrimination task ($p = 0.204$).

DISCUSSION

When an individual loses a limb, many changes occur, not only within the peripheral system but also within the central nervous system. Although descriptions of phantom sensations and phantom pain have been around since at least the sixteenth century (12), the etiology of these experiences is still not understood. After an amputation occurs, the nerves and muscles attempt to build connections wherever possible, leading to reorganization within the residual limb. Whether this reorganization fuels the central nervous system reorganization or *vice versa* needs further investigation. Results from this study indicate that cortical reorganization may be confined to the contralateral somatosensory cortex and does not significantly affect other cortical areas or spread transcallosally to the somatosensory cortex in the opposite hemisphere.

Our investigation of the effects of an amputation on the cortex were conducted through the use of facial mapping. By using a Q-tip to brush areas of an amputee's face and evoking phantom sensations in the missing limb, we were able to positively identify hand-to-face remapping in 42.1% of upper extremity amputees. Such results show that the removal of an upper extremity does indeed cause changes within the main cortical target of somatosensory input projections, the somatosensory cortex. Additionally, this study showed that cortical reorganization is not always directly linked to the experience of PLP, since half of those experiencing mislocalization of touch failed to report any PLP. The time since amputation also did not play a role in the experience of cortical reorganization. Results are encouraging, if not definitive, and provide an important first step for future studies involving the timing of the onset and overall plasticity of cortical reorganization. One very interesting finding arising from this study was the identification of a congenital amputee who experienced mislocalization of touch. Facial mapping caused sensation within the palm of the missing limb as the forehead and chin were brushed. Initially, this participant reported that they did not experience PLP or a phantom limb; however, when asked to depict the phantom limb on a piece of paper, they proceeded to trace around a limb that they still perceived, a phantom representation. The ability of this individual to feel the palm of the missing limb on their forehead and chin shows that the brain has undergone cortical reorganization. These findings raise questions about the cause of the congenital limb loss. Although this person was born without the limb, there is the possibility that the limb was formed *in utero* and then removed, such as from amniotic band syndrome. In this scenario, there was regression of the limb during development such that the limb representation developed within the brain and did not disappear when the limb was lost. If the limb never formed during development, it is possible that the cortex still maintains some innate representation of all body parts. Such findings go against multiple studies that indicate congenital amputees do not experience phantom limbs and/or RS due to cortical reorganization (3, 4, 8). Furthermore, since there was no correlation between the presence of phantom pain and whether there was detectable hand-to-face remapping, these findings suggest that cortical reorganization alone is not the etiology of phantom pain as previously postulated (13–15).

Furthermore, temporally based tactile stimulation testing was completed on upper extremity amputees to determine the effects of amputation on the temporal processing in the CNS. Temporal order judgment task and duration discrimination task are timing tests that are controlled by areas of the brain other than the somatosensory cortex. As described by multiple studies, the ability to judge which finger receives the first test pulse is controlled mainly by the pre-supplementary motor area and posterior parietal cortex (16–18). Duration discrimination, the ability to determine which test pulse lasted longer, is thought to reflect activity predominantly centered in the cerebellum (19). Results from tactile testing on the intact limb of upper extremity amputees and controls showed that there is no significant difference on timing perception tasks between the two groups. These findings suggest that amputations lead to remapping effects that do not have an impact on timing measures that take place outside of the denervated somatosensory cortex or changes within pathways controlling the intact limb.

For clinical purposes and the management of PLP, more effort into determining the utility of visualization and residual limb movement therapies is necessary, especially if cortical reorganization alone is not a key factor in the presence of phantom pain. Future research efforts should focus on the timing of cortical reorganization to gain more insight into whether the peripheral or central nervous systems cause and/or maintain the phantom experiences. Additionally, tactile testing targeting the somatosensory cortex contralateral to the amputated side will provide information regarding changes there and effects that therapies and treatments contribute to these changes. Determining the effects that an amputation has on the organization of the brain will enable researchers to gain further knowledge about the presence of PLSs. Finally, more research needs to be conducted on the experience of phantom sensations felt by congenital amputees. It is possible that determining the factor that causes a congenital amputee to experience phantom sensations may lend great insight to the understanding of overall phantom experiences.

ETHICS STATEMENT

This study was carried out in accordance with the recommendations of the human research protection guidelines, University of Tennessee Health Science Center IRB, with written informed consent from all subjects. All subjects gave written informed consent in accordance with the Declaration of Helsinki. The protocol was approved by the University of Tennessee Health Science Center IRB.

AUTHOR CONTRIBUTIONS

KC assisted with running of participants, assisted with data analysis, and lead manuscript creation. DM oversaw and completed the running of participants and completed data analysis. KH assisted with running of participants and analyzing data. MT and OF designed the protocol, completed data analysis, and assisted with the manuscript. RW assisted with data analysis, manuscript creation, and editing of the manuscript. JT oversaw study design and execution and led manuscript editing.

ACKNOWLEDGMENTS

The authors wish to thank Annie Chan, PhD, for assistance with data collection during the first year of the study.

FUNDING

This study was supported by start-up funds provided by the University of Tennessee Health Science Center.

REFERENCES

1. Weinstein SM. Phantom limb pain and related disorders. *Neurol Clin* (1998) 16(4):919–35. doi:10.1016/S0733-8619(05)70105-5
2. Carlen PL, Wall PD, Nadvorna H, Steinbach T. Phantom limbs and related phenomena in recent traumatic amputations. *Neurology* (1978) 28:211–7. doi:10.1212/WNL.28.3.211
3. Flor H, Elbert T, Muhlnickel W, Pantev C, Wienbruch C, Taub E. Cortical reorganization and phantom phenomena in congenital and traumatic upper-extremity amputees. *Exp Brain Res* (1998) 119:205–12. doi:10.1007/s002210050334
4. Simmel M. The absence of phantoms for congenitally missing limbs. *Am J Psychol* (1961) 74:467–70. doi:10.2307/1419756
5. Vetter RJ, Weinstein S. The history of the phantom in congenitally absent limbs. *Neuropsychologia* (1967) 5:335–8. doi:10.1016/0028-3932(67)90005-X
6. Giummarra MJ, Gibson SJ, Georgiou-Karistianis N, Bradshaw JL. Central mechanisms in phantom limb perception: the past, present and future. *Brain Res Rev* (2007) 54:219–31. doi:10.1016/j.brainresrev.2007.01.009
7. Flor H. Phantom-limb pain: characteristics, causes, and treatment. *Lancet Neurol* (2002) 1(3):182–9. doi:10.1016/S1474-4422(02)00074-1
8. Pons TP, Garraghty PE, Ommaya AK, Kaas JH, Taub E, Mishkin M. Massive reorganization of the primary somatosensory cortex after peripheral sensory deafferentation. *Science* (1991) 2:1857–60. doi:10.1126/science.1843843
9. Montoya P, Ritter K, Huse E, Larbig W, Braun C, Topfner S, et al. The cortical somatotopic map and phantom phenomena in subjects with congenital limb atrophy and traumatic amputees with phantom limb pain. *Eur J Neurosci* (1998) 10:10951102. doi:10.1046/j.1460-9568.1998.00122.x
10. Ramachandran VS, Rogers-Ramachandran D. Phantom limbs and neural plasticity. *Arch Neurol* (2000) 57:317–20. doi:10.1001/archneur.57.3.317
11. Karl A, Birbaumer N, Lutzenberger W, Cohen LG, Flor H. Reorganization of motor and somatosensory cortex in upper extremity amputees with phantom limb pain. *J Neurosci* (2001) 21:3609–18.
12. Finger S, Hustwit MP. Five early accounts of phantom limb in context: Paré, Descartes, Lemos, Bell, and Mitchell. *Neurosurgery* (2003) 52(3):675–86. doi:10.1227/01.NEU.0000048478.42020.97
13. Birbaumer N, Lutzenberger W, Montoya P, Larbig W, Unertl K, Topfner S, et al. Effects of regional anesthesia on phantom limb pain are mirrored in changes in cortical reorganization. *J Neurosci* (1997) 17:5503–8.
14. Flor H, Denke C, Schaefer M, Grusser S. Effect of sensory discrimination training on cortical reorganization and phantom limb pain. *Lancet* (2001) 357:1763–4. doi:10.1016/S0140-6736(00)04890-X
15. Foell J, Bekrater-Bodmann R, Diers M, Flor H. Mirror therapy for phantom limb pain: brain changes and the role of body representation. *Eur J Pain* (2014) 18:729–39. doi:10.1002/j.1532-2149.2013.00433.x
16. Conte A, Rocchi L, Nardella A, Dispenza S, Scontrini A, Khan N, et al. Theta-burst stimulation-induced plasticity over primary somatosensory cortex changes somatosensory temporal discrimination in healthy humans. *PLoS One* (2012) 7:e32979. doi:10.1371/journal.pone.0032979
17. Lacruz F, Artieda J, Pastor MA, Obeso JA. The anatomical basis of somaesthetic temporal discrimination in humans. *J Neurol Neurosurg Psychiatry* (1991) 54:1077–81. doi:10.1136/jnnp.54.12.1077
18. Pastor MA, Day BL, Macaluso E, Friston KJ, Frackowiak RS. The functional neuroanatomy of temporal discrimination. *J Neurosci* (2004) 24:2585–91. doi:10.1523/JNEUROSCI.4210-03.2004
19. Koch G, Oliveri M, Torriero S, Salerno S, Gerfo EL, Caltagirone C. Repetitive TMS of cerebellum interferes with millisecond time processing. *Exp Brain Res* (2007) 179:291–9. doi:10.1007/s00221-006-0791-1

Conflict of Interest Statement: MT is cofounder of Cortical Metrics, the company that built the tactile stimulator used in the study. No other authors have a conflict of interest.

Advantages of publishing in Frontiers

OPEN ACCESS
Articles are free to read, for greatest visibility

COLLABORATIVE PEER-REVIEW
Designed to be rigorous – yet also collaborative, fair and constructive

FAST PUBLICATION
Average 85 days from submission to publication (across all journals)

COPYRIGHT TO AUTHORS
No limit to article distribution and re-use

TRANSPARENT
Editors and reviewers acknowledged by name on published articles

SUPPORT
By our Swiss-based editorial team

IMPACT METRICS
Advanced metrics track your article's impact

GLOBAL SPREAD
5'100'000+ monthly article views and downloads

LOOP RESEARCH NETWORK
Our network increases readership for your article

Frontiers
EPFL Innovation Park, Building I • 1015 Lausanne • Switzerland
Tel +41 21 510 17 00 • Fax +41 21 510 17 01 • info@frontiersin.org
www.frontiersin.org

Find us on